

https://dspace.org/

Mining through water-bearing fissures at Northam platinum mine (Zondereinde)

Chauke, Thapelo Welcome

2025-06

University of the Witwatersrand, Johannesburg

https://hdl.handle.net/10539/49638

Chauke, Thapelo Welcome. (2025). Mining through water-bearing fissures at Northam platinum mine (Zondereinde). [Master's dissertation, University of the Witwatersrand, Johannesburg]. WIReDSpace. https://hdl.handle.net/10539/49638

Downloaded from a DSpace repository. https://dspace.org/

School of Mining Engineering



MINING THROUGH WATER-BEARING FISSURES AT NORTHAM PLATINUM MINE (ZONDEREINDE)

Student Name:	Thapelo
Student Surname:	Chauke
Student Number:	0403541w
Supervisor:	Thomas Stacey

MSc (50/50)	MSc by Research only	PhD
X		

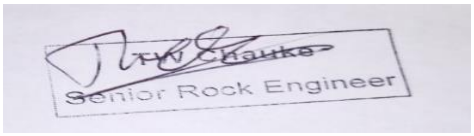
A research report presented to the Faculty of Engineering and Built Environment, University of the Witwatersrand, Johannesburg, in partial fulfilment of the fulfilment for the degree of Master of Science in Engineering

WORD COUNT	32150

DATE: 19 JUNE 2025

DECLARATION

I have acquainted myself with the Student Academic Misconduct Policy (SAMP) of the University of the Witwatersrand. I hereby assert that the work I am submitting for assessment is wholly my own. I affirm that I have not engaged in plagiarism, misrepresentation, or collusion with any individual or source. I have duly acknowledged, cited, and referenced all sources utilized in my work. Furthermore, I declare that I have employed artificial intelligence (AI) tools solely as a means of guidance. The ideas and arguments articulated in my work are entirely my original thoughts and interpretations. I recognize that any academic misconduct, such as plagiarism or collusion, will incur serious repercussions. Such repercussions may encompass a diminished grade, a fail mark, or disciplinary measures in accordance with the SAMP. The School of Mining Engineering has my consent to investigate any possible academic misconduct pertaining to my work. This inquiry may involve the use of similarity and AI detection software to assess the originality of my submission. I commit to adhering to the outcomes of any such investigation.



Signature of candidates

19/06/25

Date

ABSTRACT

Mining through water geological fissures can result in a fall of ground and loss of revenue if proper mining and support strategies are not employed. Sound mining practices and good design are recommended to ensure safe and stable excavation. The host rock at Northam Platinum Mine is Norite, with a uniaxial compressive strength of 130 MPa. The host rock is supported with conventional tendon support in the form of 1.8m length, 20mm diameter, full-column resin grouted bolts. Unfortunately, prominent and complex geological water-bearing fissures exist on the eastern and western sides of the shaft, striking North-South (N-S). The structures are associated with closely spaced joints, dykes, shear zones, and water fissures, making it challenging to install conventional tendon support due to friable ground conditions.

The study investigated a geotechnical strategy to develop excavations through these complex structures with arch sets and void fill. Three development sites at Northam Platinum Mine approaching major complex fissures are discussed in detail in this report. The strategy used for water sealing when approaching these structures and increasing tunnel development dimensions to accommodate arch sets and void fill are discussed. Geotechnical analyses using empirical methods were used to designate the characterisation and mechanical properties of the rock mass. Geological core logging and physical mapping of joints, faults, and dykes were conducted on boreholes drilled ahead of mining faces for the three development tunnels. Numerical modelling using Vantage elastic software was used to assess rock wall condition factor (RCF) on tunnels and assist in selecting suitable support units. The support used in the form of steel arches to support these structures and consolidation to enhance the strength of the rock mass is analysed and discussed. Smooth wall blasting limits hanging wall and sidewall damage, whose application requires evaluating and optimising blasting designs and was a focal point of this study. Moreover, other related case studies involving similar conditions, like tunneling under the Himalayas, and running dykes, amongst others, are also dealt with.

ACKNOWLEDGEMENTS

I wish to express my profound gratitude to my supervisor, Professor T.R. Stacey, for his invaluable guidance, unwavering understanding, patience, and encouragement. I am profoundly grateful for his steadfast support and inspiration throughout my research journey. Our discussions have consistently been enlightening, and his enduring interest and contributions to the rock mechanics community are truly commendable. A Special thanks to Northam Platinum Mine for allowing me to conduct the research.

I would also like to convey my deepest appreciation to my beloved family and cherished friends for their unwavering support.

First and foremost, I wish to express my heartfelt gratitude to God, Almighty for serving as a guiding light in every aspect of my existence. To God be the Glory.

.

Table of Contents

DECLARATION i
ABSTRACT ii
ACKNOWLEDGEMENTS iii
TABLE OF CONTENTS iv
LIST OF FIGURES viii
LIST OF TABLES xi
LIST OF ABBREVIATIONS xii
LIST OF SYMBOLS xiii

CHAPTER 1: INTRODUCTION 1

1.1 Introduction 1
1.2 Project Location 2
1.3 Geology of Northam Platinum Mine 2
1.3.1 Regional Setting 2
1.3.2 Local Geology 3
1.3.3 Hydrogeology and Seismicity 5
1.4 Problem Statement 6
1.5 Research Justification 7
1.6 Research Objectives 7
1.7 Research Methods 7
1.7.1 Qualitative Research 8
1.7.2 Quantitative Research 8
1.8 Sources of Data 9
1.9 Research Validation 9
1.10 Structure of the Research Report 9

CHAPTER 2: LITERATURE REVIEW 10

2.1 Introduction 10
2.2 Key Concepts, Theories and Studies 10
2.2.1 Engineering Geological Behaviour of Rock 10
2.2.2 Rock Mass Classification System 17
2.2.2.1 Rock Quality Designation System 18
2.2.2.2 Rock Mass Rating System 19
2.2.2.3 Mining Rock Mass Rating 20

2.2.2.4 Norwegian Q System 23
2.2.2.5 Geological Strength Index 27
2.2.2.6 Rock Mass Classification System Limitations 29
2.2.3 Excavation Support and Design 30
2.2.3.1 Key Theories 30
2.2.3.2 Excavation support ratio 32
2.2.3.3 Stand-up time and unsupported span 32
2.2.3.4 Support system characteristics 35
2.2.4 Influence of Groundwater in Mining 37
2.2.5 Numerical Modelling 39
2.2.6 Blast Design 40
2.2.6.1 Introduction 40
2.2.6.2 Types of Explosives 40
2.2.6.3 Explosives Properties 41
2.2.6.4 Evaluation of explosives characteristics in jointed areas 41
2.2.6.5. Half Cast Factor 42
2.2.6.6 Powder Factor 42
2.2.6.7 Comparison of Explosives 42
2.2.7 Case Studies 44
2.2.8 Summary of Literature Review 56
CHAPTER 3: RESEARCH APPROACH 57
3.1 Introduction 57
3.2 In-Situ Stress Measurements 57
3.3 Rock Tests 59
3.4 Numerical Analysis 60
3.5 Empirical Analysis 61
3.6 Research Design 61
3.7 Tunnel support design methodology (GAP 335) 63
3.8 Data Collection 64
3.9 Data Analysis Approach 65
3.10 Chapter Summary 66

CHAPTER 4: DATA FOR THE STUDY 67
4.1 Introduction 67
4.2 Developing through the Big John Dyke at 14-level Footwall Drive West 67
4.3 Geological core logging for 14W 70
4.4 Developing through the Little John Dyke at 37-splay 16 Drive East 71
4.5 Geological core logging for 16E 74
4.6 Developing through the Little John Dyke at 17 Drive East 75
4.7 Geological core logging for 17E 76
4.8 Chapter Summary 78
CHAPTER 5: ANALYSIS AND FINDINGS 79
5.1 Introduction 79
5.2 Structural analyses using Stereonets at 14 FDW 79
5.3 Rock Mass Classification analyses at 14 FDW 83
5.4 Numerical Modelling using Vantage Software 14 FDW 86
5.5 Structural analysis using Stereonets at 16 FDE 89
5.6 Rock Mass Classification Analyses at 16 FDE 92
5.7 Numerical Modelling using Vantage 16 FDE 95
5.8 Structural analyses using Stereonets at 17 FDE 96
5.9 Rock Mass Classification analyses at 17 FDE 100
5.10 Numerical Modelling using Vantage at 17 FDE 103
5.11 Chapter Summary 104
CHAPTER 6 SUPPORT SYSTEM DESIGN 105
6.1 Introduction 105
6.2 Arch Sets Design 105
6.2.1 Test Procedure of Different Sets 106
6.2.2 Tests Results of Different Arch Sets 109
6.2.3 Support Design Requirements Analyses 114
6.2.4 Conclusion on selection of support 117
6.3 Spiling Bolts 117
6.3.1 Introduction 117
6.3.2 Description 118
6.4 Support Design Conclusion 118

6.5 Mining Methodology 119
6.6 Chapter summary 123
CHAPTER 7: CONCLUSIONS AND RECOMMENDATIONS 124
7.1 Recommendations for Future Research Work 125
REFERENCE LIST 126
APPENDICES 135
Appendix A: Classification of individual parameters used in the Tunneling Quality Index Q 135
Appendix B: Rock Mass System (Bieniawski,1990) 137
Appendix C: Stereographic Plot data for 14 FDW, 16 FDE and 17 FDE haulages 138
Appendix D: UCS test results for done in 2011 139
Appendix E: Determination of Joint Orientation Factor, B, for Stability analyses 140
Appendix F: Rock stress factor A, for stability analysis 141
Appendix G: Determination of gravity adjustment Factor, C, for stability analysis 142
Appendix H: Geological core logging sheet for 14 FDE 143
Appendix I: Geological core logging sheet for 16 FDE 144
Appendix J: Geological core logging sheet for 17 FDW 145

LIST OF FIGURES

Figure 1: Location of Northam Platinum Mine relative to other provinces 2
Figure 2: Regional Map of the Bushveld Igneous Complex.....3
Figure 3: Schematic dip section of the Mine 4
Figure 4: Plan showing Reef Stratigraphy 4
Figure 5: Plan depicting water fissures and pillars.....6
Figure 6: Layered rock with alternating layers of sandstone and siltstone.....12
Figure 7: Alternated layers of sandstone and siltstones of flysch formation 12
Figure 8: Appearance of sheared siltstone flysch in an outcrop 13
Figure 9: Anisotropy due to bedding in sedimentary.....15
Figure 10: Anisotropic texture of gneiss showing alternating layers of mica, Quartz.....15
Figure 11: Orientations of minimum and maximum 16
Figure 12: The General Geological Strength (GSI) chart for jointed rock masses.....28
Figure 13: Rock mass classification based on Q values.....31
Figure 14: Maximum unsupported span vs stand-up time as function of RMR and Q.....33
Figure 15: Maximum unsupported span vs Q 34
Figure 16: Unsupported span as a function of RMR.....34
Figure 17: Unsupported span vs FOS as a function of Q, RMR/MRMR.....35
Figure 18: Geological map of the Himalayas 44
Figure 19: Bamboo piling at tunnel face at failed section 45
Figure 20: Failure of the ribs at the crown portions in THPS 46
Figure 21: Temporary vertical struts for crown settlements control in DKHP.....47
Figure 22: Illustration of the tunnel at Hemsil power plant 50
Figure 23: Illustration of the Tunnsjoedal power plant 50
Figure 24: Collapse at the Hanekleiv in 2006 52
Figure 25: Locality plan of the GZ block bounded by the 6 # Running Dyke 53
Figure 26: Ring sets with timber and void fill and consolidation bolts on the face 54
Figure 27: Spalling as a result of horizontal stresses 58
Figure 28: Diagrammatic representation of joint trends and principal stresses influence 59
Figure 29: Basic process for determining excavation and support measures 62
Figure 30: Indicate critical aspects to consider when designing support in a tunnel.....64
Figure 31: Plan depicting 14 Level Footwall Drive West 68
Figure 32: Borehole 14073 recorded at BL+6+18 for 14 FDW 70
Figure 33: Borehole 14073 recorded at BL+20+30 for 14 71
Figure 34: Plan showing 16 FDE 72
Figure 35: Shows drill borehole no from 16 FDE with shear zones seen on the core 74

Figure 36: Shows drill borehole no from 16 FDE core at BK-6+45 75
Figure 37: Plan depicting 17 levels of East foot wall drive passing through little john dyke...75
Figure 38: Borehole showing steep dipping joints recorded at Borehole 14072.....77
Figure 39: Shallow dipping joints with mechanical drilling break Borehole 77
Figure 40: Scatter plot of poles on an equal area lower hemisphere projection at 14 FDW .80
Figure 41: Rosette plot for 14 FDW depicting dominant joint orientations.....81
Figure 42: Kinematic analyses showing possible wedge failure on the 14-FDW drive west .82
Figure 43: Simulated wedges in the rock mass surrounding the 14 footwall west haulage ..83
Figure 44: Estimated support categories where poor ground conditions are experienced ...84
Figure 45: Unsupported span vs Q/RMR of the 3.8m span haulages 85
Figure 46: Unsupported span as a function of RMR 85
Figure 47: Plan showing 14-FDW haulage traversing Big John Dyke 88
Figure 48: RCF results above 1.4 with UCS values ranging from 60MPa to 130 MPa 88
Figure 49: Scatter plot of poles on an equal area hemisphere at 16 Foot Wall Drive East....89
Figure 50: Shows the Rosette Plot indicating the most dominant joint sets 90
Figure 51: Kinematic Analyses showing possible wedge failure on 16 Footwall Drive East .91
Figure 52: Simulated wedges in the rock mass surrounding the 16 Footwall Drive East 92
Figure 53: Estimated support categories on very poor ground conditions are experienced ..93
Figure 54: Unsupported span vs Q/RMR of the 3.8m span haulages 94
Figure 55: Unsupported span as a function of RMR Q/RMR.....94
Figure 56: Plan depicting 16 FDE and 17 FDE.....95
Figure 57: RCF results for 16 FDE at different strengths.....96
Figure 58: Stereographic plot with poles showing joints at scattered points at 17 FDE.....97
Figure 59: Depicts Rosette plot showing the most dominant joint sets at 17 FDE 98
Figure 60: Kinematic analyses showing possible wedge failure at 17 FDE.....99
Figure 61: Simulated wedges in the rock mass surrounding the 17 Footwall Drive East 100
Figure 62: Estimated support categories on very poor ground conditions.....101
Figure 63: Unsupported span vs Q/RMR of the 3.8m span 102
Figure 64: Unsupported span as a function of RMR 17 East.....102
Figure 65: RCF results for 17 FDE 103
Figure 66: Loading points for D Shaped arch sets, A3T/3 107
Figure 67: Loading points for Arch ring sets, R1T/48 107
Figure 68: Loading points for the Double square arch, S-AC1Y/5.....108
Figure 69: Loading points for the square arch, S-AC1Y/3 108
Figure 70: Load-displacement curve of 5 points, A3Y/3 110
Figure 71: Load-displacement curve for 5 points ring sets, R, 1Y/4 111
Figure 72: Load- displacements for 5 points for square arch, AC1Y/3 112

Figure 73: Load- displacements for 5 points for square arch, S-AC1Y/5.....114
Figure 74: Depicts recorded fall-out thickness in tunnels with normal ground conditions....116
Figure 75: Depicts recorded fall-out thickness for water fissures 116
Figure 76: Schematic view depicting spiling bolts in tunnel 118
Figure 77: Plan showing a five-hole ring cover array 120
Figure 78: Plan showing a nine-hole ring cover array 121

LIST OF TABLES

Table 1: Rock Quality Designation (RQD) 18
Table 2: Rock Mass Classification Table 19
Table 3: Various weighting input parameters in Bieniawski 20
Table 4: MRMR adjusted due to weathering 22
Table 5: MRMR adjusted due to joint orientation 22
Table 6: MRMR adjusted due to blasting effects 22
Table 7: Correlation between Q and Rock Mass Quality 25
Table 8: Excavation category and corresponding ESR values 32
Table 9: ANFO vs Emulsion 43
Table 10: Summary data for RMR,Q and MRMR 78
Table 11: RMR classification system guide for excavation and support in rock tunnels 86
Table 12: Deflection for D-shaped arch set, A 3Y/3 109
Table 13: Deflections for Arch ring set, R1Y/4 110
Table 14: Deflection for Double square arch set, S-AC1Y/3 112
Table 15: Deflection for Double square arch set, S-AC1Y/5 113
Table 16: Similarities with all case studies, including Northam Platinum Mine 122

LIST OF ABBREVIATIONS

ANFO	Ammonium Nitrate Fuel Oil
COP	Code of Practice
CSIR	Council for Scientific & Industrial Research
DKHP	Dordi Khola Hydroelectric Project
ESR	Excavation Support Ratio
FOG	Fall of ground
FOS	Factor of Safety
FDE	Footwall Drive East
FDW	Footwall Drive West
HCF	Half Cast Factor
GSI	Geological Strength Index
IRUP	Iron rich ultramafic pegmatite
IRS	Intact Rock Mass Strength
ISRM	International Society for Rock Mechanics and Rock Engineering
RMR	Rock Mass Rating
RCF	Rockwall Condition Factor
SRF	Stress Reduction Factor
MRMR	Mining Rock Mass Rating
MPa	Mega Pascal
NW	North West
RQD	Rock quality designation
PGM	Platinum Group Metals
PLT	Point Load Test
SE	South East
THPS	Tala Hydroelectric Power Station
TCS	Triaxial Compressive Strength
UCS	Uniaxial Compressive Strength
UCM	Uniaxial Strength Test with Moduli (UCM)
UG2	Upper Group Two Reef

LIST OF SYMBOLS

σc	Uniaxial Compressive Strength (MPa)
σv	Vertical virgin stress (MPa)
σ1	Major principal stress (MPa)
σ2	intermediate principal stress (MPa)
σ3	Minor principal stress (MPa)
ρ	Material Density (kg/m³)
Ɛ	Strain
Is	Point Load Strength Index (MPa)
ɣ	Poisson's Ratio
E	Young's Modulus (GPa)

CHAPTER 1: INTRODUCTION

1.1 Introduction

Mining through complex water-bearing geological fissures poses a significant safety risk to a mining operation's sustainability. Zondereinde Mine, owned by Northam Platinum, is mining through water-bearing fissures with challenges in ground instability when using tendon support. Poor ground conditions near these fissures increase the risk of falls of ground and complicate the implementation of support and stabilisation. Water-bearing structures are contingent upon structural settings, whereas excavation design in rock is contingent upon the geological properties of host rock and orebody geometry (Roland *et al.,* 2016).

Developing tunnels through these water-bearing structures has been historically difficult, leading to abandoned development ends, significant reserve losses, and increased dilution and mining costs. These challenges were also faced by tunneling in the Himalayan region in India (Diwakar *et al.,* 2022).

A case study at a conventional narrow hard-rock platinum mine in the Bushveld Complex examined challenges posed by water-bearing geological structures. The orebody dip runs parallel to the structures traversing the mining lease area. The research examines the application of sound geotechnical planning to safely and efficiently mine through complex geological structures. The research study aims to develop and formalise a geotechnical strategy to support mining through complex water-bearing geological structures while securing the long-term stability of development ends. In doing so, mining operations can quickly access all sections of an orebody without sacrificing safety. Several case studies were evaluated to assist in developing a common strategy for mining through the structures. This chapter summarises the geological settings of the mine, the research objective, and a brief background of the Zondereinde Mine between Northam and Thabazimbi in the Limpopo Province.

1.2 Project Location

Zondereinde Mine is located approximately 30 km from Northam in the Limpopo province, on the western limb of the Bushveld Complex. The Crocodile River runs through the mine from the southern to the northern lease area close to the eastern boundary. The mine is located on the south side of the Amandelbult mine. Figure 1 illustrates the relative location of Zondereinde Mine to Limpopo province.

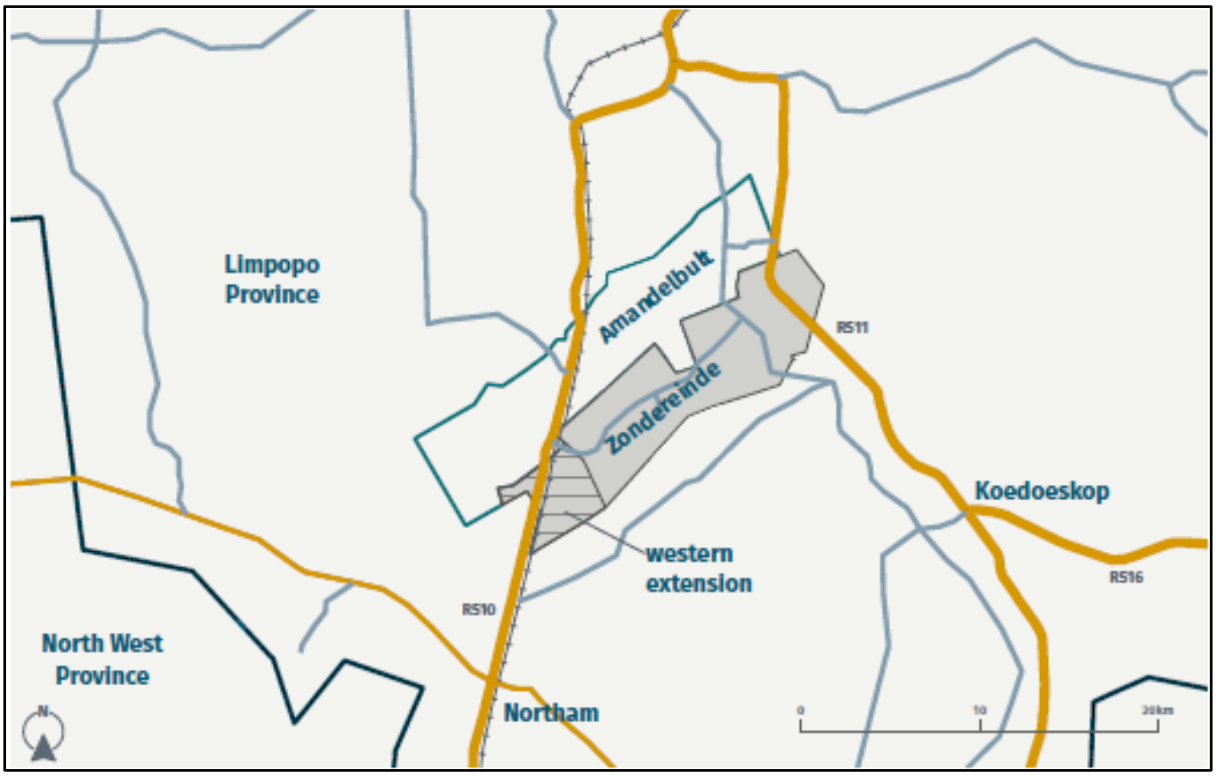


Figure 1 Location of Zondereinde Mine relative to other provinces (Zondereinde Mine COP, 2024)

1.3 Geology of Zondereinde Northam Platinum Mine

1.3.1 Regional Setting

Zondereinde Platinum Mine is at the core of South Africa's Bushveld Igneous Complex. The Bushveld Complex comprises the Rustenburg Layered Suite, the Lebowa Granites, and the Rooiberg Felsic (Figure 2). It is underlain by the Transvaal Super Group rocks and overlain by Karoo sediments. The Rustenburg Layered Suite predominantly comprises mafic igneous rocks and is subdivided into several distinct zones. The marginal zone encircles the periphery of the intrusion, while ascending from the base of the complex are the Lower Zone, the Critical Zone, the Main Zone, and the Upper Zone. The Bushveld Igneous Complex stands as the most extensive layered igneous intrusion within the Earth's crust. The Bushveld complex in South Africa comprises the richest ore bodies, including chromium, platinum, vanadium, and

others. It contains the largest reserves of platinum group metals (PGMs) and platinum group elements (PGEs). Figure 2 depicts the regional geology of the Bushveld Igneous complex.

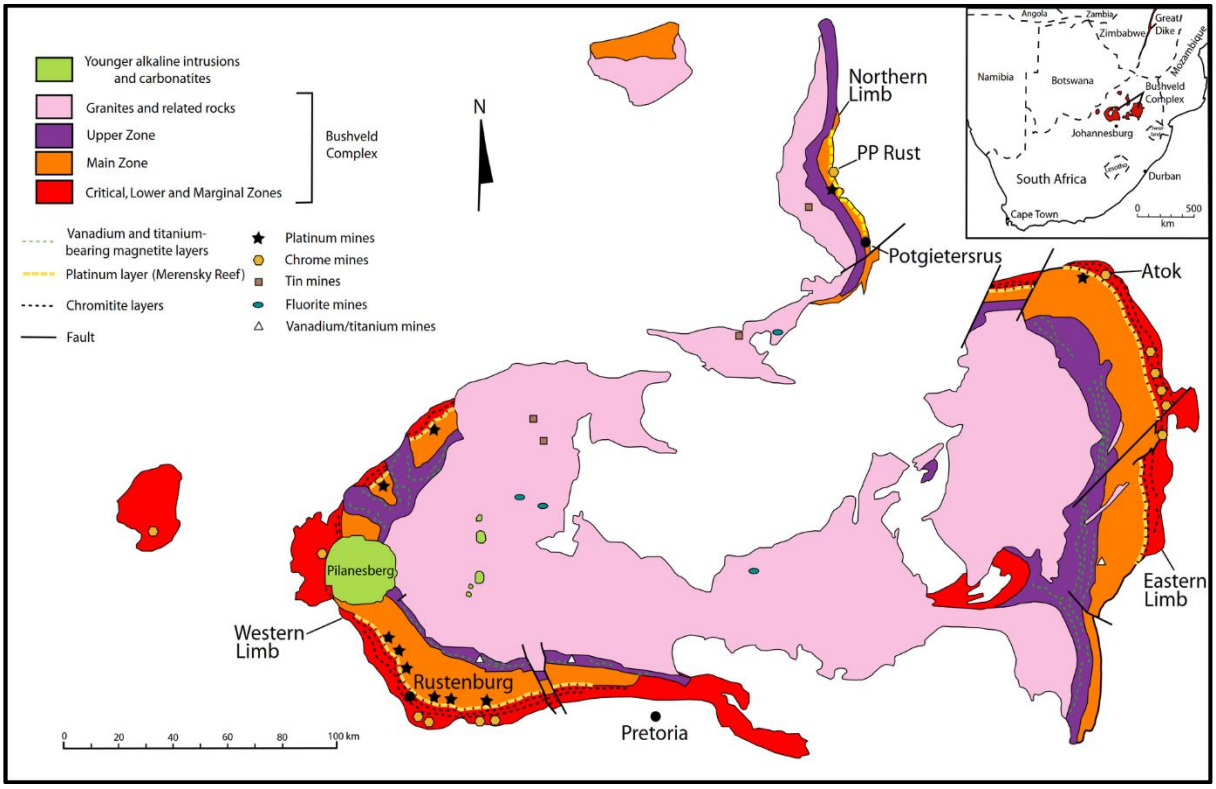


Figure 2: Map of the regional Bushveld Igneous complex (Hunter, 1975)

1.3.2 Local Geology

The stratigraphic sequence comprises the conformable norite, anorthosite, pyroxenite, dunite-harzburgite, and chromite lithologies of the Upper Critical Zone. The two economic orebodies extracted are the Merensky Reef and the UG2 Reef. These deposits are formed due to the crystallisation of platinum-bearing sulfide minerals at discrete intervals. Figure 3 is an illustration of the schematic dip section of the Mine (Zondereinde Mine COP, 2024). The depth of mining varies from 1160 and 2300m below the surface. The Merensky Reef is the primary reef mined, it is mined between 1 Level and 16 Level (1160m to 2240m beneath the surface). The UG2 reef is the secondary reef and is currently being mined between 2 Level and 12 Level (1280m to 1990m below surface).

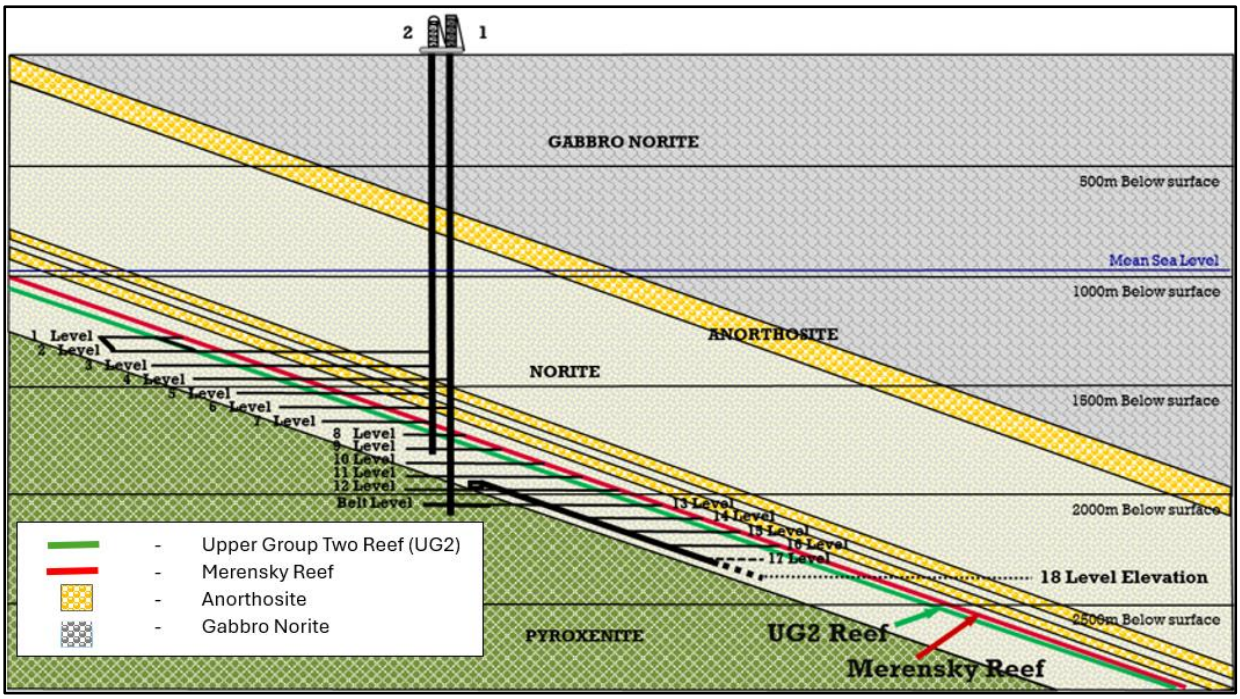


Figure 3: Schematic dip section of the Mine (Zondereinde Mine COP, 2024)

The immediate hanging wall of the UG2 Reef comprises pyroxenite and harzburgite that grades into pyroxenite. Various types of Merensky Reef emerge when the Merensky Reef shifts from its typical position into the underlying strata, creating a steep discordant transition referred to as potholes (Figure 4).

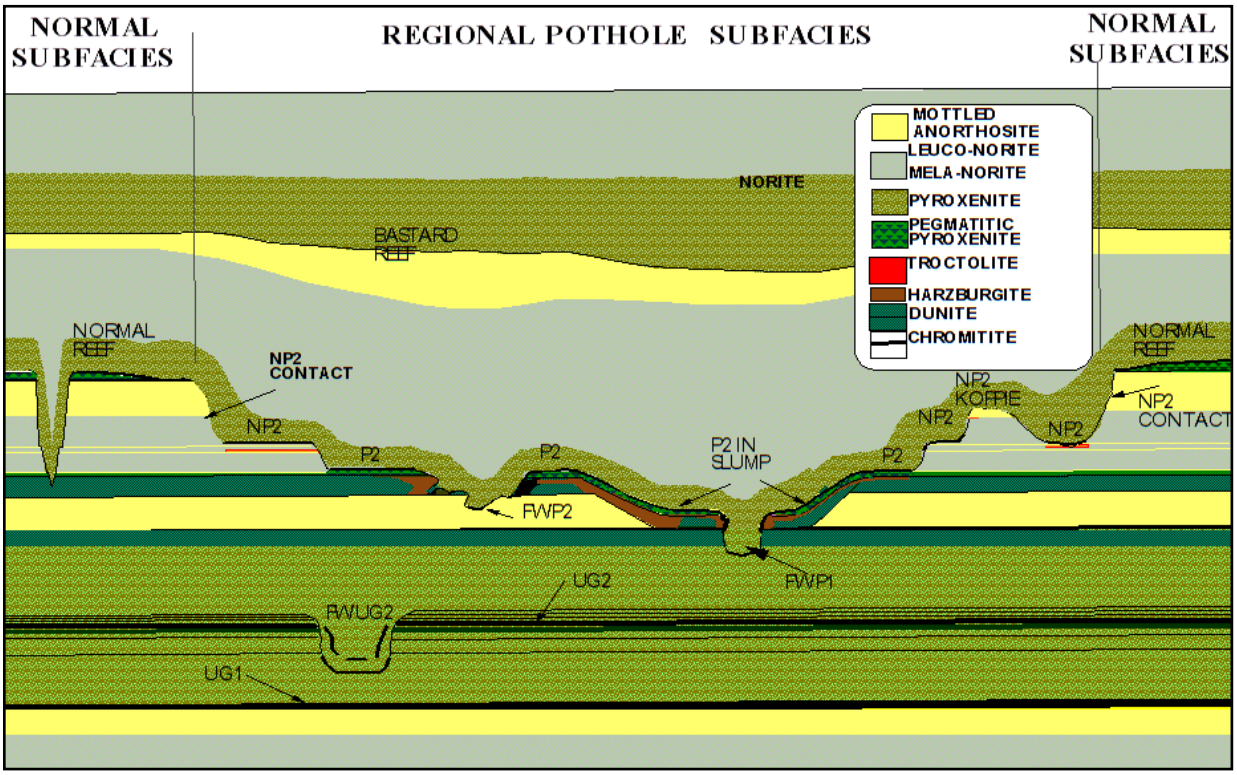


Figure 4: Plan showing Reef Stratigraphy (Zondereinde Mine COP, 2024)

The Merensky hanging wall remains consistent and comprises a fine to medium-grained pegmatitic pyroxenite, ranging from 1m to 3m thick, which grades up into a mela norite and ultimately into norite. The Merensky is overlain by mottled anorthosite and the Bastard Reef pyroxenite unit (Figure 4).

1.3.3 Hydrogeology and Seismicity

The major structures traversing the mining area include faults and dykes, including the Big John Dyke, which is 20m thick and strikes NW-SE, the Murchison Thrust Fault, which has a displacement of approximately 15m, the 21-Line Fissure, the Little John dyke, with shear zones ranging from 75m to 200m, and the 37-line Fault, with shear zones of up to 25m thick (Figure 5).

Surface water drains mainly through tributaries of the Crocodile River and the seasonal Bierspruit dam. The groundwater encountered in the mine is from secondary-type aquifers, with water occurrences restricted to geological discontinuities. Both rechargeable and non-rechargeable aquifers occur in the mine. Pilanesberg orientation structural zones act as the main rechargeable aquifer in the mine's working places. The Big John Dyke, which is 20m in width striking N-S, is a major water-bearing structure. Groundwater pressures of up to 21 MPa can be anticipated at a depth of approximately 780m with density of 2760kg/m^3, contingent upon the mining depth and the hydraulic head (Humphrey, 1910).

At Zondereinde Mine, Non-rechargeable groundwater in mines is commonly associated with iron-rich ultramafic pegmatite (IRUP) intrusions (Zondereinde Mine COP, 2024). These IRUP intrusions are generally harder, stronger (UCS between 153 MPa and 312 MPa), and more brittle than the host rock. Groundwater sources can cause hazardous gases. The groundwater temperature ranges between 43 degrees Celsius at the shallowest levels and 72 degrees Celsius at the deepest levels. The Murchison thrust fault is roughly 15m wide. The 21-line fissure ranges from 75m to 150m thick (Figure 5).

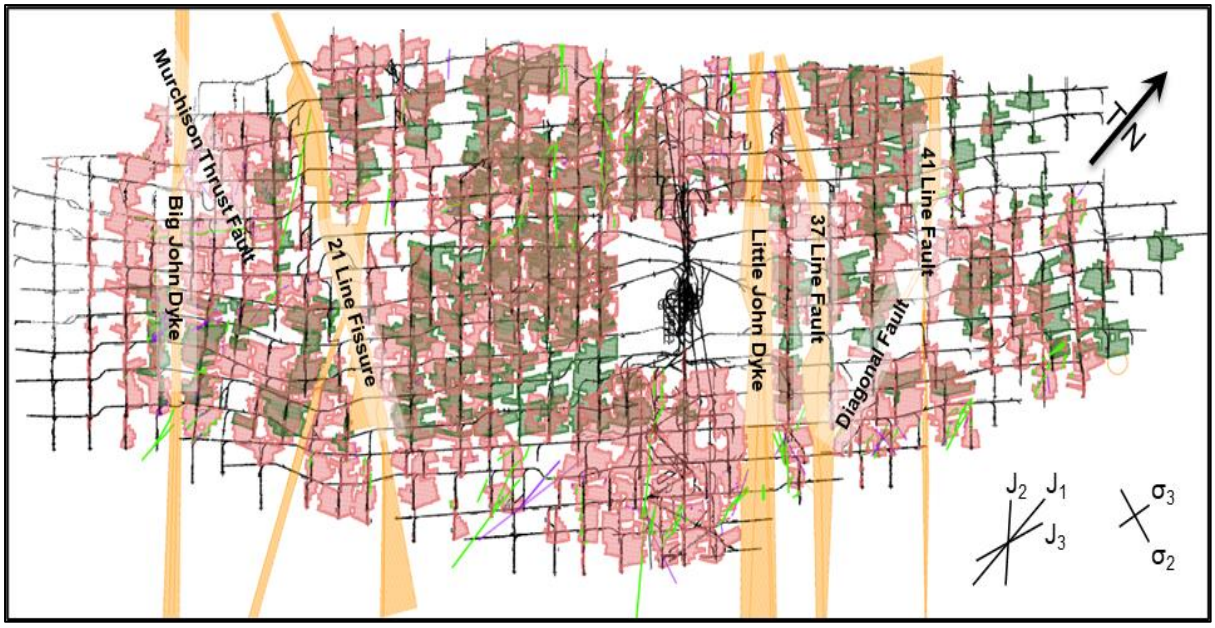


Figure 5: Plan depicts water pillars in orange on major geological structures with Merensky stopes (red) and UG2 stopes (green). (Zondereinde Mine COP, 2024)

Figure 5 illustrates prominent fault zones and dykes in the mine. Displacements of the rock mass along the contacts of the fault zone and dykes were observed. All major faults and dykes intersect both the Merensky and UG2 Reefs. Joint mapping by the CSIR in 1994 revealed that most joints (J1) trend north-south, dipping steeply to the east. Three joint orientations are indicated in Figure 5, along with the orientations of the intermediate (σ2) and minor (σ3) principal stresses. Most of the structures are the major rechargeable water-bearing fissures within the mine. Development through poor ground associated with some major structures is achieved through site-specific strategies.

The mine is classified as seismically active, with damaging seismic events occurring sporadically. Seismicity is generally concentrated at isolated pillars and active mining areas. Seismic events associated with geological features, including water-bearing fissures, did not exhibit a discernible trend and was not deemed a significant consideration in the study.

1.4 Problem Statement

Water-bearing geological fissures create unfavourable ground conditions that complicate mining operations and may result in accidents if not approached with caution. Most of these structures strike NW-SE and range from 25m to 50m thick (Big John Dyke, Little John Dyke, 37 Line Fault, 41-line Fault). These conditions are prevalent at the Zondereinde Northam Platinum Mine and have been causing challenges in ground conditions. The characteristics primarily consist of fault zones that result in displacement. Other formations are delineated by dykes linked to shear zones, creating poor ground conditions. Valuable ore reserves may be

forfeited if these regions succumb to collapse. The excavations will be mined slowly, delaying production targets; however, the scheduling of these excavations is planned.

1.5 Research Justification

The significance of the study is that ground support can be optimised to stabilise mining excavations and deliver value, (Brady & Brown, 2006). The empirical rock classification systems provide context for subdividing rock mass into manageable units. The Q-system provides primary excavation and support design recommendations. Ground support is discussed extensively by (Potvin & Hadjigeorgiou, 2020). Laubscher (1990) developed MRMR, which caters for blasting, stress effects, and joint orientation and is relevant for this study. The study will provide a better understanding of excavation development through water-bearing structures to formalise a mining and support method for efficient ore extraction to support economic viability. It will also improve aspects of support design and add value to the body of knowledge in rock engineering.

1.6 Research Objectives

The following are the objectives of this research

- To geotechnically and structurally characterise the rock mass bounded by water-bearing fissures at Zondereinde Mine by determining the ground types, including the primary stress conditions, the size and shape of the tunnel along with the ground water dynamics, and the orientations of joint sets by using stereographic projection and conducting vantage modelling to evaluate principal stress directions.
- To determine the behaviour of the rock mass induced by water-bearing fissures, identify boundary conditions, requirements, and delineate ground control districts.
- To develop a support strategy for extracting ore through water-bearing fissures and ensure the long-term stability of excavations by determining excavation and support types relevant for the water-bearing fissures.
- To develop an optimal mining strategy, including blasting and support design to mine through water-bearing fissures.
- To study and evaluate different case studies to assess similar conditions to support the proposed methods and recommendations on the Zondereinde Platinum Mine.

1.7 Research Methods

The research will be undertaken as an explorative case study and address questions regarding what, how, and why based on a detailed exploration of cases. This report employs both qualitative and quantitative methodologies. The quantitative research approach includes

data analysis, which includes statistical analyses such as fall of ground database and other numeric theories. The qualitative analyses include case studies on mining through complex fissures.

1.7.1 Qualitative Research

Moser and Korstjens (2017) elucidate that qualitative research is a mode of inquiry that reveals and offers profound insights into real-world challenges. In contrast to the collection of numerical data points characteristic of quantitative research, qualitative research aids in formulating hypotheses that facilitate the examination and comprehension of quantitative data. It delves into the underlying mechanisms and motivations rather than merely quantifying amounts. For this study, primary data was gathered through visual observations, including the identification of structural orientation, dip and dip directions, strike direction, and significant geological features such as faults, dykes, shear zones, and extensively jointed rock masses. Secondary data from existing literature reviews on complex geological features and related case studies were analysed. The literature further established a correlation between rock mass classification and both empirical and numerical modeling to evaluate and analyse tunnel mining through water-bearing fissures.

1.7.2 Quantitative Research

Bhandari (2020) elucidates that quantitative research entails the systematic collection and analysis of numerical data. This methodology can be employed to determine averages, discern patterns, and formulate predictions. It rigorously examines fundamental phenomena and extrapolates findings to broader populations. Quantitative research is distinctively different from qualitative research, which emphasises the gathering and analysis of non-numerical data. Empirical methodologies encompass Bieniawski's RMR (Bieniawski, 1989), Barton's Q system (NGI, 2022), and Laubscher's rock mass classification system MRMR (Laubscher, 1990). DIPS software was used to process the joint data and determine joint patterns. Numerical analyses were conducted using Vantage 3D elastic modelling software from IMS (Institute of Mine Seismology). Data collection encompasses geological information, including rock types and geological features, as well as the stress regime of the region. The gathered data include sets of discontinuities along with their orientations, spacing, and conditions, in addition to the presence of groundwater. Fall of ground database, including fall out-thickness was analysed. The collected numbers are presented in figures and tables.

1.8 Sources of data

The following data sets were obtained from Northam Platinum to support the main case studies.

1. Survey Data, including mining directions of haulages.
2. Underground observations on three development sites.
3. Geology: lithological units Stratigraphy, Weathering, Structural faulting.
4. Geotechnical data from laboratory and core logging: Rock Quality Designation (RQD), rock strength, Domains.
5. Structures, including Fissures, fractures, faults, Dykes, Joints.
6. A review of common case studies is a source of data to support the research.

1.9 Research validation

The rock mass around the water-bearing fissures is based on the RQD factor, which is insufficient to inform rock mass classification and characterisation schemes alone to derive support recommendations. There lies an opportunity to improve rock mass characterisation utilising industry-leading empirical systems. The rigour involved is sufficient for both academic and industrial applications.

1.10 Structure of the Report

Chapter 1 serves as an introductory, elucidating this report's main aim and justifications. Chapter 2 explores the literature pertinent to this research, investigating the fundamental theories relevant to mining within the heterogeneous rock mass. Additionally, it discusses some published studies where mining through complex fissures with groundwater and shear zones was encountered; Furthermore, this chapter examines foundational literature on rock mass classifications, numerical modelling, and blast design, incorporating several case studies. Chapter 3 covers the research approach, which focuses on data collection and where empirical designs will be developed and used to designate the quality of the rock mass and assist in choosing suitable support for water-bearing fissures at Zondereinde Northam Platinum Mine. Chapter 4 briefly discusses the data for the study. Chapter 5 is the analysis and findings, where the three haulages passing through water-bearing fissures are assessed and analysed. Chapter 6 discusses support design, where support requirements and choice are discussed in detail. Chapter 7 reviews all chapters, recommendations, and conclusions, highlights contributions to achieving research objectives, and emphasizes critical findings, future research, and their implications.

CHAPTER 2: LITERATURE REVIEW

2.1 Introduction

Sahu *et al.* (2020) state that the literature review describes the research issue's theoretical perspective and previous findings. According to Miglianico *et al.* (2020), most studies rely on published literature to either substantiate or challenge any expected research findings. The objective of the literature review is to discern existing gaps and circumvent the redundancy of previously established knowledge by comprehending what is already understood about the topic (Alvesson & Spicer, 2019). These authors contend that undertaking a literature review enhances one's grasp of the subject matter.

This chapter briefly discusses the fundamental theories related to mining through complex fissures, including the behaviour of the rock mass in heterogeneity, the theory behind the rock mass classification system, the effect of groundwater, excavations, and support principles, and the theory behind numerical modelling to assess principal stresses on tunnels. Blasting methods to limit damage in the rock walls are also briefly discussed. Several case studies of tunnels in other countries mined in geologically disturbed ground, including Northam Platinum and mining through the Himalayan mountains in India, are briefly discussed. The first aspect discussed is the key concepts and theories on the subjects.

2.2 Key Concepts, Theories and Studies

According to Kahraman *et al.* (2016), it is common for underground mining operations to develop through geological features. It is an inherent characteristic or function of underground mining that cannot be circumvented entirely or avoided. Geological features can range from typical faulting and jointing to more complex ‘running dykes’ and seismically active structures (Du Preez *et al*., 2018). Jha (2022) explained that humid conditions and groundwater contact with fault gouge can initiate tunnel collapse. The following theories related to the literature review are discussed below.

2.2.1 Engineering Geological Behaviour of Rock

Spaun & Nickmann (2006) explain that an assumed knowledge of rock behaviour is more often the basis for estimating rock properties than determining rock properties in laboratory tests. Rock behaviour is intricately linked to petro-physical properties, such as ultrasonic P-wave velocity, electric resistivity, magnetic susceptibility, density, magnetic remanence, mechanical properties, such as uniaxial compressive strength (UCS), tensile and shear strength, and elastic properties such as Young’s modulus and Poisson’s ratio (Askaripour *et al*., 2022).

The rock mass is defined as the entirety of the in-situ medium, encompassing the bedding planes, faults, joints, folds, and other structural features (Brady & Brown, 2006). A rock mass is typically characterised by considerable heterogeneity, exhibiting a variety of contrasting rock types; thus, it is not considered a homogeneous medium (Askaripour *et al*., 2022). This resonates with the study at Northam Platinum, where mining through water-bearing fissures comprises heterogeneous rocks due to different rock materials contained in the Big John Dyke, Little John dyke, and 37-line fissure. It is, thus, crucial to understand the influence of rock's texture on its geomechanical behaviour. Askaripour, *et al*. (2022) stated that a rock has heterogeneous and anisotropic engineering properties, a single type of rock can exhibit a variety of textural properties, including differences in mineral composition, grain size, shape, and orientation.

Heterogeneous layered rocks and their behaviour

Saroglou (2013) emphasises that heterogeneous layered rocks can be defined as formations comprising a minimum of two lithological units, each exhibiting distinct engineering behaviours and properties. Boggs Jr, (2009) states that this rock type displays a structure characterised by alternating layers of resilient and more fragile rocks of varying thicknesses, typically of sedimentary origin, as illustrated in Figure 6. Mizens and Maslow (2015) mention that Flysch and Molasse serve as quintessential examples of such rocks. They are distinguished by rhythmic variations of sandstone interspersed with pelitic rocks, including siltstones, marls, shales, and clay shales, as illustrated in Figure 7.



Figure 6: Layered rock with alternating layers of sandstone and siltstone in equal proportions (Boggs Jr, 2009)



Figure 7: Alternated layers of sandstones and siltstones of flysch formation (Mizens & Maslov, 2015)

Marinos and Hoek (2001) assert that obtaining a sample of "intact" core for uniaxial compressive testing in the laboratory poses significant challenges when dealing with heterogeneous rock types, such as flysch. Figure 8 depicts the characteristic appearance of such material in an outcrop. Bedding and schistosity planes, along with joints, exemplify the discontinuities typically found in nearly all samples extracted from rock masses, as illustrated in Figure 8 (Marinos & Hoek, 2001).



Figure 8: Appearance of sheared siltstone flysch in an outcrop (Marinos & Hoek, 2001)

As a result, any strength value obtained from laboratory testing on core samples will be less than the uniaxial compressive strength σc needed to be included in the Hoek-Brown criteria. According to Marinos & Hoek, 2001, including the findings of such tests would result in an unreasonably low value for the rock mass strength and a twofold penalty on the strength (in addition to the one imposed by GSI).

Renshaw *et al*. (2003) introduced an analytical model to examine the stresses within a series of horizontal layers exhibiting alternating elastic properties. Their findings affirm that elastically heterogeneous layering induces tensile stresses in the more rigid layers. The authors concluded that the heterogeneity among elastic layers may play a significant role in the formation of joints within layered sedimentary rocks.

A good example to illustrate the complexity of geology is described by Bouzeran *et al*. (2019) in terms of heterogeneous and buckling mechanisms on excavation performance at

Westwood Mine, Quebec, Canada. The relevance of this case presents the application of knowledge derived from the understanding of geology and its influence on stope and haulage performance. Knowledge of geotechnical properties of geological fissures ahead of development faces will assist in proper design in mining through water fissures at Northam Platinum Mine as experienced in this case study.

There are Several other tunneling case studies on the Himalayan region in India. Mauriya *et al*. (2010), suggest that complex and heterogeneous geology and inadequate site investigation are the main underlying challenges to project completion, stable excavation, poor safety, and cost overruns. The study's results revealed a lack of sound geotechnical investigation to support comprehension of rock mass behaviour. The main features in the complexity of geology were folds, thrust and shear zones, rock cover and in-situ stresses, water-bearing structures, and geothermal gradients (Mauriya *et al*., 2010). The Himalayan region environment suggests geological complexity like those found at Northam Platinum Mine, characterised by the challenges of mining through water-bearing fissures and poor ground conditions. The Big John Dyke, Little John Dyke and 37-line fissure, traversing the three development haulages at Northam contain/compose of amphibole, plagioclase, phenocrysts, microcrysts and Fe-To oxides which reflect heterogeneity.

Anisotropic rocks and their behaviour

According to Saroglou (2013), metamorphic rocks such as phyllites, schists, shales, and gneisses, along with slates, exhibit anisotropic behaviour attributed to the presence of foliation planes, including schistosity and banding. Özbek *et al*. (2018) suggest that marbles may also display a low degree of anisotropy, although their behaviour is predominantly isotropic. Anisotropy is frequently observed in sedimentary rocks such as siltstones, claystones, and mudstones. As noted by Matsukura *et al*. (2002), anisotropy in igneous rocks can arise due to flow structures, as seen in rhyolites.

In heterogeneous rock formations, such as flysch or molasses, characterised by thin layers of siltstone and sandstone, anisotropy arises from the orientation of these layers in relation to the principal loading axis (Saroglou, 2013). Anisotropy may be either intrinsic, resulting from the alignment of rock-forming crystals within the unaltered rock—an aspect that cannot be disregarded in laboratory samples—or structural, stemming from the emergence of inherent anisotropy on a macroscopic scale. Figure 9, exemplifies structural anisotropy in sedimentary rocks, attributed to the presence of bedding planes. Figure 10 illustrates inherent anisotropy, evidenced by the alignment of crystals at the microscopic level (Saroglou, 2013). Earlier investigations conducted by Attewell and Sandford (1974) on anisotropic rocks have demonstrated that the anisotropy curve for both uniaxial and triaxial compressive strength is

distinctive of the principal types of anisotropy. This finding is corroborated by subsequent research by Behrestaghi *et al*. (1996). Most anisotropic rocks display a U-shaped strength anisotropy curve.



Figure 9: Anisotropy due to bedding in sedimentary rock, *(Saroglou, 2013)*

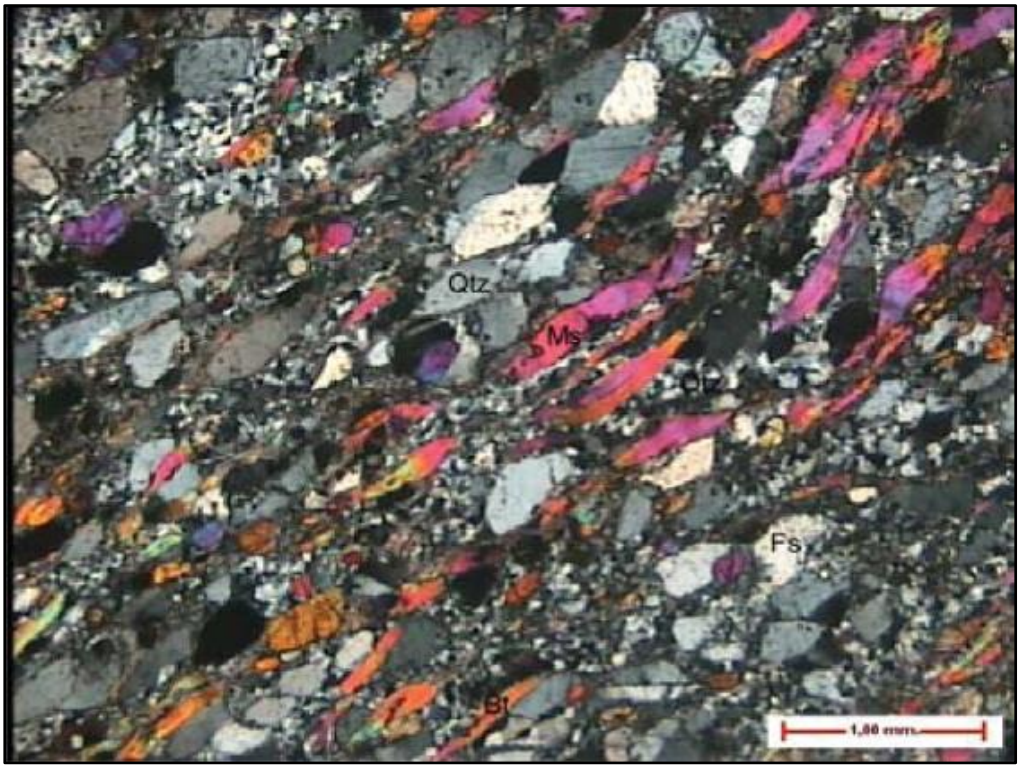


Figure 10: Anisotropic texture of gneiss showing alternating layers of Mica (Ms) , Quartz (Qtz) and Feldspar (Saraglou, 2013)

Ramamurthy (1993) classified anisotropy into three categories based on the shape of the uniaxial strength anisotropy curve, which illustrates the variation of σc with loading orientation, β (as depicted in Fig. 11). A U-type, characterised by a minimum strength at an orientation of β = 30° and a maximum when loading is perpendicular to the anisotropy plane. 2. Shoulder type, where strength attains its zenith when loading is parallel to the anisotropy plane and remains nearly constant until the loading angle approaches β = 90°. The orientation between β = 15° and 30° is where the minimum strength is observed. 3. Anisotropic behaviour may arise from the presence of multiple anisotropy planes within the rock, exhibiting an undulating configuration (Saroglou, 2013).

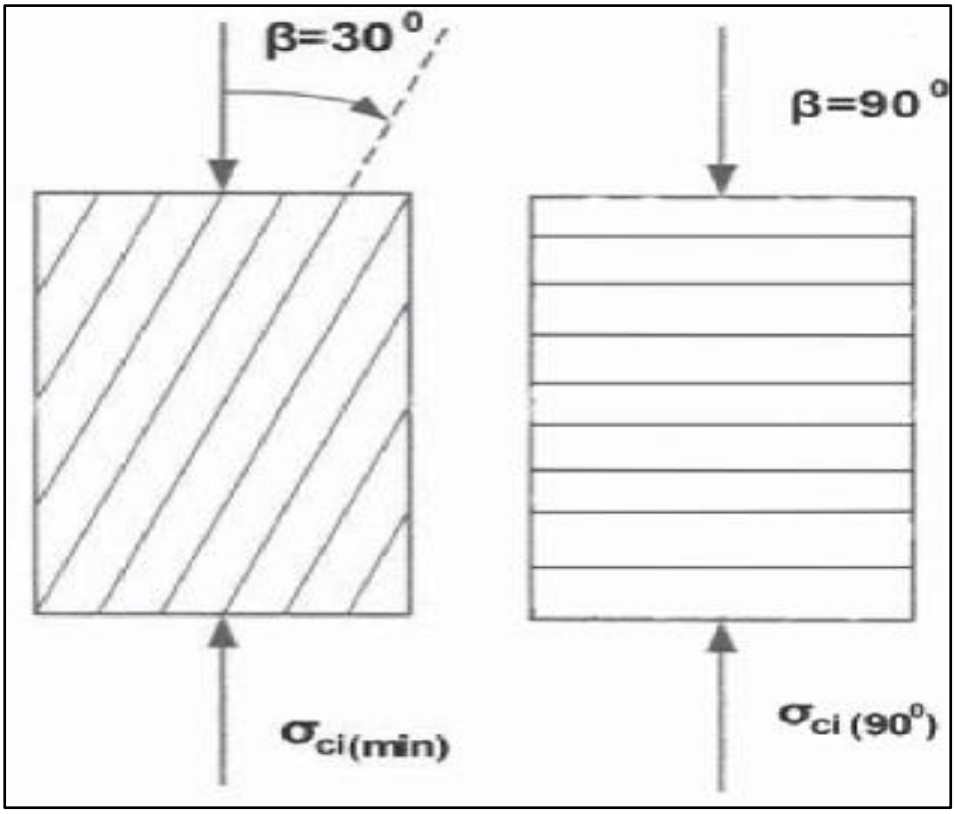


Figure 11: Orientations of minimum and maximum (Saraglou, 2013)

The following should be ascertained to understand how transversely isotropic rocks behave: −Strength and deformation modulus at primary loading directions, - Failure criteria parameters at the lowest strength orientation and perpendicular to the anisotropy planes; −Triaxial strength anisotropy curve and the impact of confining pressure on anisotropy.

Vitali et al. (2021) assert that the behaviour of tunnels within anisotropic rock masses is exceedingly intricate, contingent upon the alignment of the tunnel axis in relation to the principal geostatic stress directions and the structural planes of the rock. Numerical modelling using a 3D boundary element method is conducted. The 2D representation cannot capture the effects of such complex scenarios. The modelling of anisotropic behaviour is complex

since the tunnels are not parallel to the boundaries. The situation may become progressively more complex if the principal far-field stresses are not aligned with the principal axes of material anisotropy. This research presents a novel methodology for applying boundary conditions and far-field stresses to three-dimensional numerical models of tunnels subjected to comprehensive ground and loading conditions. This innovative approach facilitates the simulation of any tunnel orientation in relation to the principal directions of stress and material anisotropy.

According to Marinos *et al*. (2018), geology and in-situ rockmass characteristics dictate tunnels' behaviour. Further geological classification systems cannot be over-relied on without augmenting advanced site investigation methods. The case study was done in Serbia, and results were obtained using laboratory-tested mechanical properties and rock mass characterisations to analyse and classify the ground conditions. The design of suitable support for stable excavations comes after different rock mass classifications with the understanding of the tunnel failure mechanism.

Due to complex geological conditions, the anticipated ground conditions at Zondereinde Northam Platinum Mine comprise heterogeneous and anisotropic rock types. Water-bearing fissures are predominantly associated with faults, dykes, and jointing. At Zondereinde Northam8 Mine, different dykes are encountered, including Big John Dyke, Little John Dyke, and 37 Line fault fissures which comprise anisotropic types of rocks.

2.2.2 Rock Mass Classification Systems

Rock Mass Classification is the systematic process of categorising rock masses and assigning a distinctive identifier based on analogous properties, enabling the prediction of the rock mass's behaviour (Bieniawski, 1989). This methodology will be employed at Northam Platinum Mine, where three development tunnels navigate through water-bearing fissures to comprehend the behaviour and conditions of the rock mass, thus determining appropriate support. Various rock mass systems are delineated below. The classification of rock masses encompasses the Barton Q system, initially conceived by Barton *et al*. (1974) and subsequently revised by (NGI, 2022), the Rock Mass Rating (RMR) (Bieniawski, 1989), the Mining Rock Mass Rating (MRMR) (Laubscher, 2000), the Geological Strength Index (GSI) (Hoek *et al*., 1995), and the Rock Quality Designation (RQD) (Deere & Deere, 1988). These methodologies serve to evaluate rock mass quality and support requirements (Hoek & Brown, 1980). According to Moss and Kaiser (2022), rock mass classifications are instrumental in establishing Rock Mass Quality (RMQ), yet standard support selection charts may not be applicable when anticipated support capacity consumption arises. For years, the mining industry has depended on empirical rock support design systems. Support design

methodologies that excessively rely on rock mass classification systems no longer yield robust mine designs for the industry. While these classification systems are valuable for characterising rock masses, they fail to facilitate the development of efficient and effective support systems (Moss & Kaiser, 2022). It is suggested that rock mass classification systems be employed in conjunction with numerical modelling to achieve precise outcomes.

2.2.2.1 Rock Quality Designation System

Developed by Deere in 1963, the Rock Quality Designation (RQD) serves as a quantitative metric for assessing the quality of rock masses derived from borehole cores. The RQD is calculated by summing the lengths of core pieces exceeding 10 cm and dividing this total by the overall length of the core. Prior research has indicated that RQD does not provide a dependable measure of rock mass quality when joint spacings approach 10 cm, as it results in an RQD of 100%, categorizing the rock mass as of the highest quality. The subsequent formula delineates RQD:

$$RQD = \sum \frac{length\ of\ core > 100mm}{total\ length\ of\ core}\ x\ 100\% \qquad [1]$$

Higher RQD values indicate good ground conditions and lower RQD values show poor ground conditions (Table 1).

Table 1: The RQD values and volumetric jointing (Deere, 1963)

1 RQD (Rock Quality Designation)			**RQD**
A	Very poor	(> 27 joints per m³)	0-25
B	Poor	(20-27 joints per m³)	25-50
C	Fair	(13-19 joints per m³)	50-75
D	Good	(8-12 joints per m³)	75-90
E	Excellent	(0-7 joints per m³)	90-100
Note: i) Where RQD is reported or measured as ≤ 10 (including 0) the value 10 is used to evaluate the Q-value ii) RQD-intervals of 5, i.e., 100,95,90, etc., are sufficiently accurate			

The RQD can also be determined by the frequency of joints or discontinuities per unit volume (Jv) on the rock surface, as outlined in Equation 2 (Palmstrom, 1982). The RQD was modified

by (Palmstrom, 2005) where no geological core is available, and the formula is given in equations 2 and 3:

$$\mathrm{RQD} = 115 - 3.3\,\mathrm{Jv} \quad [2]$$

Where $Jv = \frac{1}{J1}\ x\ \frac{1}{J2}\ x\ \frac{1}{J3}$ [3]

where J1, J2, and J3 are the average spacing of joints.

The RQD calculated from three development tunnels mining through fissures are, 45-60% at 14 footwall drive west indicating poor to fair ground conditions, 38-48% at 16 Footwall Drive East indicating poor ground conditions and 40-50% at 17 Footwall Drive East showing poor ground conditions. The RQD is included as one of the parameters to calculate the MRMR.

2.2.2.2 Rock Mass Rating System

The Geomechanics classification system, widely referred to as Rock Mass Rating (RMR), was devised by Bieniawski between 1972 and 1973 to assess tunnel stability and support requirements (Bieniawski & Lowson, 2013). Over the years, this system has undergone refinement through numerous case studies. The RMR system serves as a numerical classification (ranging from 0 to 100) of rock mass, which has been meticulously reviewed and enhanced (Bieniawski, 1989). It encompasses five essential parameters (Bieniawski, 1989). The parameters employed, as highlighted, include:

1: Uniaxial compressive strength (UCS) of the rock material.
2: Rock Quality Designation (RQD).
3: Spacing of discontinuities.
4: Condition of discontinuities.
5: Groundwater conditions.

The RMR value is established by selecting the relevant ratings for the parameters from the table and summing them. Bieniawski classified the rock mass into five classes, as illustrated in Table 2.

Table 2: RMR classification table (Bieniawski, 1989)

Class	RMR (Rock Mass Rating)	Class
I	81-100	Very good rock
II	61-80	Good rock
III	41-60	Fair rock
IV	21-40	Poor rock
V	<21	Very poor rock

The advantages of Bieniawski's (1989) RMR are:

- Determines joint condition in conjunction with spacing.
- Commonly and widely applied.

The disadvantages of Bieniawski's (1989) RMR are:

- It is designed for civil engineering.
- It ignores the influence of weathering when newly exposed rock is present.
- Disregards the impact of mining stresses on the stability of excavations.
- The roughness and modifications of the joints are regarded independently.

The average RMR rating calculated from all three development haulages was 36, indicating poor ground conditions. The reliable rating to determine ground conditions on water fissures is MRMR, discussed below, which accounts for the influence of blasting, induced stresses, joint orientation, and weathering.

2.2.2.3 Mining Rock Mass Rating (MRMR)

Laubscher (1990) introduced a methodology for evaluating rock masses in mining contexts. The MRMR is derived by aggregating four key parameters: Intact Rock Strength (IRS), Rock Quality Designation (RQD), joint condition, and groundwater, along with Joint Spacing (JS). Stacey and Swart (2001) noted that the MRMR framework incorporates the same parameters as the Geomechanics system, yet it combines groundwater and joint conditions, culminating in a concise set of four parameters. The MRMR system is more adept at facilitating accurate stability assessments. The latest update was discussed by (Jakubec & Laubscher, 2000), and introduces the influence of mining disturbances on in-situ stresses. This method is appropriate for the Northam case study as it accounts for the effects of blasting, joint orientations, weathering, and stress.

Table 3: Various weighting input parameters in Bieniawski's (1989) and Laubscher's RMR (1990)

Laubscher's MRMR Input parameters	**Maximum MRMR Rating**	**Bieniawski's RMR Input parameters**	**Maximum RMR rating**
Intact Rock Strength (UCS)	20	Intact Rock Strength (UCS)	15
RQD	15	RQD	20
Joint spacing	25	Joint spacing	20
Joint condition and Groundwater	40	Joint condition Groundwater	30 15

The MRMR can be determined using the following equation:

MRMR = IRS + RQD + spacing + condition

In which:

MRMR = Laubschers Mining Rock Mass Rating

IRS = Intact Rock Strength

RQD = Rock Quality Designation

Spacing = spacing of discontinuities

Condition = condition of discontinuities

MRMR = RMR * adjustment factors

Adjustment factors encompass weathering, joint orientation, mining-induced stresses, and the repercussions of blasting (Laubscher, 1990).

Laubscher (1990) further observed an additional parameter crucial for the design of support systems intended for mining applications: design rock mass strength (DRMS).

The DRMS represents the rock mass strength modified according to four parameters: weathering, mining-induced stresses, joint orientation, and the repercussions of blasting. Rock mass strength (RMS) is characterized by the intrinsic rock strength (IRS) and the rock mass rating (RMR). The IRS is determined through mechanical tests conducted on diminutive specimens and is subsequently reduced by eighty percent.

$$RMS = \frac{(A-B)}{80}\ x\ C\ x \frac{80}{100} \qquad [4]$$

Where: A = Total RMR rating,

B = IRS rating and

C = IRS in MPa.

The MRMR, RMR, and DRMS can be adapted to many different functions for rock masses. The factors of adjustments are clearly shown in the Table 4. In the study area, on all three haulages at Northam Platinum Mine, the extent of weathering, even after four years of mining, is moderate due to water and gases. Therefore, the adjustment is taken as 90%, as shown in the Table 5.

Table 4: Adjustments to MRMR due to weathering (Stacey & Swart, 2001)

The pace of weathering and modifications (%)					
Description of the extent of weathering	**6 months**	**1 year**	**2 years**	**3 years**	**4+ years**
Fresh	100	100	100	100	100
Slightly	80	90	92	94	96
Moderately	82	84	86	88	90
Highly	70	72	74	76	78
Completely	54	56	58	60	62
Residual soil	30	32	34	36	38

The modifications in the case study area of the Zondereinde Northam Platinum Mine at three haulages was taken as 85% as four Joints defined the excavations, and two faces faced away from the vertical, as shown in Table 5.

Table 5: Adjustment to MRMR due to joint orientation (Stacey & Swart, 2001)

The quantity of joints that delineate the block	**Adjustments (%) Number of faces tilted away from the vertical**				
	70	75	80	85	90
3	3	-	2	-	-
4	4	3	-	2	-
5	6	4	3	2	1
6	6	5	4	3	2 or 1

The mines studied employ conventional drill and blasting methods. The RMR was amended by 94% to account for the blasting effects within the study area; shot advances with smooth wall blasting, and emulsion explosives are advised in these areas.

Table 6: Adjusted to MRMR due to blasting effects (Stacey & Swart, 2001)

Excavation Technique	Adjustment (%)
Boring	100
Smooth wall blasting	97
Good conventional blasting	94
Poor blasting	80

The MRMR for the area of interest concerning the haulages, with an initial calculated RMR of 36, averages 32. Following adjustments of 90% for weathering, 85% for joint orientation, 120% for mining-induced stresses, and 94% for blasting effects, the revised MRMR is.

Adjusted MRMR = 36 x 0.9 x 0.85 x 1.2 x 0.94 = 32

The advantages of MRMR are:

- It examines the ramifications of blasting.
- It recognises the effects of joint orientation and weathering on rock surfaces.
- It is meticulously crafted for mining applications and is devoid of any limitations on maximum span.
- It provides guidelines for suitable support.

The disadvantages of MRMR are:

- An advanced comprehension of the system and rock mechanics is crucial for precisely evaluating the effect of joint orientation and induced stresses.
- It suggests that water solely influences joint conditions, a notion that is not necessarily accurate, particularly in soft rock formations.
- It was conceived in accordance with the caving mining system, and the majority of the case studies were conducted within this environment.

Most Platinum Mines use rock mass rating and a Q system to evaluate rock behaviour. This case study at Zondereinde Northam Platinum Mine requires MRMR which accommodates the influence of blasting, stress fractures, joint orientations due to the highly jointed rock mass, and weathering due to different rock types, water, and gases on water fissures traversed.

2.2.2.4 Norwegian Q-System

The Q rating serves as an indicator of the stability of rock masses surrounding underground openings within jointed rock formations. This system was initially established by Barton *et al.* in 1974 and has since undergone revisions, the most recent being by NGI in 2022. Elevated Q-values signify robust stability, whereas diminished values suggest inadequate stability. The Q system is employed in the mining and tunneling sectors to evaluate the rock mass's potential and to devise optimal support structures, as noted by NGI in 2022. The foundational work by Barton *et al*. (1974) demonstrated that the Q value could be derived using the equation presented in Equation 5. The subsequent research conducted by NGI in 2022 revealed that the Q value can alternatively be calculated using Equation 6. In this equation, a normalisation factor is incorporated for a modified Qc, reflecting the significance of the intact rock's unconfined compressive strength (UCS), as elucidated by Barton in 2002 and Rehman *et al*.

in 2018. Additionally, Barton in 2002 indicates that Equation 7 may also be utilised to estimate the unconfined compressive strength of the rock mass ($\sigma c\mathrm{m}$). Barton *et al*. (1974) provides more details on the origin of the Q rating, and the latest update is found in (NGI, 2022).

$$\mathrm{Q} = \frac{\mathrm{RQD}}{\mathrm{Jn}} \mathrm{x} \frac{\mathrm{Jr}}{\mathrm{Ja}} \mathrm{x} \frac{\mathrm{Jw}}{\mathrm{SRF}} \quad [5]$$

$$\mathrm{Qc} = \frac{\mathrm{RQD}}{\mathrm{Jn}} \mathrm{x} \frac{\mathrm{Jr}}{\mathrm{Ja}} \mathrm{x} \frac{\mathrm{Jw}}{\mathrm{SRF}} \mathrm{x} \frac{\sigma \mathrm{c}}{100} \quad \text{or} \quad \mathrm{Qc} = \mathrm{Q} \mathrm{x} \frac{\sigma \mathrm{c}}{100} \quad [6]$$

$$\sigma \mathrm{cm} = 5 \rho \mathrm{Q}^{\frac{1}{3}} \quad [7]$$

Where:

RQD is the Rock Quality Designation

Jn is the Joint set number (the number of discontinuity sets)

Jr is the Joint roughness number (the degree of alteration or weathering of the discontinuity surfaces)

Ja is Joint alteration number (the degree of alteration or weathering of the discontinuity surfaces);

Jw is the Joint water reduction factor (groundwater inflow)

SRF is the stress reduction factor

The stress reduction factor can be calculated using the formulas below:

ρ is the rock density measured in kg/m³

σcm is the uniaxial compressive strength of the rock mass.

σc is the uniaxial compressive strength of intact rock measured in MPa, and the value of σc is its rating in equation 6;

$$SRFq = \left(\frac{RQD}{Jn}\right) x \left(\frac{Jr}{Ja}\right) x \left(\frac{Jw}{Q}\right) \quad [8]$$

$$SRFqc = \left(\frac{RQD}{Jn}\right) x \left(\frac{Jr}{Ja}\right) x \frac{Jw}{Qc} x \frac{\sigma c}{100} \quad [9]$$

NGI, (2022) illustrates that wall support can also be achieved by adjusting the Q value, as demonstrated in the equations.

$$\text{For } Q > 10 \qquad Qwall = 5Q \qquad [10]$$

$$\text{For } 0.1 < Q < 10 \qquad Qwall = 2.5Q \qquad [11]$$

$$\text{For } Q < 0.1 \qquad Qwall = Q \qquad [12]$$

Swart and Handley, (2005) pointed out that the advantages of Q systems are:

- Considers the impact of mining-induced stresses on excavations stability.
- Can be utilised to assess the deformability of rock.
- Widely recognised and extensively acknowledged.
- The roughness and alteration of joints are considered separately.

Swart and Handley, (2005) pointed out that the disadvantages of Q systems are:

- Generally regarded as more pertinent in tunnelling.
- It does not consider the aspects of joint separation and continuity.

Table 7: Correlation between Q and rock mass quality (Barton & Grimstad, 1994)

Q	**Class**
0.001-0.01	Exceptionally poor
0.01-1	Extremely poor
1-4	Poor
4-10	Fair
10-40	Good
40-100	Very good
100-400	Extremely good
400-1000	Excellently good

The Q rating calculated at Zondereinde Northam Platinum Mine for the three development haulages mining through Little John Dyke, Big John Dyke, and 37 Line fissure ranges between 0.3-0.4, indicating extremely poor ground conditions. In this study the MRMR is the proper system to be used to classify ground conditions as stated above due to its relevance to ground conditions mined at three development haulages mining through water fissures.

Watson (2004) evaluated fourteen rock mass rating systems; among these classification systems, four were deemed pertinent for assessing slope stability in the Bushveld Platinum Mines. These conclusions align with an evaluation conducted by Swart *et al*. (2005) regarding the chrome mines in the Bushveld Complex. The systems are categorised as follows:

- The Geomechanics Classification, also known as the Rock Mass Rating (RMR) system, was pioneered by Bieniawski (1989).
- The rock quality index (Q) system, established by the Norwegian Geotechnical Institute, was formulated by Barton (1974) and collaborators.
- The Mining Rock Mass Classification, or Modified Rock Mass Rating (MRMR) system, was introduced by Laubscher (1990).
- The Modified Stability Graph method, utilising the Modified Stability Number (N'), was initially developed by Mathews and associates in 1981 and subsequently refined by Potvin (1988).

Watson (2004) discovered that the N' system consistently correlates with observed ground conditions and reduces personal interpretation.

The stability number N'' can be defined as follows

N'' = Q x A x B x C [13]

Where:

$$Q = \frac{RQD}{Jn}\ x \frac{Jr}{Ja}\ x\ \frac{Jw}{SRF}$$

A = is the rock stress factor

B = A modified Matthew's factor for joint orientation.

C = A modified Matthew's factor for the influences of sliding and gravity

The graphs for B and C are listed on Appendix (E-G).

This system served as a foundation for the development of the New Modified Stability Graph Method (N''), particularly within the platinum industry (Watson, 2004). The N'' method was utilised in rock mass rating analysis, culminating in the compilation of a database encompassing assessed stable, unstable, and collapsed sites within the UG2 Reef of the Bushveld Complex. Comprehensive statistical analyses were conducted on the amassed data to ascertain the significance of each parameter. This system can be integrated with other methodologies to enhance the precision of rock mass quality assessments.

2.2.2.5 Geological Strength Index (GSI)

The Geological Strength Index was established by Hoek (1994). This index is extensively utilised to assess the strength reduction from intact rock to the rock mass. Carter and Marinos (2000) demonstrated that the GSI system can effectively characterise rock masses, enabling the determination of input data pertaining to the properties that influence the mechanical behaviour of these masses.

Figure 12 presents the GSI chart for jointed rock masses.

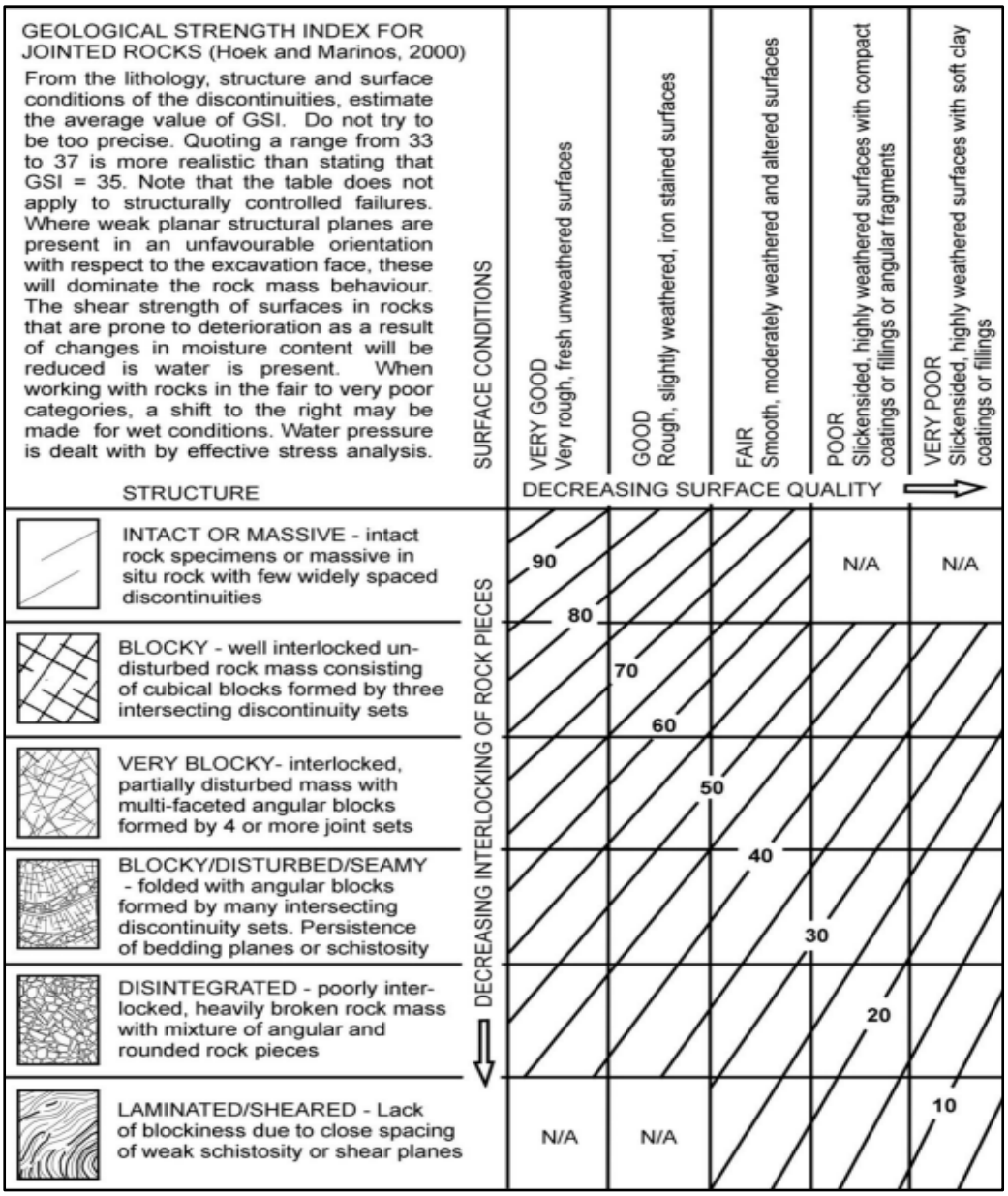


Figure 12: Present the General Geological Strength Index (GSI) chart for jointed rock masses derived from the geological observations *(*Marinos *et al.,* 2000*)*.

The GSI classification system has been devised to satisfy the demand for dependable input data regarding the properties of rock masses, which is essential for numerical analyses in the design of tunnels and slopes, while also providing a comprehensive geological characterisation of the rock mass.The GSI on all three development haulages/Tunnels (14 west, 16 east, and 17 east) mining at Northam Platinum is low, indicating very poor ground conditions on all three development haulages. The tunnels/haulages are bounded by at least 4 or more joint sets.

Correlation between RMR, Q and Geological Strength Index (GSI)

The correlation between Barton's rock mass quality index Q, Bieniawski's rock mass rating RMR, and GSI was examined following the case studies conducted by Bieniawski in 1984.

This included case studies in the United States, South Africa, and Scandinavia.

Brady (2005) observed that the correlation between rock mass rating (RMR) and Q rating is expressed by the following formula:

$$RMR = 9 \ln Q + 44 \quad [14]$$

Hoek *et al*. (1995) Suggested that GSI in relation to RMR is given by the following formula 15. After further research, Hoek et al. (2013) proposed another formula 16 as cited by (Somodi, 2021).

$$GSI = \mathrm{RMR}_{89} - 5 \text{ for } \mathrm{RMR}_{89} > 23 \quad [15]$$

$$GSI = 0.5\, RQD + 1.5\, Jc \quad [16]$$

Jc refers to the joint wall condition as delineated by Bieniawski (1989), while RQD signifies the rock quality designation.

2.2.2.6 Rock Mass Classification Limitations

Potvin *et al*. (2012) assert that the application of rock mass classification or characterisation necessitates a degree of interpretation, accompanied by inherent uncertainties in the methodologies employed. The deficiencies of rock mass classification methods lie in their inadequacy to accurately represent the intricate nature of geological formations. Hadjigeorgiou and Harrison (2011) suggest that uncertainties are associated with rock mass classification systems, highlighting criticisms regarding the limitations of RQD estimation in relation to fracture intensity. Such systems cannot function in isolation. The Geotechnical Strength Index (GSI) tool, likewise, is inappropriate as a standalone instrument for tunnel design, as it presupposes a homogeneous rock mass and therefore lacks universal applicability (Marinos *et al*., 2007). The approach to rock mass classification is fundamentally grounded in a compilation of experience-based site data for the interpretation of rock mass behavior (Mikula & Lee, 2007). Palmstrom and Broch (2006) contend that the use of rock mass classifications in isolation reveals significant limitations in addressing the necessity for permanent support and in predicting the behavior of rock masses under poor ground conditions. The Q and RMR values do not represent factual data concerning the engineering geology of the rock mass (Pells & Bertuzzi, 2007). The Q system inadequately considers critical factors such as joint

orientations, joint continuity, joint aperture, and rock strength. In the Northam case study, the rock mass rating system, specifically the Q system, fails to account for the effects of blasting, whereas the MRMR does take such effects into consideration.

2.2.3 Excavations Support and Design

2.2.3.1 Key Theories

Excavation support and design are critical to ensuring the stability of excavations. This theory covers the support systems and design of excavations. This theory of support and excavation design will be used for the current study at Zondereinde Northam Platinum Mine, where three development tunnels are mining through water-bearing fissures. Brady & Brown (2006) discussed support systems in underground mines. According to Potvin and Hadjigeorgiou, (2015), ground support stabilises underground excavations. Developing an excavation in rocks using blasting methods results in deformation and displacement due to energy impact on structures. The behaviour of rock mass and the potential failure mechanism are essential in selecting a support system. Kaiser *et al*. (2000) assert that two primary scenarios arise when undertaking underground construction in hard rock: 1) structurally controlled, gravity-driven failures, and 2) stress-induced failures manifesting as spalling and slabbing. The former occurs predominantly under conditions of low radial and tangential stresses, while the latter becomes significant when elevated tangential stresses precipitate the failure of the rock mass (Kaiser *et al*., 2000).The three haulages mining through water fissures at Zondereinde Northam Platinum Mine are structurally controlled due to complex geological features. According to Potvin and Hadjigeorgiou (2015), a significant challenge confronting underground hard rock mines lies in the engineering design of ground support systems. This complexity is particularly pronounced during the pre-feasibility and feasibility phases, where access to geomechanical data is often constrained. Rock mass classification systems frequently represent the sole methodologies available for estimating the properties of large-scale rock masses. Potvin and Hadjigeorgiou (2015) further assert that these classification systems are essential components of empirical design, effectively categorizing areas with analogous geomechanical attributes. They offer valuable guidelines concerning excavation stability and facilitate the selection of reinforcement and support mechanisms. Moreover, they delineate in-situ rock mass properties that serve as crucial input parameters for numerical models. In the mining sector, the Q classification system proposed by Barton *et al*. (1974) and the rock mass rating (RMR) developed by Bieniawski (1976) underpin numerous empirical design methodologies.

According to Yilmaz (2023),underground excavations,i.e. openings with different dimensions are developed either by conventional drill and blast or mechanically excavated.

The behaviour of rock masses and potential failure mechanisms is crucial in the selection of an appropriate support system. Potvin and Hadjigeorgiou (2015) and Laubscher and Taylor, (1976) attribute the widespread adoption of the RMR and Q systems to their advantageous application in various extensively utilised empirical designs relevant to caving mines and open stope mining operations. According to Barton and Grimstad (1994), the support recommendations for the majority of underground mines in Australia and Canada are predicated on the Norwegian Method of Tunneling. Distinct ground conditions, geological contexts, and rock mass characteristics are categorised using the Q rating system, wherein the rock mass rating dictates the appropriate support. In this study, the MRMR serves as a reliable instrument for evaluating the quality of the rock and determining the requisite support, as it accounts for the effects of blasting, the orientation of joints, and weathering influences. Figure 13 below demonstrates the relationship between the Q rating and the span divided by the excavation support ratio.

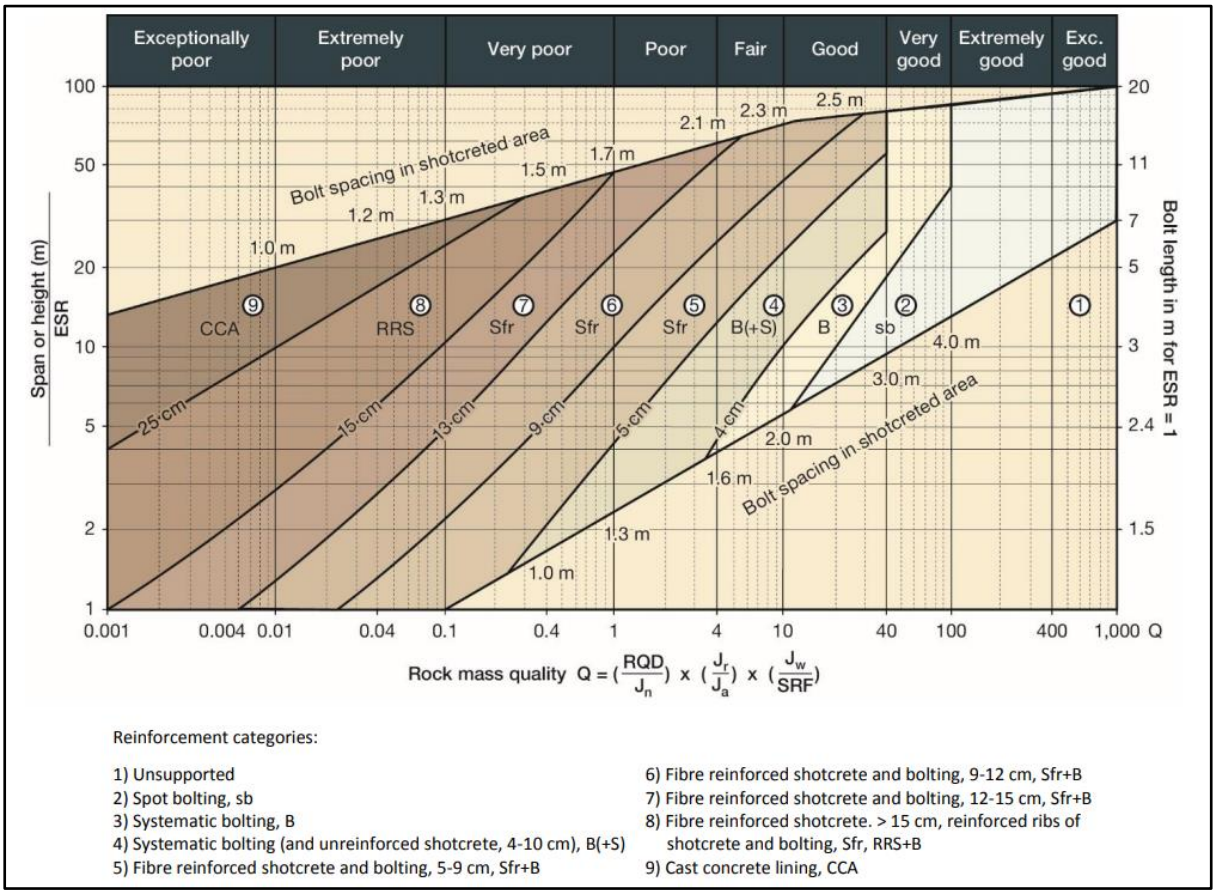


Figure 13: Rock mass classification – permanent support recommendation based on Q. (Barton & Grimstad, 1994)

2.2.3.2 Excavation Support Ratio

The study conducted by NGI in 2022 introduced an additional parameter known as the Equivalent Dimension (De) of the excavation, which correlates the Q value to the stability and support requirements of underground excavations. To compute De, one divides the span, diameter, or wall height of the excavation by the Excavation Support Ratio (ESR). The value of ESR pertains to the intended purpose of the excavation and the level of security required by the support system implemented to uphold the excavation's stability (see Table 8). At Zondereinde Northam Platinum Mine, the access tunnels serve as permanent haulages, with an excavation support ratio of 1.3. The resultant De was charted against the Q value to determine the various categories of support.

Table 8: Excavation category and corresponding ESR values (Barton *et al*., 1974)

	Excavation category	**ESR**
A	Temporary openings	3-5
B	Permanent mine entrances, water conduits for hydropower, exploration tunnels, drifts, and the headings of substantial excavations	1.6
C	Storage facilities, water treatment plants, minor roadway and railway tunnels, surge chambers, and access passages	1.3
D	Power stations, significant roadways and railway tunnels, civil defense shelters, and portal intersections.	1.0
E	Underground-nuclear power plants, railway stations, sports and public venues, and manufacturing facilities	0.8

2.2.3.3 Stand Up Time and Unsupported Span

Drilling and blasting are employed when excavating tunnels or stopes, which require an excavation to remain stable and unsupported for a particular time after the blast, after which the support can be installed. It is of paramount importance to determine the length of time that an excavation can remain unsupported and stable for mine logistics and safety purposes. It usually takes 3-4 hours or half a shift to clean the blasted ore from the development face and prepare the face support. Rehman et al. (2018) explain that when the rock mass is excavated and remains unsupported for an extended duration, it can precipitate instabilities, potentially culminating in the failure and collapse of the excavation. For this reason, it is critical to

determine the stand-up time for all the underground excavations. The maximum stable unsupported span is determined using the following chart (Figures 14, 15 & and 16).

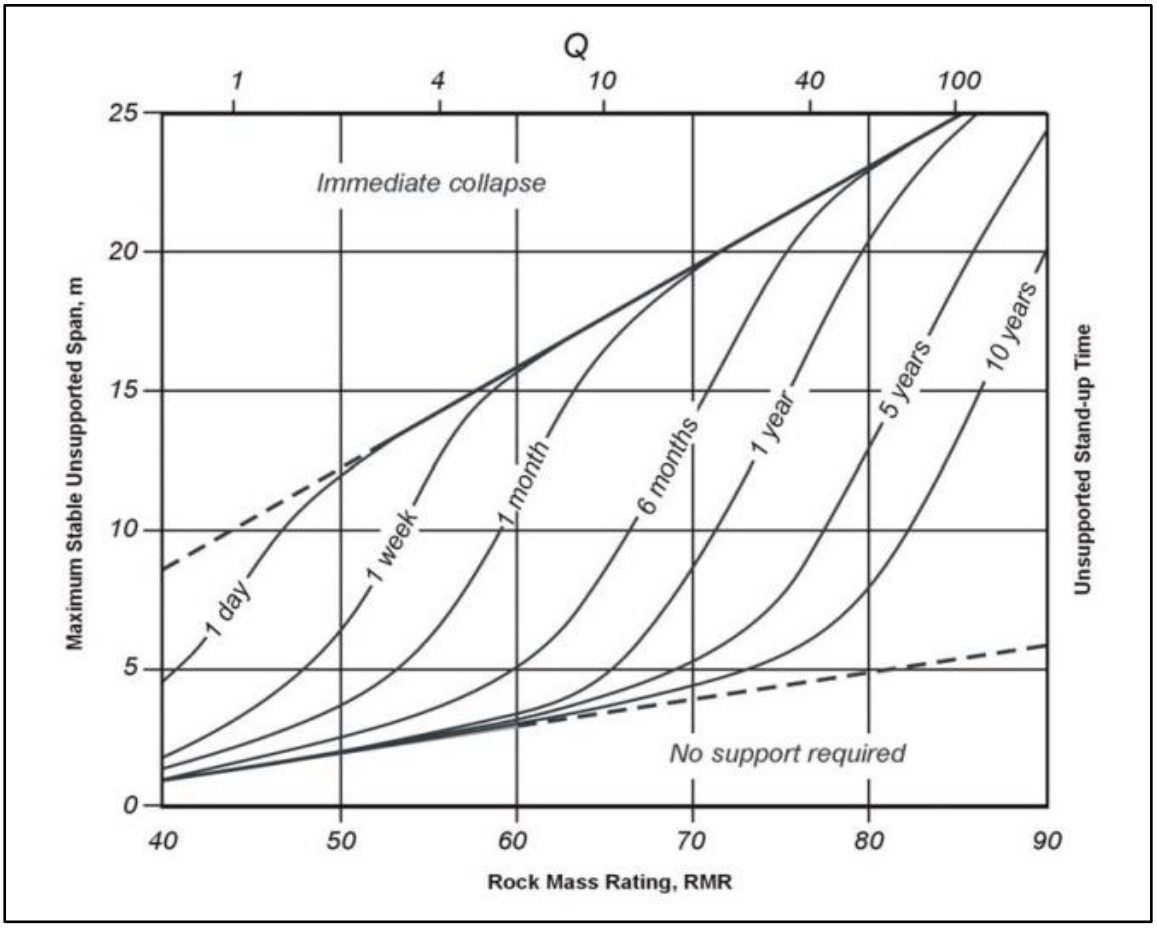


Figure 14: Maximum unsupported span vs stand-up time as a function of RMR and Q (Stacey, 2001)

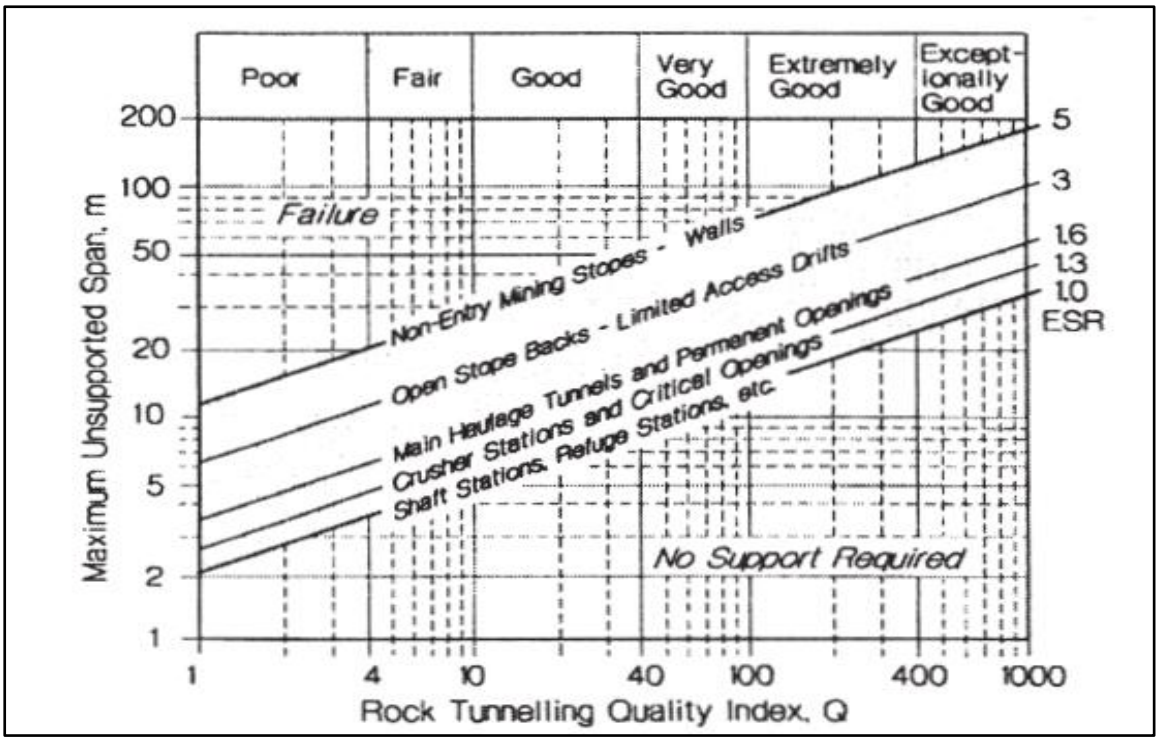


Figure 15: Maximum unsupported span vs Q (Barton *et al*., 1974)

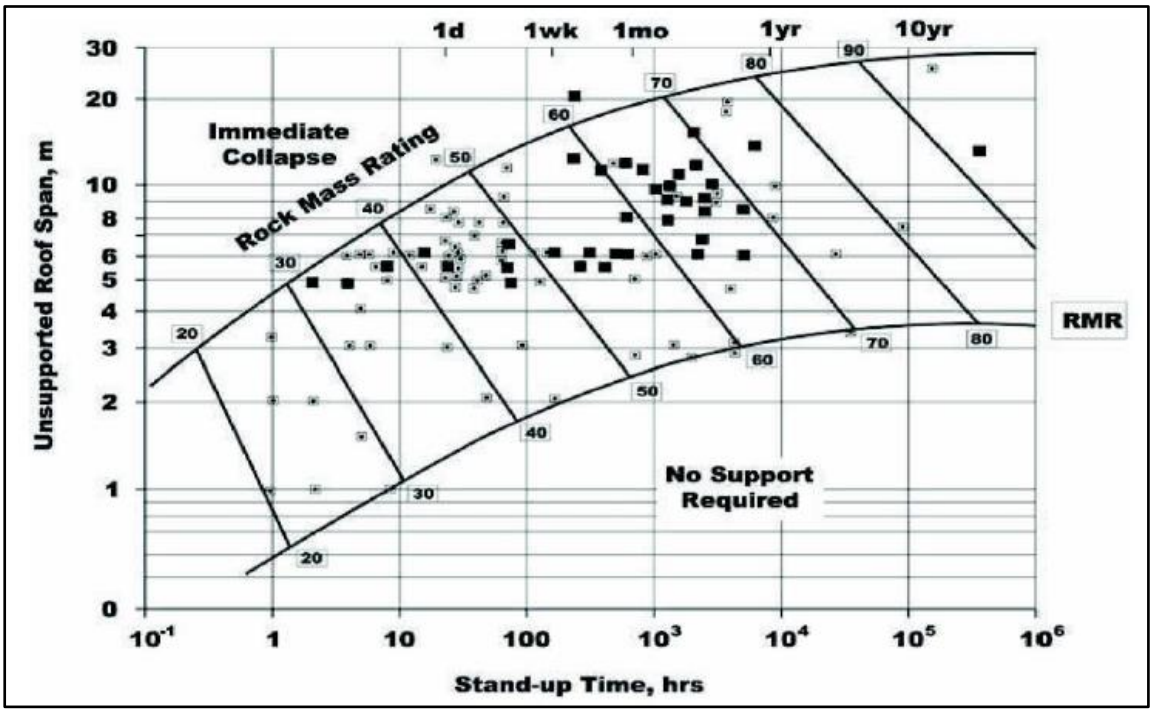


Figure 16: Unsupported span as a function of RMR (Bieniawski & Lowson, 2013)

The recommended safety factor for tunnels according to industry best practice is 1.5. FOS can be determined by plotting the Q or RMR/MRMR value against the unsupported span (Figure 17).

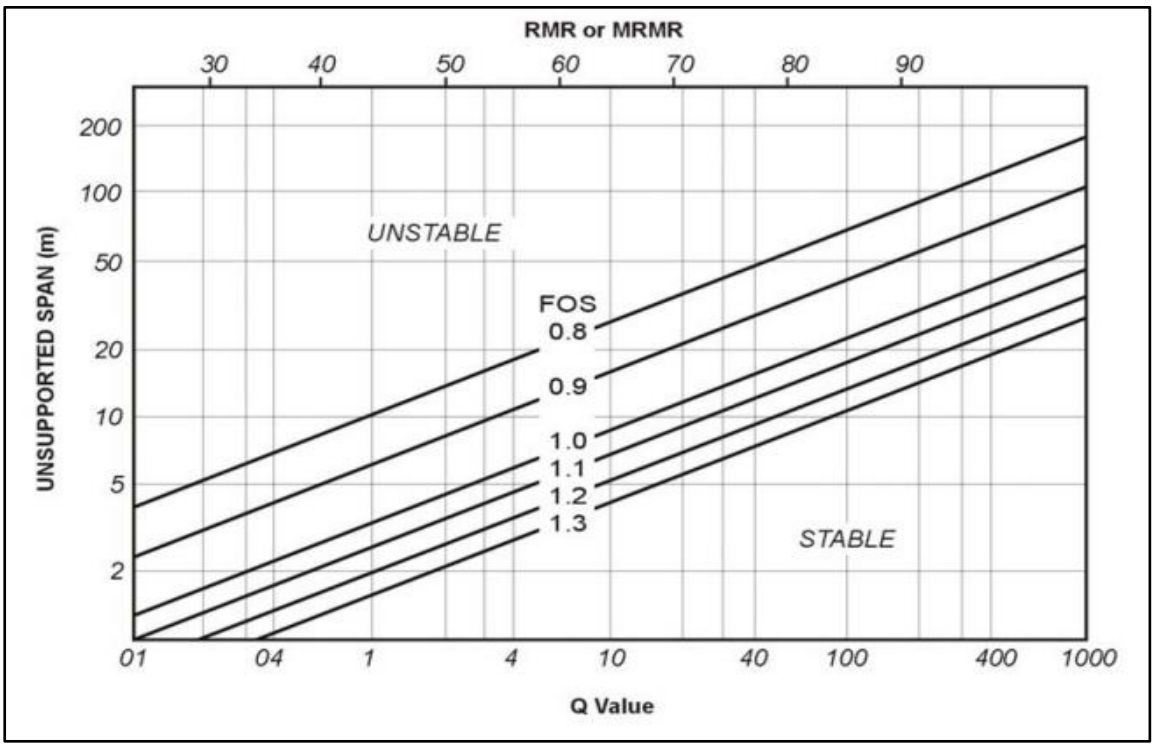


Figure 17: Unsupported span vs FOS as a function of RMR, MRMR/Q (Stacey, 2001)

2.2.3.4 Support System Characteristics

The support units can be classified as active or passive support. Active support types apply forces immediately resisting rock mass deformation, and passive support requires deformation to take place before the support system can generate resistive loads (Jager & Ryder, 1999).

Key support characteristics are summarised below.

Initial Stiffness

The initial stiffness refers to the rate at which a load is manifested within the support system as a result of the deformation of the rigid mass. Examples of support with high initial stiffness are grouted bars and cables, pre-tensioned rock bolts, and shotcrete. Low initial stiffness systems include steel arch sets, mesh, and lacing areal coverage support.

Energy Absorption and Yieldability

A yieldable support system is essential where rock mass deformation is anticipated due to a high-stress environment, particularly in the presence of significant stress fluctuations, or dynamic conditions. These units can withstand in high seismic areas and include cable anchors that can accommodate large deformations.

Length of Tendon

The length of the tendon will dictate the degree of interaction within the rock mass. It Is essential for the tendon's length to be adequate to accommodate the depth of the instability while ensuring sufficient anchorage throughout that depth. In the event where the depth of the rock mass instability is greater than the length of the tendon, then the length of the tendon should be evaluated based on the creation of the reinforced rock mass shell of adequate shape and dimension.

Spacing of Tendons

The spacing of the tendons within a support system can influence their loading contingent upon their interaction with the rock mass. Under static loading conditions, the loading of the support system may be expressed in relation to the necessary support resistance requirements. Under dynamic loading, this is expressed as the energy absorption requirements of the support system. In highly discontinuous rock mass, the spacing of the tendons will influence the degree of any areal coverage support between the tendons.

Areal Coverage

To maintain the overall integrity of the excavation, the unstable rock mass between the tendons needs to be confined by an aerial type of support system. Requirements for area coverage depend on the stability of the rock mass between tendons and differ between static and dynamic conditions. As the rock mass becomes more discontinuous, the direct interaction between the tendon and the rock mass is reduced. The capacity and load deformation criteria for the areal coverage support will be dictated by the loading conditions of the rock mass, the degree of instability between tendons, and the permissible deformation limits of the excavation rockwalls.

Conclusion Regarding Application to Zondereinde Northam Platinum Mine on Rock Mass Classification and Excavation Support Design

Most Platinum mines use rock mass rating and a Q system to evaluate rock behaviour. The case study at Zondereinde Northam Platinum Mine requires MRMR due to the effects of blasting on haulages, which can lead to stress fractures, joint orientations resulting from the highly jointed rock mass, and weathering caused by different rock types, water, and gases. The adjusted MRMR (Mining Rock mass rating) for the water fissures at three sites averaged 32 as calculated above, depicting poor ground conditions. The MRMR factor influences the selection of excavation design and support. The unsupported span and RMR/MRMR relationship were also discussed in detail. The support system characteristics were also looked at, assessing all the critical factors when designing the support system.

2.2.4 Influence of Groundwater in Mining

Groundwater has an adverse impact on the underground environment by weakening the rock mass. This topic covers several case studies where the rock mass is influenced by groundwater. These are pertinent to the Zondereinde Northam Platinum Mine, as there three development haulages mining through water fissures contain water. Nguyen *et al*. (2021) elucidated the impact of rising groundwater levels on the geomechanically changes occurring within the jointed rock mass surrounding tunnel support structures. The study concludes that groundwater levels in the underground haulage affect the rock mass instability and the supporting structure behaviour. In a similar vein, Rahimi *et al*. (2020) assert that the instability of rock masses stems from geotechnical structural imperfections within the rocks, as well as from static and dynamic loading conditions resulting from stress concentration, seismic occurrences, released energy, drilling and blasting activities, gravitational forces, groundwater influences, and temperature variations. Park *et al*. (2004) indicate that Numerical modelling using software such as UDEC numerical modelling can assist in predicting the mechanical behaviour of the rock mass and the support. Groundwater can cause a change in the water pressure, which can cause a magnitude of forces in the supporting structure (Bobet, 2003) . Proper modelling can have a good influence on predicting and selecting suitable support types. Nguyen *et al*. (2021) state that the influence of groundwater can reduce rock strength, adhesion force of the interface, and friction, which leads to an unstable state of the rock mass. The water contained on the Big John Dyke, Little John Dyke and 37-line fissure on the three haulages at Zondereinde Northam Platinum Mine has a weakening effect on the rock mass inducing instabilities.

Hongri *et al*., (2014) explain that underground rock porous media are deformable bodies. The application of load and fluid pressure can give rise to deformations in the porous medium, which in turn may lead to alterations in the pore and fracture structure. Such modifications can induce changes in the velocity within the rock matrix, ultimately impacting its behaviour (Stanchits *et al*., 2011).

According to Anagnostou (2006), water can influence both the stability and deformation of a tunnel by diminishing effective stress and, consequently, resistance to shear; by generating seepage forces directed towards the excavation boundary; and by eroding fine particles from the surrounding earth. The flow of seepage may result in a lowering of the water level and induce time-dependent subsidence as a consequence of consolidation. Moreover, when tunneling through soft ground, the seepage forces directed towards the opening may compromise its stability. The movement of water through low-permeability soil is a significant contributor to time-dependent phenomena in tunneling (Anagnostou, 2006). Additionally, in a

broader context regarding environmental ramifications, substantial water inflows may obstruct excavation efforts or severely affect the tunnel's functionality during its operational phase.

According to Jakubec et al. (2018), the Ekati and Diavik diamond mines demonstrated that water could compromise tunnel stability and induce deformations by diminishing effective stress, thereby reducing resistance to shearing and creating seepage forces directed towards the excavation boundaries, which can precipitate instabilities. Wang *et al*. (2016) investigated the collapse of a rock slope that was excavated in the Autumn of 1997, situated within the alternating strata of sandstone and mudstone in Chongqing, China. This rock slope experienced a sudden failure on April 28, 2014, marking approximately 16.5 years since its excavation. The failure was primarily attributed to the initial excavation coupled with prolonged weathering (Wang *et al*., 2016). The authors identified water as a crucial element that expedited the weathering process, thereby compromising the mechanical integrity of the rocks.

Nihayat (2022) defines swelling behaviour in tunnels as a time-dependent process that causes an increase in volume and inward movements in the tunnel. This behaviour is the result of numerous interacting mechanisms, which cause additional complications in excavation projects (Butscher *et al*., (2016). Stability problems introduced by swelling clay depend on several internal and external factors (Nihayat, 2022). Nihayat (2022) indicates that internal factors are type and structure of the clay mineral, particle size and amount of clay infilling, the water content and dry density before swelling, concentration of ions and the dominant cation type of the clay mineral, and available diagenetic cementation (Nihayat, 2022). External factors are: access to free water for imbibition and ion concentration in water, the possibility of volume increase in the swelling process, and eventual counter-pressure (Nihayat, 2022).

This phenomenon occurs with relative infrequency, as noted by Selmer-Olsen and Palmstrom (1989). The swelling materials may be confined to select faults or joint surfaces within a geological province; both younger and older systems traversing the same area may lack the presence of swelling clays. Typically, rock powder and fragments coexist with the swelling minerals; additionally, a suite of secondary minerals such as calcite, quartz, chlorite, talc, zeolites, kaolinite, and hydromica/illite may be found in conjunction with the swelling clay minerals within the infillings, as observed by Selmer-Olsen and Palmstrom (1989).

Swelling rocks pose a distinct challenge in tunneling operations as they can potentially give rise to substantial excavation difficulties (Sharifzadeh et al., 2017). In numerous instances, areas of swelling or rocks imbued with expansive minerals have precipitated tunnel collapses, leading to significant extra expenses and delays for the project. Additional financial losses ensue if the complications posed by swelling rocks compel the closure of a facility (Selmer-

Olsen & Palmstrom, 1989). The water-bearing fissures at Zondereinde Northam Platinum Mine can exhibit similar problems as in the cases mentioned above. Understanding the effects of groundwater will be essential in the final design of the planned excavations.

2.2.5 Numerical Modelling

Numerical modelling is a tool used to model stresses and deformations around underground excavations. Major and minor principal stresses were modelled on the three haulages mining through water fissures at Zondereinde Northam platinum Mine. This chapter briefly discusses the theory behind the Numerical Modelling. Rock material is a natural geological occurrence comprising different minerals (Nikolic *et al*., (2016). It is inhomogeneous, anisotropic, discontinuous, and inelastic and consists of oriented potential failure zones. Because of its irregular nature, predicting the behaviour of the rock mass is challenging. Numerical modelling has different approaches to solving this challenging occurrence. Numerical methods are classified into continuum, discontinuum, and hybrid continuum/discontinuum methods. The most notable continuum numerical models are Finite Difference Method (FDM), Finite Element Method (FEM), and Boundary Element Method. The discontinuum methods are the Discrete Fracture Network (DFN) and the Discrete Element Method (DEM).

Swart and Handley (2005) state that while most fall of ground incidents are linked to the failure of geological formations, the design methodologies employed are primarily confined to structural analyses. In certain instances, complex numerical analysis programs are utilised on an ad hoc basis to evaluate the stability of structurally controlled panels. Numerical modelling is vital for optimum support design because empirical methods are limited. Esterhuizen and Streuders (1998) assert that unstable key blocks of rock with the potential to fall are usually found in the hanging wall of excavations and can be delineated by geological structures. Dips software was used to obtain the orientation of joint sets and possible failure mechanisms. An underground mapping exercise was performed to ascertain the orientations of joint sets and significant geological formations. Possible kinematic analyses were described for the three tunnels at Zondereinde Northam Platinum Mine.

A case study at Zondereinde Northam Platinum Mine was conducted on three development sites where elastic modelling was conducted. Elastic Vantage software was utilised, and principal stresses were calibrated using the Rockwall condition factor as a parameter to determine different ground conditions to obtain suitable support.

Numerical Modelling Limitation

Numerical Modelling of rock mass behaviour is complicated when numerical and empirical modelling is employed due to the existence of discontinuities and the heterogeneous,

anisotropic, and non-elastic characteristics of the rock mass (Hussain et al., 2018). Although empirical methods, such as statistical analyses, are used to assess the stability of the stope panels/development at Zondereinde Northam Mine, they are limited in verifying the anticipated performance of the designed excavation. It can be difficult to obtain the desired result without knowing the parameters. The Vantage software utilised is elastic and capable of forecasting stress; however, it cannot anticipate the rock mass's failure. There is no one generalised method that can solve all rock mechanics problems.

Conclusion On Numerical Modelling regarding the application at Zondereinde Northam Platinum Mine

The Vantage elastic modelling results depict that the rock wall condition factor is beyond 1.4, which indicates poor ground conditions that require stringent support due to stress fractures induced by high principal stresses. The three haulages were modelled, and the high vertical stresses induced severe sidewall fractures.

2.2.6 Blasting Design

2.2.6.1 Introduction

Blasting aims to achieve maximum face advance per blast with minimal damage to the rock walls. This is achieved through accurate drilling and blasting with the correct explosives. The ground conditions where water fissures are intersected at Zondereinde Northam Platinum Mine are generally incompetent due to closely spaced joints infilled with serpentinite, fault zones, and shear zones. These conditions and stress fractures created due to depth induce blocky ground conditions. Therefore, blasting methods for these excavations must be used to reduce the damage to the rock wall. This chapter discusses blasting methods, types of explosives used, and blasting techniques that are better and can improve conditions in mining through water fissures at Zondereinde Northam Platinum Mine.

2.2.6.2 Types of Explosives

Explosives characterised by a low-velocity detonation (VOD) possess greater gas energy and diminished shock energy (Maranda, 2011). Such explosives are ill-advised in complex geological conditions, as the gas may infiltrate joints and fractures, further deteriorating the ground's integrity. This infiltration can lead to instability within the stratified rock, particularly where distinct parting planes are situated in the hanging wall. At Zondereinde Northam Platinum, cartridge emulsion explosives are employed in both stoping (29mm x 270mm) and development (32mm x 270mm) operations.

Ammonium nitrate-fuel oil (ANFO) is a high-energy explosive that widens the joints, leading to the uncontrollable unraveling of the rock walls. It is not recommended in poor ground conditions encountered in water fissures. Examining charging and blasting practice in challenging ground conditions where the water fissures intersected are vital.

2.2.6.3 Explosives properties

Various types of explosives were examined, and their advantages and disadvantages were analysed for design considerations. Ammonium nitrate-fuel oil (ANFO) is a supreme explosive utilised in the mining sector. The initial examination of ANFO suggests that it will yield a substantial frequency of the critical blocks, thereby contributing to an unstable hanging wall (Bohanek *et al*., 2013). This can result in overbreak, which can worsen the conditions. Ammonium nitrate-fuel oil has certain drawbacks, including inadequate water resistance and suboptimal detonation characteristics, which limit its applicability for dry blasting in truncated compact rock masses (Maranda, 2011). Its advantages, however, encompass straightforward production processes, cost-effectiveness, and insensitivity to mechanical impacts during the loading phase into drill holes (Mathew, 1997). Dealing with water fissures at Zondereinde Platinum Mine, this kind of explosive will not work.

Other types of bulk explosives encompass emulsions and water gels. Bulk emulsion's advantages over ANFO comprise their ease of transportation, water resistance, minimal gas emission, string charging, optimal coupling, increased velocity detonation, and improved work environment (Maranda, 2011).

2.2.6.4 Evaluation of explosives characteristics in jointed areas

Ammonium nitrate-fuel oil explosives cause longer cracks and damage the hanging wall further (Sellers, 2011).

Smooth wall blasting works more efficiently with bulk emulsion. In smooth wall blasting, the final row of holes features a charge lighter than usual and should be detonated subsequent to the main charge to restrict the confinement of the holes and mitigate damage to the sidewalls. Mining through water fissures requires smooth wall blasting to limit rock wall damage. Elevated heave energy explosives adversely affect the stability of excavations (Chikande & Zvarivadza, 2016). Chikande and Zvarivadza, (2016) furthermore, explain that high-brisance explosives are preferred in the anisotropic jointed rock mass.

At Zondereinde Northam Platinum Mine the water fissures are highly jointed, hence the types of explosive characteristics in geotechnically challenging ground conditions are critical. The research area at Northam Platinum Mine is bounded by water fissures, shear zones, and joints, so different types of explosives were examined in challenging ground conditions. When

haulages are blasted with the correct explosives and good blasting practices, ground conditions improve, and several associated economic benefits result.

2.2.6.5 Half-Cast Factor

The concept of the half-caste factor is delineated as the proportion of the total visible drill barrel length in the sidewalls and hanging wall following the blast in relation to the total drilling length (Dey & Murthy, 2010). This factor is essential in assessing the extent of developmental overbreak. Since development overbreak affects the support quality, the effect of blasting on these fissures was analysed. According to Singh, (1992), blasting is destructive, and blast damage can be deleterious to safety and productivity.

The dimensions and quantity of the barrels, along with the half-cast factor, were ascertained utilising Equation 17 as follows:

$$HCF = \frac{\sum_{i=1}^{n} Li}{\sum_{r=1}^{n} Lr} \quad [17]$$

Where HCF = Half cast factor

Li = Post–blast drill mark length visible (m)

Lr = Pre-blast drilled length (m)

At Zondereinde Northam Platinum Mine, poor blasting and improper half-cast factor induce adverse ground conditions.

2.2.6.6 Powder Factor

The powder factor is a ratio that defines the relationship between the volume of rock fractured and the quantity of explosives employed to achieve this fragmentation. It can be articulated as the volume of rock broken per unit weight of explosives utilised. The smooth wall blasting technique reduces the amount of damage to rock walls by reducing burden and spacing and using small quantities of explosives to improve explosive distribution in the rock mass.

2.2.6.7 Comparison of Explosives

Table 9 below displays a comparison between ANFO and Emulsion. This comparison was done to choose the explosives type with the most merit and suitable for good ground conditions at Zondereinde Northam Platinum Mine. Emulsion is a better choice as it results in less damage to rock walls in poor ground conditions.

Table 9: ANFO vs emulsion

Parameter	**ANFO**	**Emulsion**
Advance	Average 2.8m	Average 3m
Capital cost	Low-ANFO loader is cheaper	High-MCU expensive to buy
Cost per blasted tonnage	Low	High
Charging time	More time	Less time
Powder factor	Low	High
Productivity	Decreased productivity	Increased productivity
Safety	Generate bad hanging	Improved safety, less damage
Overbreak	More	Less
Water resistance	Dissolves easily	Excellent

The hanging wall and sidewalls improved with the use of emulsion on the three haulages mined at Zondereinde Northam Platinum Mine. The adoption of bulk emulsion presents further enhancements in regions encountering difficulties such as minimal advancement and inadequate fragmentation.

Conclusion on blasting on haulages mining through water fissures at Zondereinde Northam Platinum Mine

Various explosive types and methods were discussed, including the explosives used at Zondereinde Northam Platinum Mine. Smooth wall blasting is essential in ensuring the stability of excavations bounded by water-bearing fissures. The emulsion explosives are used in stoping (29mm x 270mm) and development (32mm x 270mm) to limit damage to rock walls. The observations with emulsion explosives show that the ground conditions improve, reducing accidents and falls of ground. This explosive promotes safety and efficiency in blasting quality. The extent of overbreak is constrained, enhancing the conditions of the rock mass and the integrity of the support, while concurrently yielding a reduction in installation and remediation costs.

2.2.7 CASE STUDIES

CASE STUDY 1: Challenges in Tunneling in the Himalayas in South Asia (Diwakar, *et al*., 2022)

This case study was carried out Himalayas of India; this parallels the Northam Platinum Mine due to the region's intricate geological formation. The Himalayas is a mountain range in Asia and is the most unstable region globally. The rock mass in these mountains is fragile due to complex geological structures, tectonic forces, and faulting. A number of underground excavation tunnels were examined, including a headrace tunnel project from Nepal and six further tunnel projects from Bhutan, India, and Pakistan. The emphasis was placed on the prevalent challenges faced during tunneling, along with their potential causes and corresponding solutions. The study will discuss only two projects from Bhutan and Nepal. The conclusion from all projects will be discussed, as well as strategies. Figure 18 below depicts the geological map of the Himalayas.

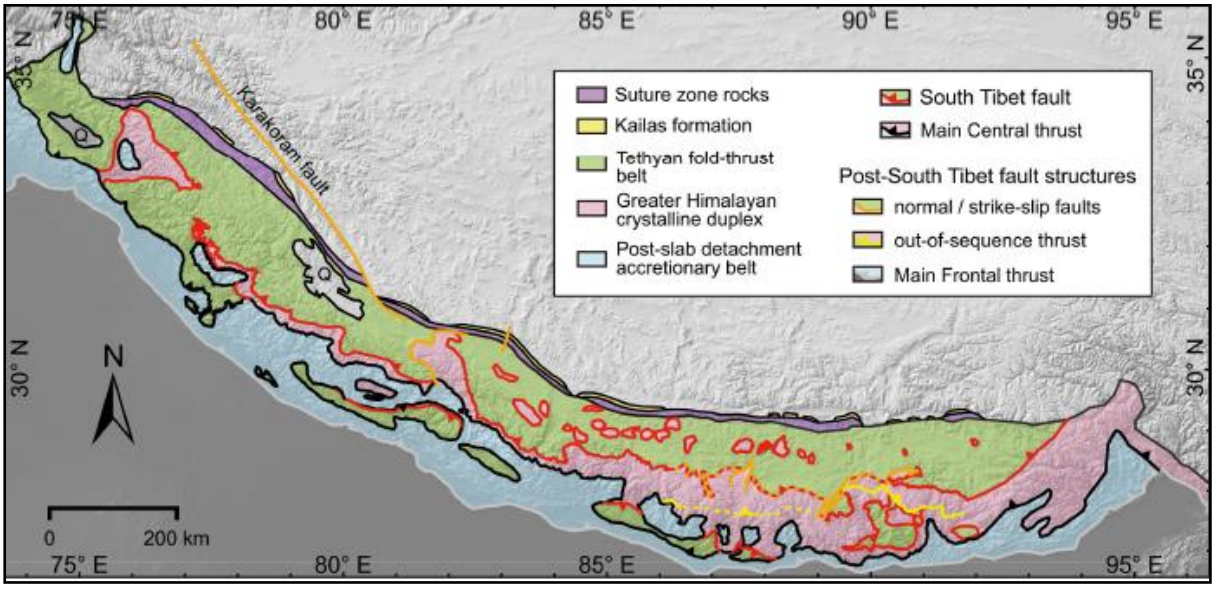


Figure 18: Geological map of the Himalayas (Diwakar *et al*., 2022)

Tala Hydroelectric Power Station (THPS)

The Tala Hydroelectric Power Station (THPS) is located in the Chukha district, adjacent to the Wangchu River in Bhutan. The geological context of the project is encompassed within the paleo-Proterozoic strata of the Shumar Formation of the Daling-Shumar Group, situated within the Lesser Himalayan rock sequence. This formation consists of light grey to white, subtly weathered, very fine-grained, medium to thick-bedded, cliff-forming quartzite, typically characterised by interlayers of thin to thick-bedded green muscovite-biotite schist and phyllite, adorned with distinctive sigmoidal quartz vein boudins. Along the tunnel alignment, there are high to medium-grade metamorphic rocks. In moderately adverse geological conditions, one

encounters highly shattered and moderately to heavily weathered amphibolite, biotite schist, and foliated interbeds of quartzite, featuring foliation shears that can reach up to half a meter in thickness. The rock mass is significantly saturated with water. The ground conditions bear a resemblance to those found at Zondereinde Northam Platinum Mine, where the Big John Dyke, Little John Dyke, and the 37-line fissure are intersected.

Mining Strategy

The tunnel was excavated utilising the drill and blast method, except in regions with unfavourable ground conditions constrained by shear zones, where manual removal was necessary. The headrace tunnel boasts a diameter of 6.8m and extends over a length of 23km.

The Q ratings indicated values ranging from 0.05 to 0.14 indicating poor ground conditions. This suggests that the rock has undergone significant fragmentation, weak, and vulnerable to water problems.

The geological conditions between chainage 699m and 709m of the adit situated at the Kalikhola stream were unfavourable. The tunnel experienced multiple collapses, occurring even after grouting, consolidation, and the installation of steel ribs and drainage pipes. To stabilize the tunnel face, bamboo piling was employed, alongside the installation of a forepole umbrella (Figure 19).



Figure 19: Bamboo piling at tunnel face at failed section (Diwakar *et al*., 2022)

Figure 19 illustrates the bamboo piling at the tunnel's entrance; this method has demonstrated its efficacy in preventing face collapse. To circumvent unfavourable geological circumstances, it was advisable to alter the tunnel's initial trajectory; nonetheless, analogous ground conditions were subsequently encountered.

Figure 20 illustrates the failure of the ribs at the crown; the excavation was conducted with a 2m pull, accompanied by the installation of ribs at 0.5m intervals. However, five ribs succumbed to the substantial dead load imposed by the sheared rock mass. Thirteen anchors, each 8m in length and 51mm in diameter, were installed at a 20° angle ascending, into which grout was injected.

Twenty-seven perforated pipes 8m long and 50mm in diameter were installed, followed by grouting. The support system consists of steel ribs at 0.5m spacing, 5-6m long rock bolts, 25mm in diameter, every 2m, 175mm steel fibre (temporary) shotcrete, and concrete lining. These measures were successful and very effective and allowed the project to proceed.



Figure 20: Failure of the ribs at the crown portion in THPS (Diwakar *et al*., 2022)

Dordi Khola Hydroelectric Project (DKHP)

The Dordi Khola Hydroelectric Project (hereafter referred to as DKHP) is located in the Lamjung district, nestled within the Lesser Himalayan Zone of Western Nepal. Geologically, it resides in a tectonically deformed area characterised by two central thrust sheets, where a thrust fault distinguishes the surface rocks. The project site is composed of formations from

the Ranimatta, Naudanda, and Ghanapokhara. The Naudanda Formation is characterised by white, massive quartzite that is fine to medium-grained and features ripple marks, interspersed with green phyllites. The Ghanapokhara Formation consists of black to grey carbonaceous slates and green shales, primarily composed of white to grey, compact dolomite and dolomitic limestones, which are layered together.

Challenges Encountered and Potential Solution

A 2780m long head race tunnel to convey water was excavated. The excavated diameter is 3.8m, and the final dimension is 3.3m. The tunnel was mined, and drill and blasting methods were used. However, manual excavation was carried out in poor geological conditions where the tunnel passed through the colluvium deposits. Groundwater problems and poor geological conditions were encountered. The tunnel collapsed due to weak weathered rocks and groundwater. The tunnel's face and hanging wall experienced a collapse; the face was reinforced with a 25mm thick layer of shotcrete to serve as a protective shield. Struts were installed to halt the further movement of the muck. To manage the crown settlement, temporary ISMB-150 steel beams were implemented to bolster the ribs (see Figure 21).



Figure 21 Temporary vertical struts for crown settlement control in DKHP (Diwakar *et al.,* 2022)

The ground at the invert level was exceedingly soft, resulting in one of the supporting ISMB-150 struts becoming submerged and ultimately lost (Figure 21). As the tunnel progressed, the geological composition transitioned from phyllite to quartzite. In that segment, ISMB-150 struts, each spaced 50cm apart, were installed as provisional support. Further reinforcement in the form of ISMB-200 struts, also at a spacing of 50cm, was introduced without the removal of the temporary support, owing to the unfavourable ground conditions.

The Himalayas Relation to Zondereinde Northam Platinum Mine

Mining in the Himalayas comprises complex geological features, including shear zones, closely spaced joints, and faulting. The THPS is bounded by thin beds, with weathered quartz veins. The rock mass is charged with groundwater, like Zondereinde Northam Platinum Mine.

The distinction between the two studies is that the Himalayas are mined in a shallow environment characterised by less stress fractures. In contrast, the Zondereinde Northam Platinum Mine, operates where at an intermediate depth, where intense stress fracturing significantly deteriorates ground conditions. The mining strategy employs drilling and blasting techniques characterised by a diminished face advance per blast, such as those utilised at Zondereinde Northam Platinum Mine. The support strategy used was steel beams and arches, which was successful.

CASE STUDY 2: Geotechnical investigations and preliminary support design for the Gecimez tunnel: A case study along the Black Sea coastal highway, Giresun, northern Turkey. (Akgun *et al*., 2014)

This case study was conducted in Turkey along Black-sea This resonates with Northam Platinum Mine because the highway is bounded by igneous rocks with highly weathered joints. This study includes geotechnical investigations, stability assessment, and design of support systems for the Gecimez tunnel in Turkey, constructed to improve the highway to the Black Sea coast. The geological setting of this study comprises basic and acidic volcanic rocks. Some of the rock types are Basalt, which is black to greenish and has a weathered porphyritic texture. It is moderately to highly jointed with 15-60cm spacing and 1-10m persistence.

The other rock type in the area is Agglomerate, which is dark green to green. It exhibits weak to moderate weathering, with localised areas showing significant weathering, interspersed with calcite veins. The ground conditions resonate with the study at Northam Platinum.

A geotechnical investigation was done to comprehend the geotechnical characteristics of the rock mass in the tunnel. The empirical methods, including rock mass classification, Q system, and Geological Strength Index classification systems, were followed to determine the geotechnical parameters and to determine the suitable support systems.

Kinematic analysis was used in the portal where the tunnel will be located to determine possible failures. Dips software was used to plot the stereographic projection, where different failures were evaluated. The results showed two failure zones in this study: planar and wedge failure zones.

Numerical analyses of wedges and Phase 2D for tunnel deformations were used to determine the suitable support to clamp the wedge. The safety factor was calculated, and the optimum support was installed to cater to the desired load.

The water pressure permeability of this study ranged from low to very low. Shotcrete was adequate to support the rock walls.

The approach to determining rock mass behaviour is like that of Zondereinde Northam Platinum Mine, where the start is to determine rock mass behaviour by using empirical methods, then use kinematic stereographic plots and numerical modelling for stress analyses.

Related to Zondereinde Northam Platinum Mine

The Gecimez tunnel consists of volcanic, igneous rocks like those found in the Zondereinde Northam Platinum Mine. The rocks are highly jointed with sympathetic jointing, which comprises calcite veins. Empirical methods are conducted to determine rock behaviour. The Dips software was used to determine possible kinematic failure, wedge, or planar. This was also used with the Zondereinde Northam Platinum Mine case study. Geological exploration was conducted ahead of mining faces to comprehend the behaviour of the rock.

CASE STUDY 3: Examples of previous tunnel collapses due to swelling clay in Norway (Nihayat, 2022)

This case study was conducted in Norway on swelling clay, which relates with Zondereinde Northam Platinum Mine study because the rock mass is charged with water with induces swelling of the rock mass. The following examples demonstrate stability problems caused by the appearance and behaviour of swelling clay: Hemsil I hydropower plant, Tunnsjoedal hydropower plant, and Hanekleiv tunnel.

Hemsil I hydropower plant

Figure 22 indicates a tunnel collapse discovered in a 14km long 12m^2 headrace tunnel at the Hemsil I hydropower plant in southern Norway. The weakness zone was located 150m below the surface and was surrounded by rocks of Precambrian age. The clay filled zones had brecciated montmorillonite and swelling clay infilling with a thickness ranging from 1cm to 8m and steep dipping angles. During the construction period in 1959, the observed larger clay filled zones were supported by a horseshoe concrete lining, whereas smaller faults were sprayed with shotcrete and sealed. After 8 months of tunnel operation, the tunnel was closed for inspection. During the inspection in 1960, a 200m^3 slide was discovered. The mechanism of the slide showed that water was imbibed in montmorillonite causing a high swelling pressure that the shotcrete was unable to withstand. During the swelling process, the shear strength of the montmorillonite was non-existent, resulting in sliding. When the material swelled, some of it was washed out and others fell out by its own weight. This process allowed more material to have access to water, eventually causing a release between the two faults. The three haulages mining through water fissures at Zondereinde Northam Platinum Mine also intersect fault zones and swelling similar to the Hemsil power plant; a collapse can be experienced if proper methods and support are not employed.

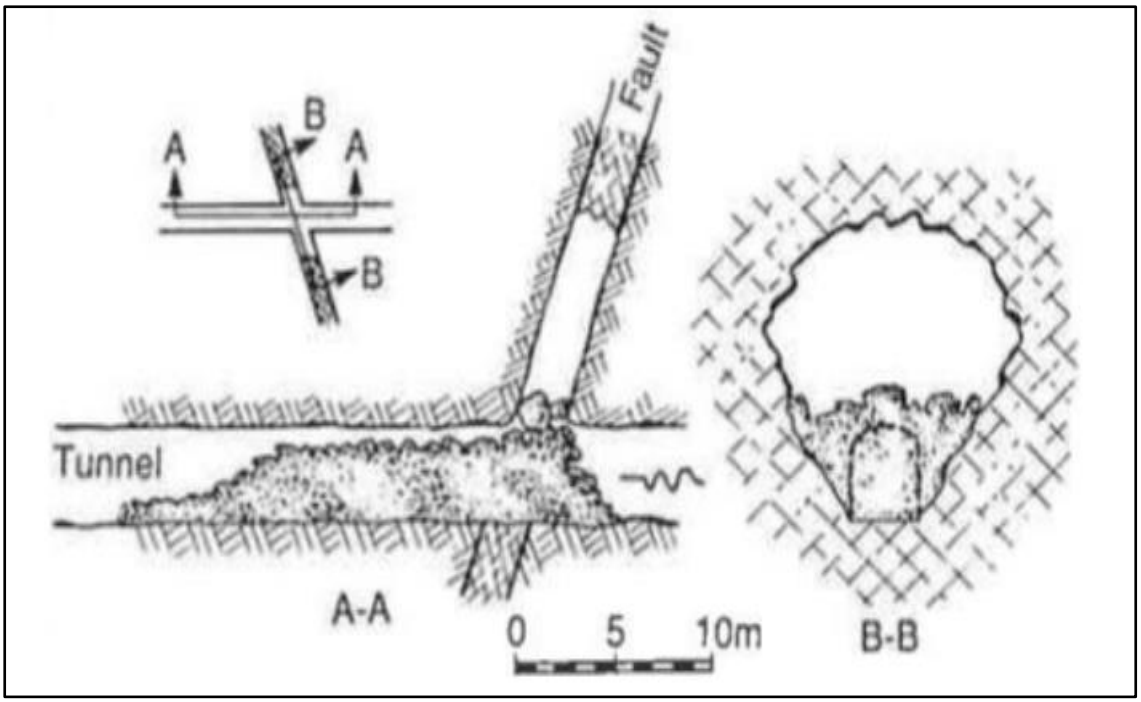


Figure 22: Illustration of the tunnel at Hemsil power plant (Nihayat, 2022).

Tunnsjoedal hydropower plant

An example of a tunnel collapse due to high leakage from surrounding rock is the 35m^2 tail race tunnel at Tunnsjoedal hydropower plant in Norway. The tail race tunnel passes through Caledonian rock. During the excavation of the tunnel in 1961-1962, a thin feather joint system was discovered, as illustrated in Figure 23 below.

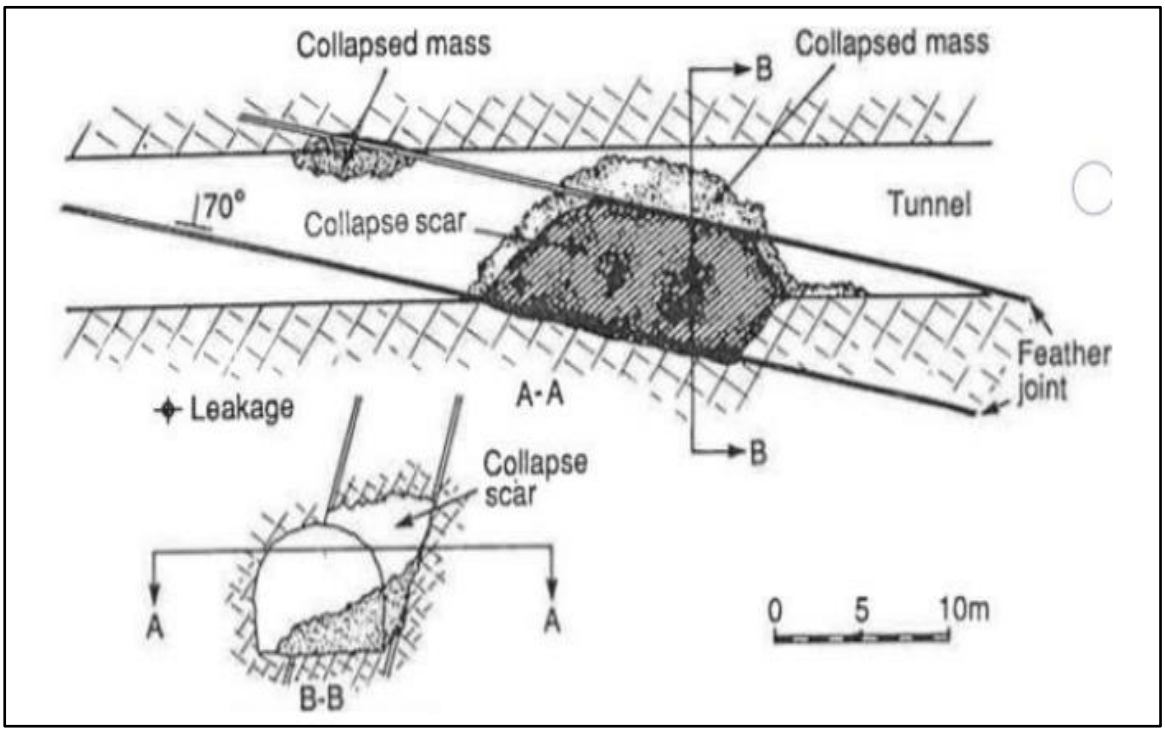


Figure 23: Illustration of the tunnel at Tunnsjoedal power plant (Nihayat, 2022)

The encountered joints were oriented parallel to the tunnel axis and had montmorillonite filling. Beside the joints, the montmorillonite was also located in the side rock. At first, these joints were neglected due to their small size and orientation to the tunnel face. In addition, the surrounding rock behaved as a good quality rock in dry conditions. However, this changed two weeks after excavation work started. A section with a length of approximately 30m started to slide. The sliding was due to a leakage from the side rock. When the water was imbibed in the montmorillonite material, a swelling pressure was mobilized and the rock disintegrated and turned into clayish mud. During this event, the tunnel blast was put on hold and concrete lining was used to stabilize the weakness zone. The three haulages mining through water fissures at Zondereinde Northam Platinum Mine also intersect prominent weathered joints similar to the Hemsil power plant; A collapse may be avoided if meticulously managed.

Hanekleiv tunnel

Usually, instability problems related to the occurrences of swelling clay have been discovered during the construction period. For the Hanekleiv road tunnel in southern Norway, the rock slide occurred 10 years after the tunnel was built. The 1,765m long tunnel passes through the bed of Permian basalt and Permian syenite and was characterised as a fairly-good rock. During the construction work in 1996, minor stability problems were encountered in the northern part. When excavating the southern part, a fault zone consisting of swelling clay was discovered. This part was stabilized with 15cm reinforced shotcrete. In addition, 10cm extra shotcrete was added where the cracks were located. In addition, a frost-protective and waterproofing cover was installed. After the faults were supported with shotcrete and rock bolts, no further stability problems were reported. This changed in December 2006, when a rock mass of 250m^3 fell down on the road, as illustrated in Figure 24. Nobody was injured due to the event happening at Christmas midnight when there was limited traffic. After the incident, the collapsed material was analysed and two thick parallel joints with swelling clay filling were identified. This structurally controlled fall of ground was supported with shotcrete and bolts, the structures resonated with mining through fissures at Zondereinde Northam Platinum Mine, The experience reveals that alternatve support measures can be used to enhance safety in mining through these features.



Figure 24: Collapse at the Hanekleiv tunnel in 2006 (Nihayat, 2022)

Relation to Zondereinde Northam Platinum Mine

Consequently, groundwater can result in the swelling of the rock mass. The water fissures contain water, and the experience of the above study can assist in anticipating rock behaviour, thereby enhancing better support systems to avoid collapses at Zondereinde Northam Platinum Mine, where three haulages approaching water fissures are mined.

CASE STUDY 4 : Tunnelling through a running Dyke – Tau Lekoa Mine (Oelofse & Judeel, 1999)

This case study was conducted in South Africa at Tau Lekoa Mine tunnels, it pertains to the Zondereinde Northam Platinum Mine, which is mining through a running dyke and is the intermediate depth with high vertical stresses inducing intense stress fractures in addition to the geological structures.

Location

Tau Lekoa Mine is situated in the Northwest Province of South Africa (Figure 25). The 6-shaft running Dyke was intersected by the development planned to access the high-grade block of ground in the northeastern corner of the mine. The running dyke forms the north-eastern boundary between African Rainbow Minerals 6 shaft, Tau Lekoa Mine, and Weltevreden lease area.

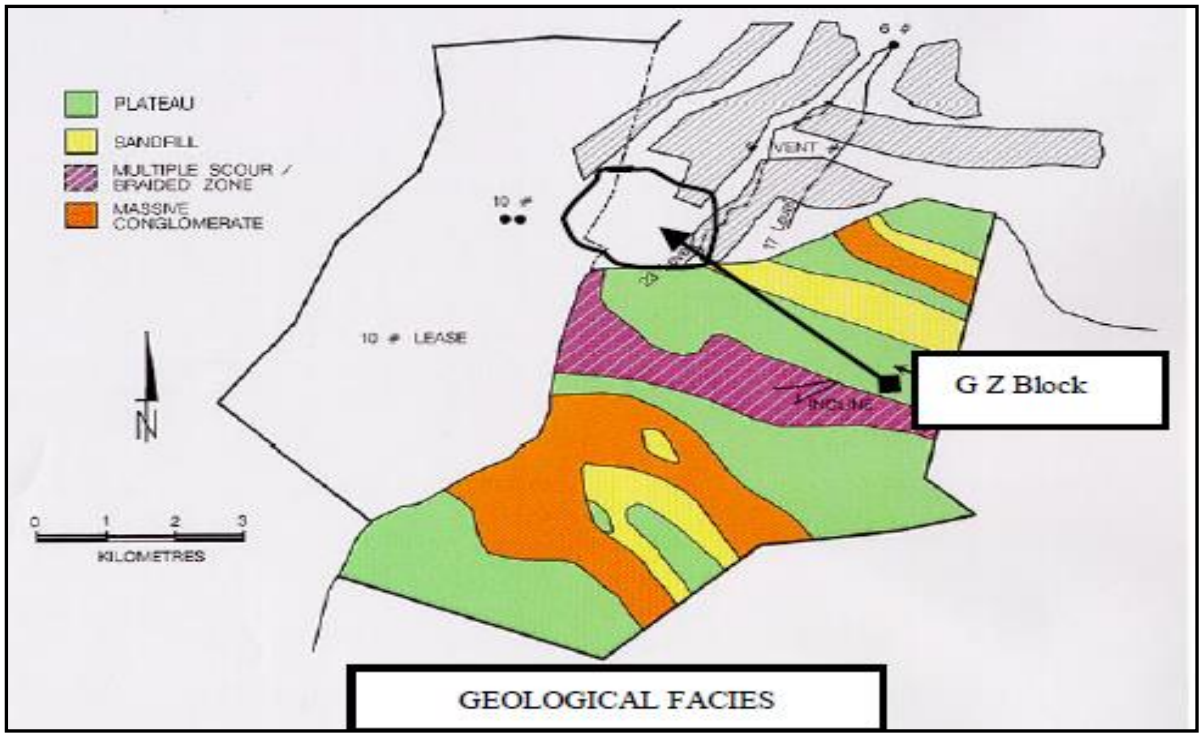


Figure 25: Locality plan of the GZ block bounded by the 6 # Running Dyke (Oelofse & Judeel, 1999)

History and Geology

Tau Lekoa Mine (Vaal Reefs 10 Shaft) was sunk between 1985 and 1989 to a depth of 1743m below the surface. The mine utilises twin shaft systems to access the Denny's and Vaal Reef economic horizons across 6 levels from 900m to 1650m below the surface. A 40m wide running dyke was intersected at 1130 N3 tunnel, documented by (Oelofse & Judeel, 1999). The dyke was dark green to black, consisting of pyroxene fragments set in a matrix of serpentinite ferromagnesium and chlorite material. Due to its highly altered nature, the dyke tended to rapidly disintegrate into a granular, unconsolidated 'sand' mixed with largefragments on exposure to water or air; hence it is called a 'running' dyke.

The Uniaxial Compressive Strength (UCS) of the dyke was determined using point load tests. The values obtained range from 5-15 MPa, 40 MPa, and 100 MPa. Estimations of the rock mass rating RMR after Bieniawski's (1989) classification system suggested a rating of approximately 40. The angle of repose of the muck pile observed underground was measured to be roughly 40° and tied up with the estimation of the friction angle. The density of the dyke material was measured to be between 3400kg/m³ and 3800kg/m3, which is higher than the host rock.

Mining Strategy

The tunnel shape and dimensions were then altered to circular and a diameter of 3.9m, respectively. Ground consolidation started at 3m from the Running Dyke contact zone and continued 5m beyond the dyke. The 4m-long consolidation holes were drilled straight into the face every 3m, and resin was grouted into the charging sticks to prevent runaways. The tunnel was advanced to a maximum of 1m per shift to facilitate the installation of the next steel ring arch set. Spiling rounds were repeated every 3m to ensure sufficient overlap of consolidated ground around the tunnel to prevent collapses.



Figure 26: Ring sets with timber and void fill and consolidation bolts on the face (Oelofse & Judeel, 1999)

Figure 26 illustrates consolidation bolts enhancing the rock mass strength ahead of the face. The tunnel was successfully mined with arch sets and void fill.

Tau Lekoa Mine in Relation to Northam Platinum Mine (Zondereinde)

Tau Lekoa mine is mining at the same depth as haulages at Northam Platinum Mine with depth ranging from 1000m to 2200m. The dyke material is highly altered and contains water. The Rock mass rating and MRMR are less than 40 depicting poor rock mass conditions. The mining strategy is reducing blast to 1m and increasing tunnel dimension before supporting the

structures with ring sets. The most important thing is the installation of self-drilling spiling bolts through which resin is injected into the rock mass to bind the blocky rock mass.

ADDITIONAL CASE STUDIES

Sharifzadeh *et al.* (2013) conducted a study on the Shibli twin tunnels in Bostanabad in Iran. The surrounding rock formations of the tunnels consist of grey shale, marl, and calcareous shale. The tunnels are mining through heavily jointed rock masses, which induce poor ground conditions. Rock mass classification systems were used to classify the ground conditions according to the severity. It was argued that rock mass classification was inappropriate for the incompetent combinations of the ground conditions. Hence GSI was used to rate the poor rock mass on the tunnel. Tunnels in weak rocks experience ground deformation and threats to the stability of the excavation as creep develops. The Shibli twin tunnels were examined through laboratory testing techniques, data monitoring, rock mass classification systems, core logging and numerical modelling.

Aicha and Mezhoud, (2021) conducted a study on the Djebel El Quahch tunnel in Algeria; the tunnel crosses the Djebel El-Quahch Mountain in the northeast province of Constantine. The tunnel traverses through weak argillite soil. Numerical modelling was used to determine the suitable methods and support of the tunnel. The following support was used for reinforcement: steel sets, a 40cm layer of shotcrete, wire mesh, and lacing and anchor bolts. Plaxis 3D numerical software was used to calculate the stresses and strains around the tunnel boundaries.

Faris, (2022) examined the design of tunnel support on swelling clay; this study was conducted in Sweden. This factor can be exacerbated by water, which induces challenging ground conditions like the Zondereinde Northam platinum Mine on three haulages mining through water fissures. Laboratory tests were conducted to comprehend the amount of swelling clay in haulages. The tests results were used in numerical analyses and empirical methods to determine suitable support systems. The results from laboratory tests indicate that clay samples could be characterised as active respectively moderately active clay. The Plaxis 3D model results depict that the swelling zone's width and swelling pressure impact shotcrete thickness and rebar spacing.

Relation to Zondereinde Northam Platinum Mine

In all the above studies, the ground conditions are poor with low Q and RMR, Laboratory tests were conducted to obtain rock mass properties to conduct numerical modeling. Numerical modeling was conducted to determine expected rock mass behaviour and assist in the selection of the support.

2.2.8 Summary of Literature Review

Mining through water fissures will result in poor ground conditions exacerbated by stress fracturing at depth and geological complexity. This chapter delineates the theory underpinning rock mass classifications, which are employed to obtain the expected rock mass quality and to identify appropriate support systems. The theory behind groundwater and several case studies were also studied to comprehend the impact of water on ground conditions. Numerical modeling background and theory were also employed to determine the expected principal stresses that would lead to stress fractures in the tunnel. Proper blasting techniques, including smooth wall blasting, are required to limit further blast damage and ensure stable rock walls. This chapter elaborates on the types of explosives and properties that suit this ground condition at Northam Platinum Mine. The literature review also included case studies in different countries of tunnel mining through complex fissures with similar conditions to Northam Platinum Mine. It was a common feature that mining without proper geological investigation was experienced in most case studies. Most case studies were done in other countries, and a few case studies done in South Africa were not published. Mining of running dyke at Tau Lekoa mine is an excellent example for the current case study as this is mining in similar ground conditions with Zondereinde Northam Platinum Mine case. More case studies in platinum mines need to be studied and published where mining through water fissures is experienced. The Zondereinde Northam Platinum Mine case study is one example. The information gained from the review of case studies contained in the chapter will be considered in evaluating the requirements for the Zondereinde Northam Platinum Mine Case. The aim of this report is mining three development haulages through water-bearing fissures at Zondereinde Northam Platinum Mine. The observations and plans showing areas of interest are shown in Chapter 4. The findings and analyses of mining through these structures are discussed in Chapter 5. SIMRAC GAP 335 is also discussed under the research approach in chapter 3, where the behaviour of ground conditions associated with the relevant support systems is detailed.

CHAPTER 3: RESEARCH APPROACH

3.1 Introduction

This chapter will explore the modes and methods employed to devise an effective and successful strategy for mining through water fissures, encompassing investigative, analytical, and logical techniques. It will also reflect on the insights gained from the case studies reviewed in the preceding chapter. In situ stress measurements were performed to assess the deformations within the rock to determine the rock stresses. Geological boreholes were drilled ahead of the three developments ends where core logging was conducted. Observations and analyses were conducted on the geological structures encountered to ascertain the characteristics and extent of the jointing and faulting system within the formation. Rock mass classification systems, including RQD, RMR, MRMR and Q values, were used to analyse and classify ground conditions and determine the required support. Rock parameters, including UCS, UCM, Poisson's ratio and Young's Modulus were determined through Rock tests done in (2011). They were used in numerical modelling software Vantage to calculate the rockwall condition factor in the tunnels.

3.2 In Situ Stress Measurements

Virgin Stress Field

In-situ stress measurements conducted on the 4 level (1014m below the surface) determined the virgin stress field at Northam Platinum Mine. The results revealed that the major principal virgin stress (σ_1) dips approximately 71° to the northeast and that the vertical virgin stress (q_v) is roughly equivalent to the weight of the overburden. The average horizontal-to-vertical stress ratio (k-ratio) measured was 0.65. The north-south k-ratio was 0.48, and the east-west k-ratio was 0.72. The orientation of the intermediate (σ_2) and minor (σ_3) principal virgin stresses about geology and mining outlines is illustrated in Figure 23.

Reliable values for the k-ratio are important for understanding rock mass behaviour, designing support, mining layouts, and use for stress modelling. Apart from the measured virgin k-ratio, variations of the k-ratio can be estimated by observing the profile of blast-generated fractures around shot holes and measuring the horizontal and vertical dimensions of the sockets. The shapes and orientation of sockets in off-reef development vary significantly across the mine. Indications of localized high horizontal stress areas were observed on the eastern side of the mine, between 9 and 12 Levels, and from about the 42 line to 48 line see (figure 27).

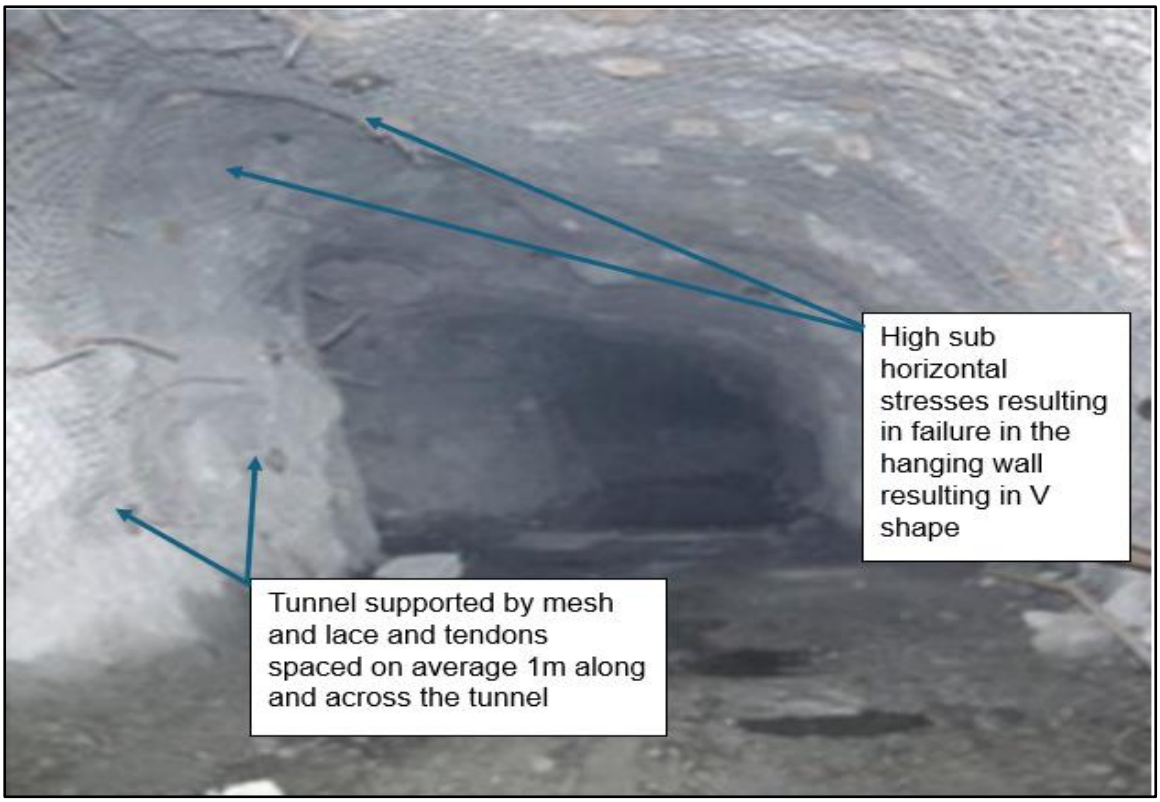


Figure 27: Spalling failure as a result of high horizontal stresses (Villaescusa *et al*., 2016)

Stress-induced fracturing in the deeper tunnels below the 13 Level is more prevalent along the sidewalls than on the hanging wall. The fracturing is quite intense along the top southern corner of the 13-level haulage. There is, however, no compelling evidence to invalidate the assumption of a vertical major principal virgin stress orientation.

Joint mapping by the CSIR in 1994 revealed that most joints (J1) trend north-south, dipping to the east. These joint orientations are indicated in Figure 23, along with the orientation of intermediate (σ2) and minor (σ3) principal stresses. The intermediate (σ2) stress tends to effectively clamp N-S trending extension fractures, while the minor principal stress (σ3) will tend to clamp the Pilanesberg joint set. Pilanesberg joint sets are parallel to cross-cut sidewalls, intersecting haulages perpendicularly (Zondereinde Mine COP, 2024). The principal stress orientations indicate that haulages will be more stable than cross-cuts because excavations subjected to the major and intermediate principal stresses (σ1 and σ2) will be more stable than excavations subjected to the major and minor principal stresses (σ1 and σ3), as illustrated by the RCF equation (Jager & Ryder, 1999). In general, haulages will be more stable because jointing intersects haulages perpendicularly and will be orientated at a favourable angle to the ambient field stress.

Figure 28 illustrates intermediate, and Minor principal stress orientations in relation to Pilanesberg joints and Extension fractures.

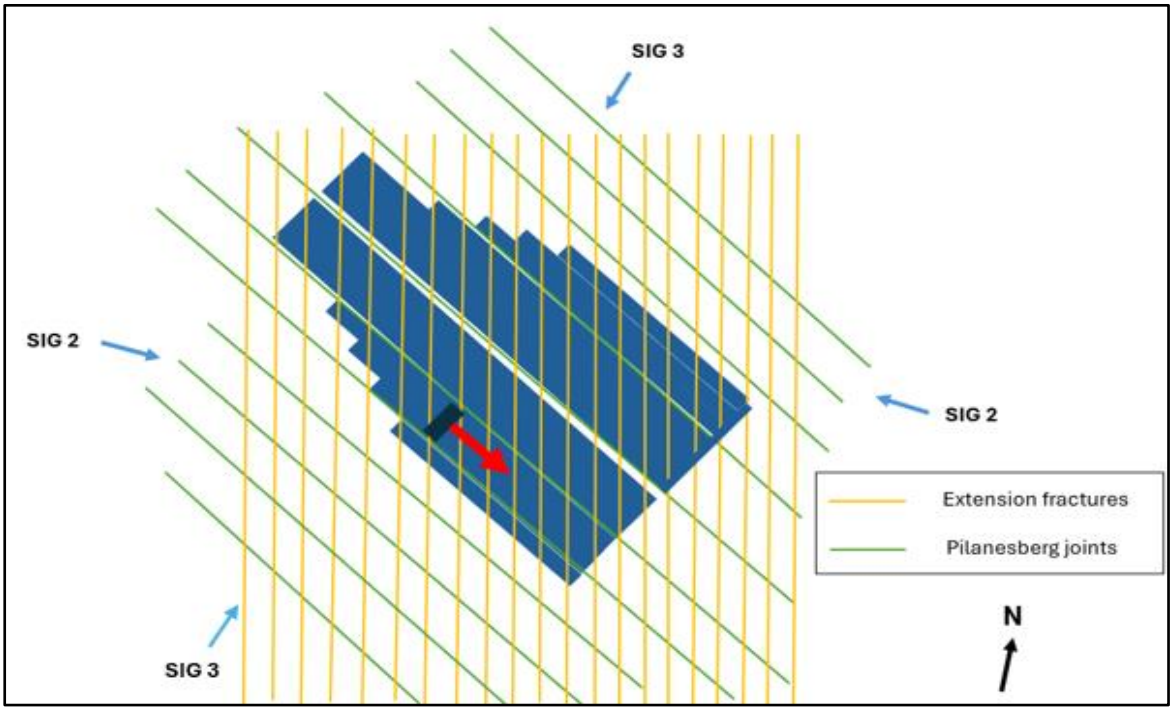


Figure 28: Diagrammatic representation of joint trends and principal stresses influence (Zondereinde Mine COP, 2024)

3.3 Rock Tests

Anticipating the strength of rock and rock masses is crucial for understanding excavation behaviour and performance. The strength and deformability of rock masses can be employed to estimate and foresee failures in mining excavations. Laboratory testing of rock specimens is an input on the characteristics of rock masses for design and numerical modeling, in addition to rock mass classification systems for quality design and forecasting (Russo & Hormazabal, 2016).

The CSIR (1991, 1993, 1994, and 1999) and ROCKLAB (2011 and 2018) laboratories determined the rock strength of the hanging wall and footwall lithologies through various point load tests and laboratory compression tests of the drilled core at Zondereinde Northam platinum Mine.

Uniaxial Compressive Strength (UCS) tests and Triaxial Compressive Strength (TCS) tests were performed at Rocklab on core samples to define the rock strength for the development haulages at Zondereinde Northam platinum Mine. The diameter of the specimens tested was as per the standard core diameter of 54mm, as recommended by (ISRM). The height to

diameter of all rock specimens was measured to be 2.5 to 3 as recommended by (ISRM). The rock specimen was a piece of core with ends ground or lapped parallel and to within 0.02mm.

The UCS, alongside the elastic modulus and Poisson's ratio, was evaluated using a servo-controlled hydraulic stiff-compression testing apparatus. The rock core specimen, characterised by a height-to-diameter ratio ranging from 2.5 to 3.0, was positioned between the upper and lower loading platens. The load was incrementally applied until failure ensued. Axial and lateral deformations were meticulously monitored through computerized instrumentation equipped with strain gauges. The UCS, elastic modulus, and Poisson's ratio were derived from the acquired data and the dimensions of the specimen. Analyses of the UCS reveal an average strength of 130 MPa.

In 1994, approximately 3000 Point load tests were conducted at 5cm intervals along the lengths of boreholes 91341P and 11-1354, and the loads recorded (P) were converted to UCS.

The Point Load Test (PLT) entails the evaluation of rock samples, whether axial, diametrical, blocks, or irregular fragments—conducted either in situ or within a laboratory environment. This test is employed to estimate the Uniaxial Compressive Strength of the rocks. The specimens are subjected to loading along the diameter for the diameter test and along the core axis for the axis test until failure occurs, at which point the peak load is meticulously recorded. The average UCS calculated was 130 MPa. Where haulages were 50-65m below Merensky reef, and where haulages were sited deeper than 75m in the footwall, design strength would be considerably less than 90 MPa due to weak rock type.

3.4 Numerical Analyses

The study utilises Vantage elastic modelling Software which is 3D and can model stresses and seismicity in underground mining. Numerical Modelling using Vantage software was used to determine RCF on tunnels. Mine plans were taken from the planning department, where dxf files for the haulages were important to Vantage software, and the model was built. The numerical simulation requires input including joints, dykes and fault properties, rock mass properties, strength properties, in-situ stresses, and geometry. The numerical modelling in this study employed in-situ stress and characteristics of the rock mass. The in-situ stresses were acquired from CSIR, where overcoring was performed at four haulage level, as previously mentioned.

3.5 Empirical Analyses

Rock Quality Designation was used from the cores drilled ahead of three haulages mining through water fissures and was assessed and evaluated using the approach of Deere (1963) and Palmstrom (1982). The empirical methods that were used after determining RQD were Laubscher's Rock Mass Rating (Laubscher, 1990), Bieniawski's RMR (Bieniawski, 1989) ,Q system (NGI, 2022) and MRMR (Laubscher, 1990). The empirical methods are applied to ascertain ground class categories within the study region, identify efficacious approaches, and recommend suitable support systems for implementation. The stress reduction factor (SRF) was assessed utilising the methodology established by (Peck, 2000) for high-stress conditions in jointed rock.

3.6 Research Design

The study encompasses three tunnels excavated through water fissures characterised by challenging ground conditions. Geological assessments, including core logging, underground observations, and mapping to ascertain Q, RMR, and MRMR values for rock mass classification, were conducted. Geotechnical analyses, comprising rock testing and in-situ stress measurements, were performed to evaluate the mechanical strength of the rocks for design purposes. Furthermore, consultations with mining teams were undertaken to gain a comprehensive understanding. Goricki *et al*. (2004) examined the behaviour of rock masses in the context of the design and construction of Alpine tunnels. The flowchart in Figure 24 delineates the tunnel design methodology (Schubert *et al*., 2003). This flowchart illustrates a direct relationship between excavation and support systems and the rock mass model, which defines the behaviour of tunnels.

Figure 29 illustrates 11 general steps that are critical to conclude a geotechnical design, and the steps are briefly discussed below:

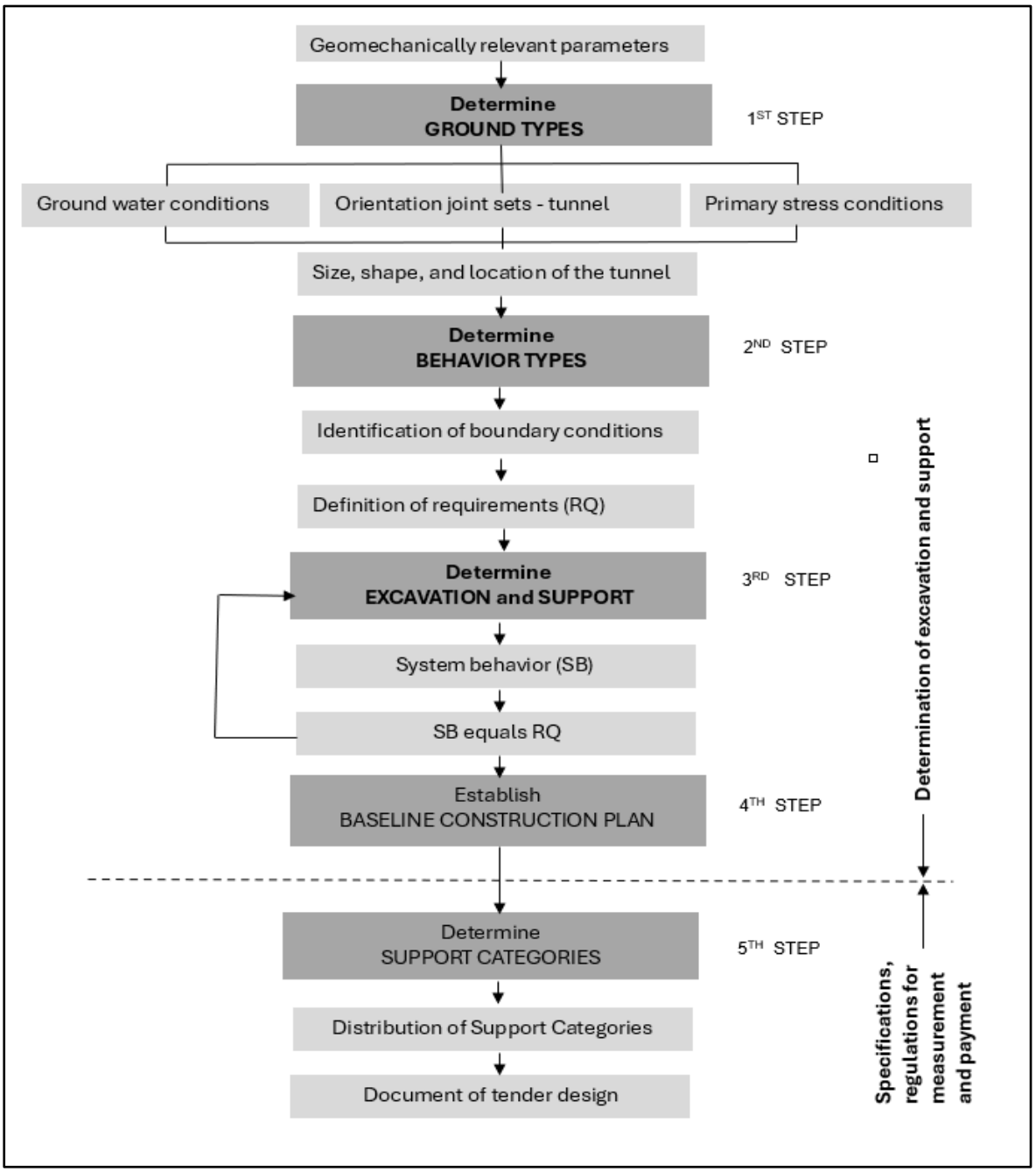


Figure 29: The basic process for determining excavations and support measures based on the behaviour of the ground types (from the Austrian Society of Geomechanics, 2010 v.2.1: Guidelines for the geomechanical design of underground structures for conventional tunneling, Salzburg)- Schubert, *et al.,* (2003).

Step 1 – Determination of ground support types (GTs)

This phase reveals the geological and geotechnical parameters delineated for each rock type. The ground types are then classed according to their geological characteristics.

Step 2 – Determination of ground/rock mass behaviour types (BTs)

The second step entails evaluating the behaviour of the ground by considering various types of ground conditions and local factors, such as groundwater presence, orientations of discontinuities, and stress conditions.

Step 3 – Determination of the excavation and support

Various support and excavation strategies are assessed, and the appropriate methods are identified. Once the support and excavation techniques have been finalised, both risk and economic analyses ought to be performed for through evaluation.

Step 4 – Geotechnical report and baseline construction plan

This step is determined based on steps 1-3. It is segmented into homogeneous areas characterised by comparable support and excavation needs.

Step 5 – Determination of excavation classes

The geotechnical design must be assessed in terms of cost and time. The categories of excavation are delineated by the methods employed for excavation and the supporting measures implemented.

The research for the Zondereinde Northam Platinum Mine Case considers the design and strategy of mining through water fissures. Geological data for design, including core logging, will be studied and analysed. The mining strategies and blasting design for this excavation will also be assessed. Geotechnical design employing empirical methods will be examined and utilised to formulate support recommendations. The core logging conducted from 14-west, 16-east, and 17-east haulages was done in 2023. The RQD, RMR, and Q ratings (NGI, 2022) were used, and rock strength tests done in 2011 will be used to design mining and support strategies.

3.7 Tunnel Support Design Methodology- GAP 335 (Haile *et al*. 1998)

The environment in which tunnels are located varies with depth; They may differ from igneous rocks to sedimentary rocks. In a low-stress environment, the control of potentially unstable key blocks is defined by geological structures. In a high-stress environment, the environment is influenced by stress, which may result in stress fractures. The main objective of tunnel design is to understand the interplay between the elements of the support system and the

surrounding rock mass (Haile *et al.,* 1998). In this case, the ground conditions where water-bearing fissures intersect must be understood to determine the correct support.

The following aspects need to be understood.

- An appreciation of how the characteristics of the rock mass structure affect the efficacy of the support system – To comprehend the characterisation of the rock mass surrounding the water-bearing fissures extracted and the performance of support in this environment.
- An understanding of the interplay between excavation geometry, the surrounding rock mass environment, and the dynamics of the support mechanism.
- Capability to engineer the capacity of the components within the support system through mechanistic analysis.
- The paramount significance of understanding the interplay between the tunnel support system and the highly fragmented (fractured) rock mass structure.

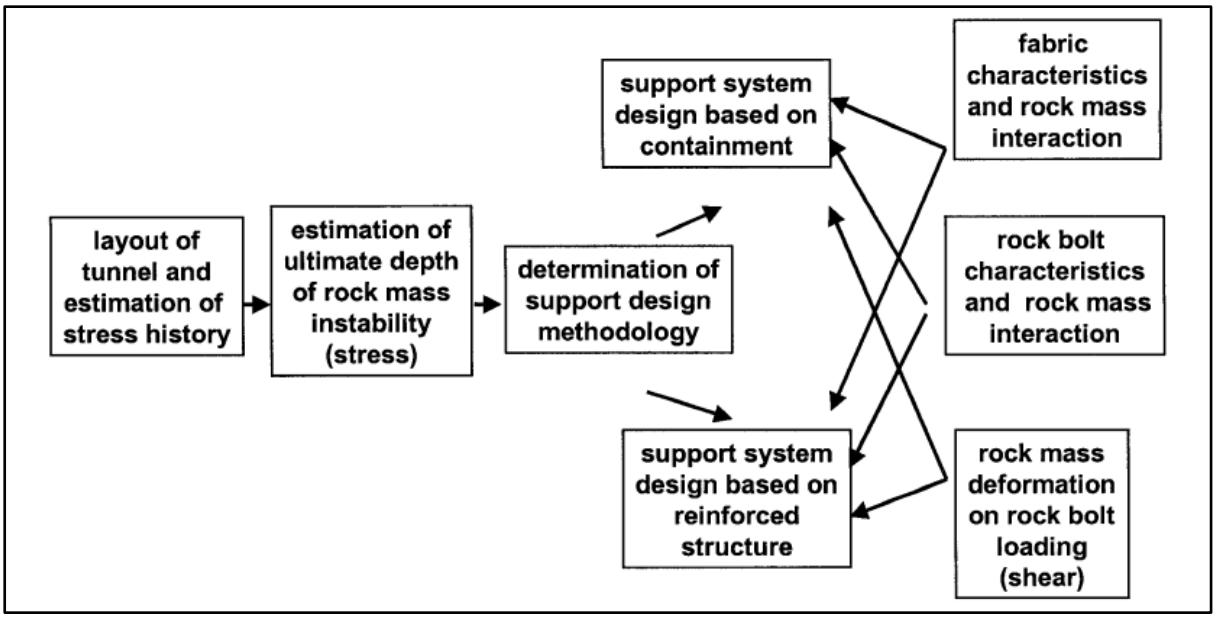


Figure 30: Indicate critical aspects to consider when designing a support in a tunnel (Haile et al. 1998)

3.8 Data Collection Process

The data was collected from the Northam Geology department, where core logging analyses were conducted. The information assisted in the calculation of RQD, Q rating, RMR, and GSI. Scan line mapping underground was performed to obtain the orientation of geological structures. Additionally, to the primary data gathered from underground observations and mapping, secondary data was sourced from a literature review that encompassed a thorough examination of case studies. A myriad of documentary resources can be employed to collect

data for any study (Mouton & Marais, 1994). Sources may include library collections, mass media materials, or archival records. According to Leedy and Ormrod, (2001) It is essential to employ a diverse array of data collection methods when undertaking qualitative research. The sources of data collected for the Northam study are as follows

Literature review on mining through water-bearing fissures.

- Visual underground observation on development mining through fissures at Northam Platinum Mine.
- Peer-reviewed journals for the literature review.
- Textbooks and handbooks addressing mining through complex fissures.
- Maps and sections, Borehole logs and Geological logs.
- The engineering properties of rock masses are delineated through both field and laboratory investigations.

3.9 Data Analysis

Data analysis serves as a formidable approach to tackling intricate challenges (Mouton & Marais, 1994). Analysis can reveal underlying patterns that may not be readily apparent when examining the dataset in its entirety, due to potential discrepancies. The data analysis includes interpreting, visualising, and exploring insights from clean datasets. It involves several steps, including defining the problem, collecting data, analysing the results, and interpreting. Vithal and Jansen (2019) assert that data must undergo a meticulous process of scanning, cleansing, and reorganisation, encompassing three essential steps in the analytical procedure. The steps are defined below

- Prudent examining and identifying trends to ensure accuracy.
- Analyse the data to identify patterns and trends and.
- Interpreting the data to derive significant conclusion.

By adopting these exemplary practices, researchers can ensure that their findings are precise, dependable, and actionable. To proficiently process research data, it was essential to present it in a structured and comprehensible manner. This work entails organising data into tables, graphs, and statistical summaries, thereby allowing for the emphasis of key study details (Vithal & Jansen, 2019). In this investigation, rock mass classification was displayed in tabular form, and support design charts were employed for the selection of supports. The response of the rock mass was elucidated through numerical modeling simulations.

3.10 Chapter Summary

This chapter presents a comprehensive overview of the research methodology. and design and articulating the methods employed to ensure the validity and reliability of the study. This includes data collection, underground mappings, and data analysis. This research encompasses both qualitative and quantitative methodological designs, as it examines numerical data and case studies to formulate recommendations for the study. The rock mass classification systems were employed to assess the quality of the rock formation. The Q system (NGI, 2022) , RMR (Bieniawski, 1989) and MRMR (Laubscher, 1990) were used. The reliability of the research was fortified through a diverse array of data collection methods, including desktop studies, literature reviews, and field observations. Furthermore, the analytical, empirical, laboratory, and numerical analysis techniques were thoroughly examined. The GAP 335 on tunnel design, which necessitates a comprehension of rock mass behaviour and the performance of support systems for effective support design, was briefly discussed. Laboratory testing was performed by reputable service providers such as CSIR and Rocklab. Likewise, numerical modelling analysis was employed to validate empirical and analytical solutions in comparison with field data.

CHAPTER 4 DATA FOR THE STUDY

4.1 Introduction

This chapter briefly summarises the primary data collected for the study. Geological cores were drilled ahead of mining faces to understand the quality of the rock and to facilitate rock mass classification. The three haulages mining through water fissures experienced similar ground conditions as the case studies discussed in the literature review, the haulages mine through geological complex regions. As in the previous chapter, where the research approach was discussed, this chapter discusses the data required which will be used to obtain the results. This dataset encompasses a variety of parameters, including different types of rock, joint properties, joint frequency, and joint orientations on three haulages mining through water fissures. Physical underground observations for the three haulages are also discussed. The two haulages are on the eastern side of the mine which is 16 Footwall Drive East and 17 Footwall Drive East mining through Little John Dyke and 37-line fissure respectively, and one haulage is on the western side of the mine, which is 14 Footwall Drive west, mining through Big John Dyke. The data presented in this research report will facilitate suitable methods and support mining through water-bearing fissures.

4.2 Developing through the Big John Dyke at 14-level Footwall Drive West

Location of 14 FDW

The 14-level Footwall Drive West is on the western side of Zondereinde Northam Platinum Mine, approximately 2094 m below the surface (virgin stress ~61 MPa). The footwall drive is in Norite rock type (UCS ranging between 100 MPa and 130 MPa). The development end is approaching the Big John Dyke, which is 40m thick and striking NW-SE (refer to Figure 31).

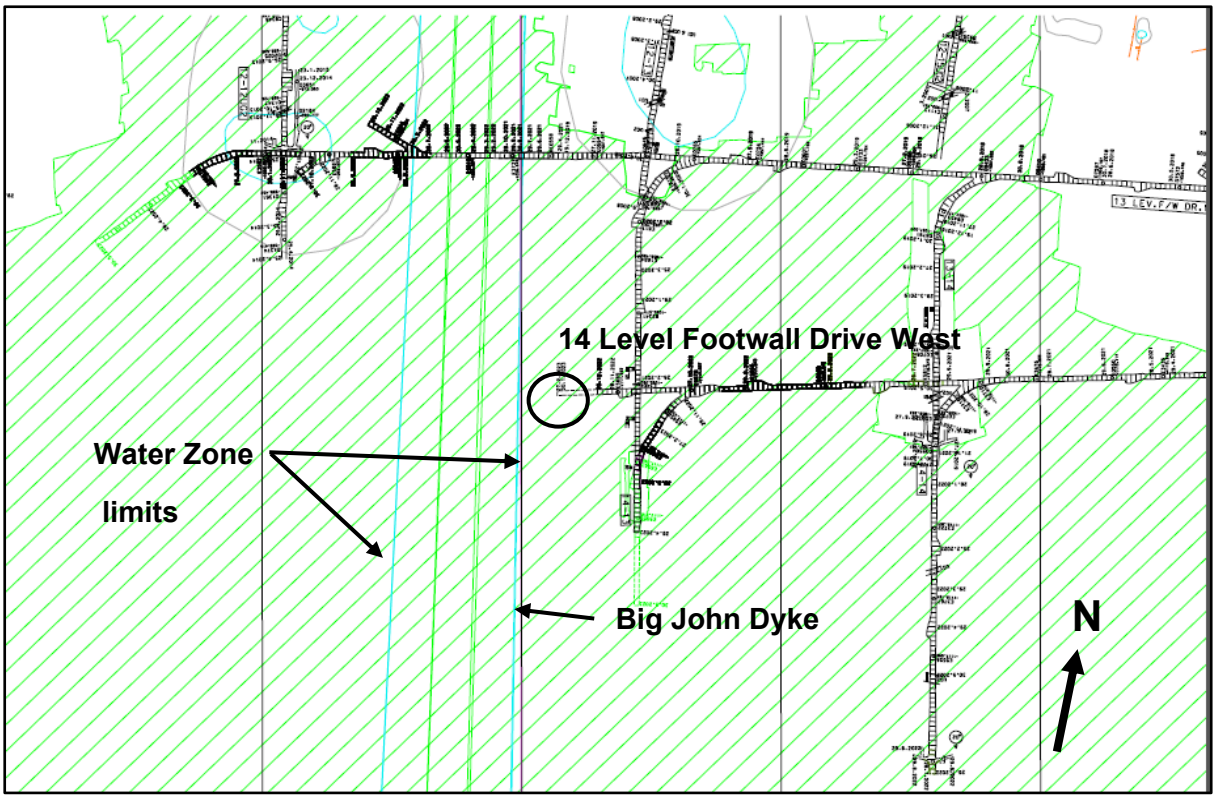


Figure 31: Plan depicting 14 Level Footwall Drive West

Geology and Seismicity in this Area (Big John Dyke area)

The dyke is brittle and weak in its contact with the host rock. More prominently, it comprises a shear zone on its eastern contact and is of the major water-bearing fissures in the mine. The dyke is composed of medium to coarse calcic plagioclase and clinopyroxenene olivine and quartz with laminated rocks. The contact zones are fine-grained and glassy with closely spaced joint creating blocky condition. Usually, these dykes would be considered a significant seismic hazard at this depth, mainly if the mine was situated in the Witwatersrand Basin (i.e., deep-level gold mines). However, seismic studies at Zondereinde Mine (i.e., deep-level platinum mine) have indicated that these dykes are not sources of seismicity; the rock types are more ductile (COP Zondereinde Mine).

Physical Underground Conditions Observations at 14 FDW

This area was visited on 23/01/24 by the Rock Engineer, and detailed assessment and observations were conducted. The host rock is still Norite; the haulage is approximately 6m from the Big John Dyke contact.

Observations at the face area

The following observations were made at 14 Footwall Drive West

- The footwall drive was measured at Peg E5706 +17m.
- The Q rating of the development is between 0.1-0.3, indicating poor to very poor conditions.
- The MRMR calculated is 32 showing poor ground conditions.
- The dimensions of the excavation were measured at a width of 3.8m and a height of 3.7m, respectively.
- The host rock is Norite traversed by prominent shallow dipping joints that create a wedge in the hanging wall. The dip of the joints is approximately 30°- 45°. The joint surfaces are smooth and filled with serpentinite.
- Shallow dipping joints are inherently unstable if not adequately supported.
- Prominent steep dipping joints (70°-80°) were also observed in both sidewalls at the face area. The joints strike in a North-South direction.
- The joint surfaces were smooth and infilled with serpentinite.
- This excavation is approaching Big John Dyke, and extremely poor ground conditions are expected ahead.
- There was water dripping from the hanging wall.
- Intense stress fractures were observed in the tunnel's sidewalls. These, in combination with prominent joints, exacerbate poor ground conditions.
- Loose rocks were observed on both sidewalls.
- This tunnel is high risk, with a rock mass rating of 36 and MRMR of 32, which indicates poor ground.

Conclusion

The current ground conditions are blocky with highly weathered joints. The ground conditions will worsen as the tunnel approaches Big John Dyke, which is known to have shear zones.

4.3 Geological Core Logging from Faces (14 FDW)

Figure 32 illustrates a core drilled horizontally from HT030 ahead of 14 Footwall Drive West; the core exhibits moderately weathered rock walls due to rock type change from Norite to Dolerite dyke. Intermediate to steep dipping joints were observed on the core. The Rock Quality Designation ranges from 48-60%. A major factor that reduces the Q rating and MRMR is the presence of water in this area.



Figure 32: Borehole HT030 drilled, moderately weathered joints were recorded at Borehole HT030 from 24-28.4m.

Figure 33 illustrates discing in HT030 cores due to closely spaced joints and stress fractures. Shallow dipping joints were also recorded in the core. Empirical methodologies were employed to scrutinise the data. The Rock Quality Designation ranges from 50-66%. The presence of water in this region significantly diminishes the Q rating and MRMR.



Figure 33: Shows Borehole HT030 drilled, with some areas with disc failure at the core at Borehole HT030 from 8.8-16.4m.

4.4 Mining between Little John Dyke and 37-line Fissure at 16-level East

Location of 16 Footwall Drive East (Figure 34)

The 16-level east haulage is currently mining in a shear zone between Little John Dyke and the 37-line fissure with dripping water in the hanging wall. The tunnel is approaching 37-line fissure, which is highly weathered and jointed. The level is approximately 2235m below the surface (virgin stress ~65 MPa).

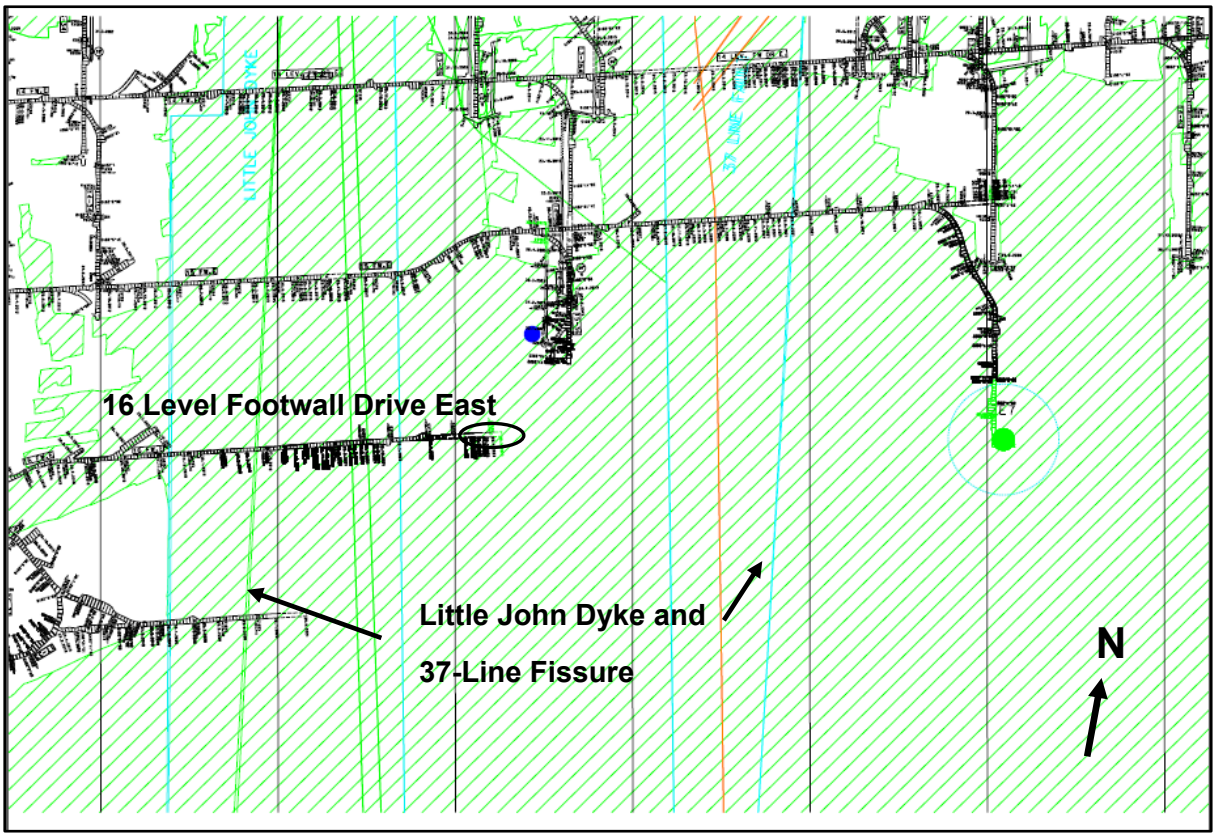


Figure 34: Plan depicting 16 Footwall Drive East approaching 37-line fissure and Little John Dyke associated with poor ground conditions.

Geology and Seismicity in this area (Little John Dyke and 37-Line fissure)

The dyke is brittle and weak in its contact with the host rock. More prominently, it has a shear zone on its eastern contact. This dyke composes of modal olivine and quartz veins, with closely spaced joints inducing blocky ground conditions and is also one of the major water-bearing fissures in the mine and has serpentinite infilling.

Physical Ground Conditions Observations at 16 FDE

This tunnel was visited on 03/07/23 by the Rock Engineer, and the following observations were made. The end has intersected Little John Dyke.

Observations

The following observations were conducted at 16 Foot wall Drive East.

- The face of the footwall drive was measured at Peg E6506 +13.4m.
- The Q rating of the development is between 0.3-0.7, indicating very poor conditions.
- The MRMR calculated is 32, indicating poor ground.
- The end is mining through incompetent ground conditions affected by multiple joints infilled with serpentinite.

- The host rock is Norite traversed by prominent shallow dipping joints that create a wedge in the hanging wall. The dip of the joints is approximately 45°-55°. The joint surfaces are smooth and filled with serpentinite.
- Water dripping from the hanging wall was also observed.
- Cross-cutting joints in combination with stress fractures were also observed in the hanging wall.
- Dimensions were 3.8m high and 4.1 m wide.
- This end is high risk, with a rock mass rating of 40 and MRMR of 32, which depicts poor ground.

Conclusion

The current ground conditions are blocky with highly weathered joints. The ground conditions will worsen as the tunnel approaches Little John Dyke, which is known to have shear zones.

4.5 Geological Cores (16 FDE)

Figure 35 illustrates the shear zone associated with closely spaced joints with infilling. Shallow dipping joints were also recorded. Discing was observed due to dyke and stress fractures. The Rock Quality Designation ranges from 38% to 48%. The presence of water in this region significantly contributes to the diminished Q rating and MRMR.



Figure 35: Shows HD 14051 borehole number from 16 FDE with shear zones seen at the core at HD 14051 from 50.1-57.8m

Figure 36 illustrates altered joints and crushed rock with discing in some areas. Shallow dipping joints were also recorded. Blocky ground conditions are anticipated. Low RQD values are expected. The presence of water in this area is a major factor in reducing the Q rating and MRMR.



Figure 36: Shows Highly jointed rock mass with discing at HD 14051 from 40m-47m

4.6 Mining through Little John Dyke at 17 level east

Location of 17 FDE

The 17-level east haulage is currently mining in a shear zone on the Little John Dyke with dripping water in the hanging wall. The tunnel is approaching 37-line fissure associated with shear zones (Figure 37). The level is approximately 2317m below the surface (virgin stress ~67 MPa).

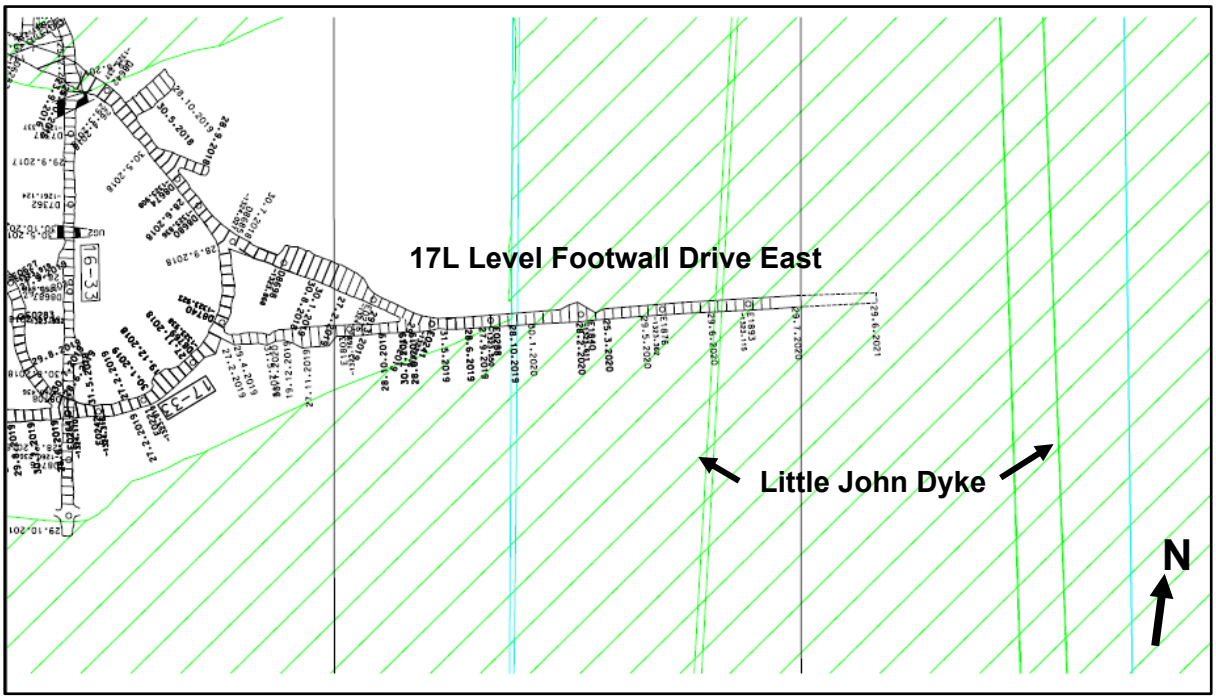


Figure 37: Plan depicting 17 level East foot wall drive passing through Little John Dyke

Geology and Seismicity in this area (Little John Dyke)

The dyke is brittle and weak in its contact with the host rock. More prominently, it has a shear zone on its eastern contact and composes of modal olivine and quartz veins, with closely spaced joints inducing blocky ground conditions. The dyke is also one of the major water-bearing fissures in the mine and has serpentinite infilling.

Physical Ground Conditions

On June 25, 2023, the Rock Engineer conducted a site visit, during which the following observations were made. The end has intersected Little John Dyke.
The end has intersected Little John Dyke.

Observations

- Multiple joints striking north-south were observed on the face. The joints are infilled with Serpentinite and are spaced 0.8m apart.
- Loose rocks were observed on both sidewalls.
- The dimensions were 3.7m high and 3.8 m wide.

Conclusion

This tunnel is currently temporarily stopped because of ventilation issues.
The current ground conditions are blocky with highly weathered joints. The ground conditions will worsen as the tunnel approaches Little John Dyke, which is known to have shear zones.

4.7 Geological Cores from face of 17 Footwall Drive East

Figure 38 illustrates the core drilled from a 17-foot wall drive east with steep dipping joints. This core's RQD is between 40-50%, however, owing to the anticipated presence of water in the vicinity, both the Q rating and MRMR are projected to be low.



Figure 38: Borehole showing steep dipping joints recorded at Borehole HD 14072 m 19-25m

Figure 39 reveals shallow dipping joints and partially altered joints. The core yielded low values of RQD due to closely spaced joints. The availability of water in this region significantly contributes to the decline in both the Q rating and MRMR.



Figure 39 Shallow dipping joints with mechanical drilling break HD 14072 from 35-42m

Table 10: Shows a summary of the RMR and MRMR for the three haulages

Working Place	**Q Rating**	**RMR_{89}**	**MRMR**	**Ground condition**
14 Footwall Drive West	0.2	36	32	Poor to very poor
16 Footwall Drive East	0.3-0.7	40	32	Poor to very poor
16 Footwall Drive East	0.1	33	28	Poor to very poor

4.8. Chapter Summary

This chapter summarised all the data used for the project. Geological core logging was conducted to assess the condition of the rock mass and to derive the Q, RMR_{89}, and MRMR values for evaluating rock quality and formulating support recommendations, the rock mass is classified as poor to very poor. Physical and geological data on the three haulages were discussed.

CHAPTER 5 ANALYSIS AND FINDINGS

5.1 Introduction

This chapter discusses and analyses the findings and results of the three development haulages approaching water fissures at Zondereinde Northam Platinum Mine. The research approach and data are discussed in previous chapters. The techniques for rock characterisation, including geotechnical logging and the mapping of excavations, as well as structural analysis to ascertain joint set orientations and kinematic analyses including dips and unwedge softwares, are examined. Numerical modelling using elastic software analyses to assess the major and minor principal stresses was conducted using Vantage software and results are shown. All the above concepts including fall of ground data base in the next chapter, case studies, and theories assisted in selecting suitable support for mining through these water fissures at the Zondereinde Northam Platinum Mine.

5.2 Structural Analysis using Stereo Nets for 14 Footwall Drive West

Figure 40 illustrates a scatter plot of poles using Dips software. The plot illustrates three orthogonal joint sets: shallow, intermediate, and steeply angled joints, along with their respective strike directions on the 14-west footwall development.

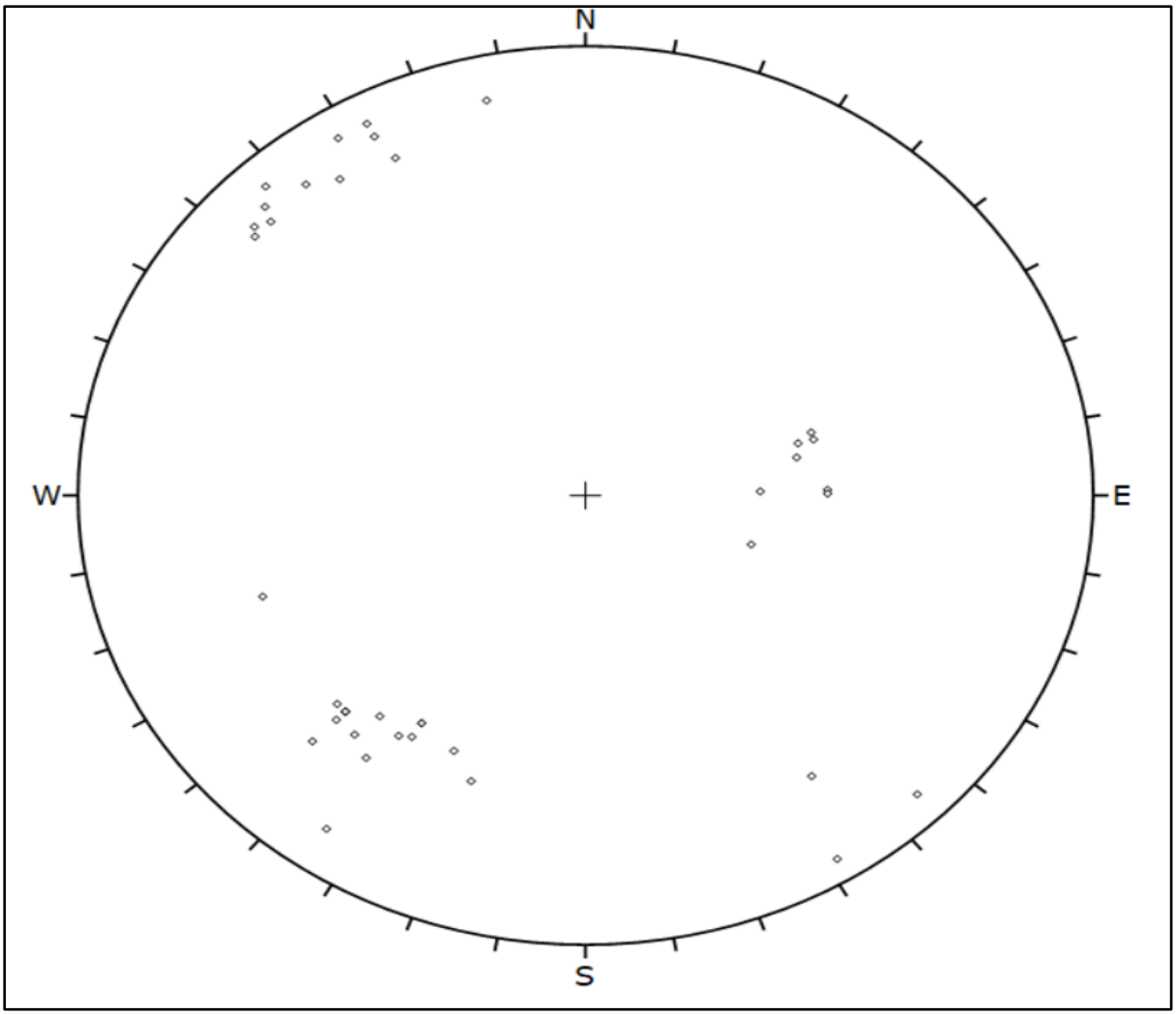


Figure 40: Scatter plot of poles on an equal area lower hemisphere projection at 14 FDW

Figure 41 illustrates the Rosette Plot. The NW-SE joint set is the most predominant configuration, exhibiting an average strike direction of 125° and an average dip of 61°. This set is known as the J1 joint set. This joint set forms wedges in the hanging wall, which are challenging to support with standard rock bolts/resin bolts. According to the joint mapping presented in Appendix C, most joints exhibit a dip towards the east in the southern sections. Among all the surveyed joints, ten exhibited a dip angle beneath 60°, indicating a significant prevalence of low-angled joints. The J2 joint trends from northeast to southwest, boasting an average strike direction of 240° and an average dip angle of 70° in its northern section.

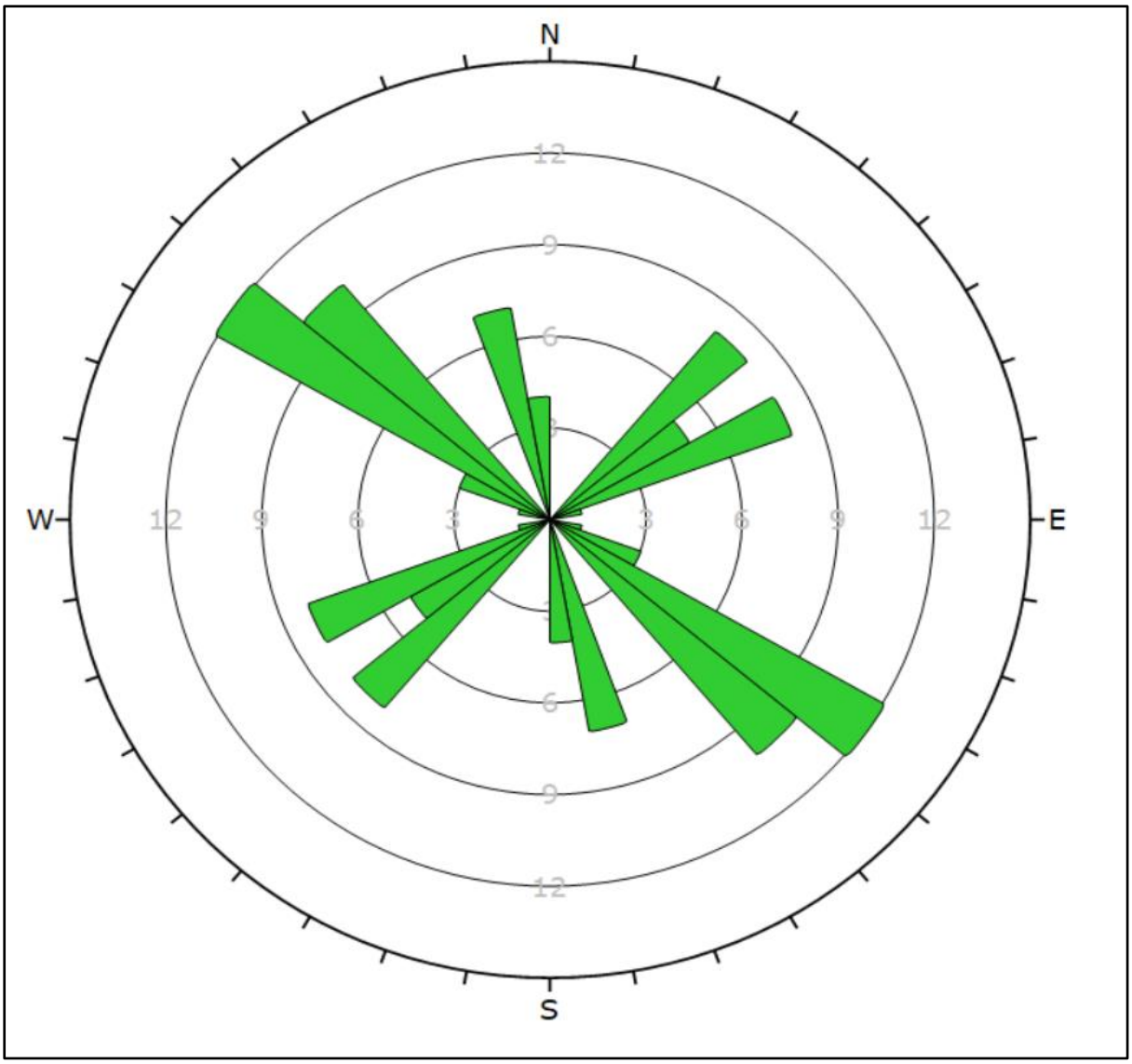


Figure 41: Rosette Plot for 14 FDW depicting dominant joint orientations

Figure 42 illustrates kinematic analyses, which indicate possible wedge failure due to the intersection of three joints. Wedges and shear zones in the hanging wall can cause a large fall of ground if not properly supported. The projection reveals shallow and steep dipping joints with closely spaced joints (Figure 42).

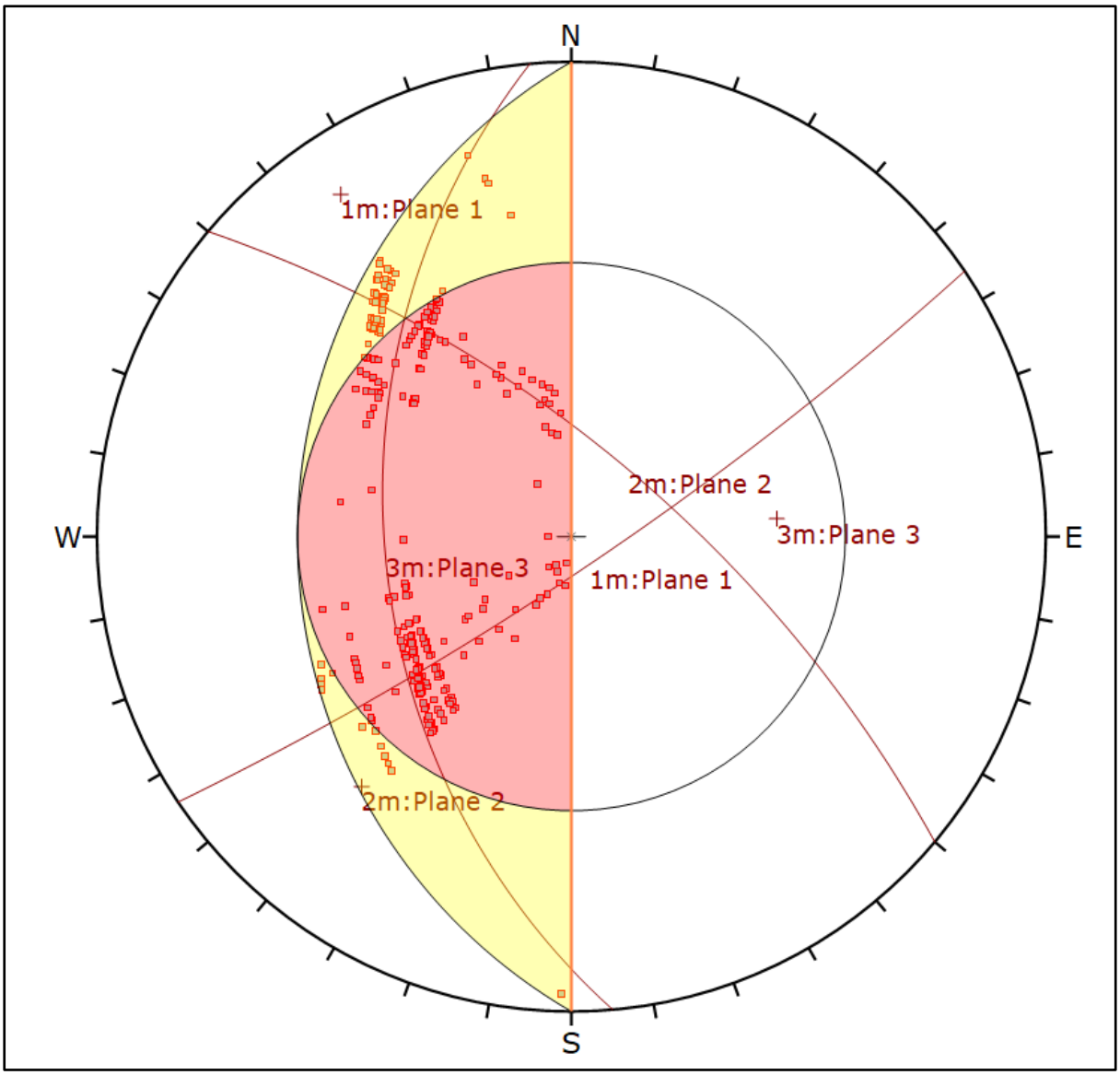


Figure 42: Kinematic analyses showing possible wedge failure on the 14-footwall drive west

The unwedge analysis program for the joint sets for the 14 FDW was conducted (Figure 43). A potentially unstable block has been identified, with an apex height of 3.7m. The anticipated failure mechanisms include wedging, sliding, and crushing. The intersection of the three joint planes is expected to induce possible wedge failure at the hanging wall and sidewalls. The

1.8m bolts and long anchors could not contain the wedges in the hanging wall, as the safety factor was calculated below the 1.5 threshold.

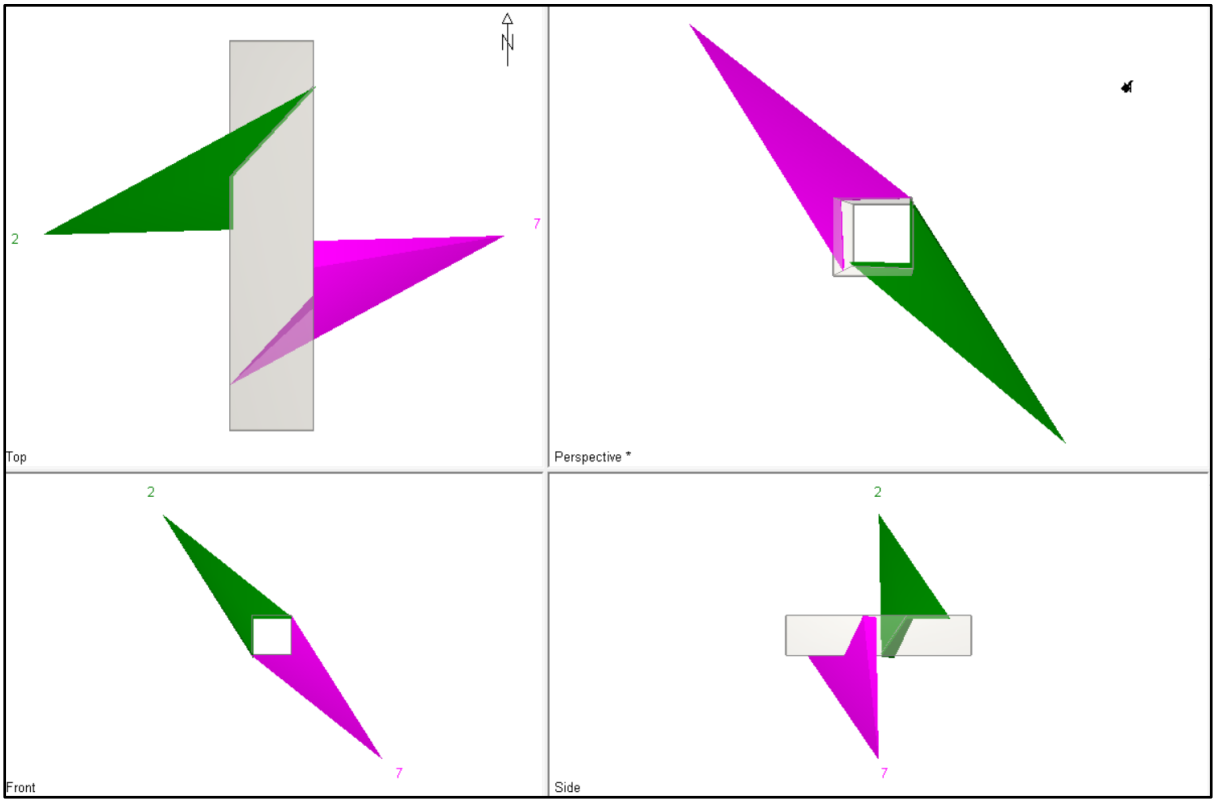


Figure 43: Simulated wedges in the rock mass surrounding the 14-foot wall haulage

5.3 Rock Mass Classification Analyses at 14 FDW

Rock mass classification data was collected from the geotechnical core recovered from cover drilling ahead of the development end faces. Cover hole data indicates poor rock mass conditions with an average Q, RMR, and MRMR of 0.2, 36, and 32, respectively. Water was intersected near the dykes. The GSI ranges from 25 to 30, denoting substandard to exceedingly poor ground conditions attributed to a fractured rock mass and the presence of moisture. Figure 44 illustrates the Q support charts.

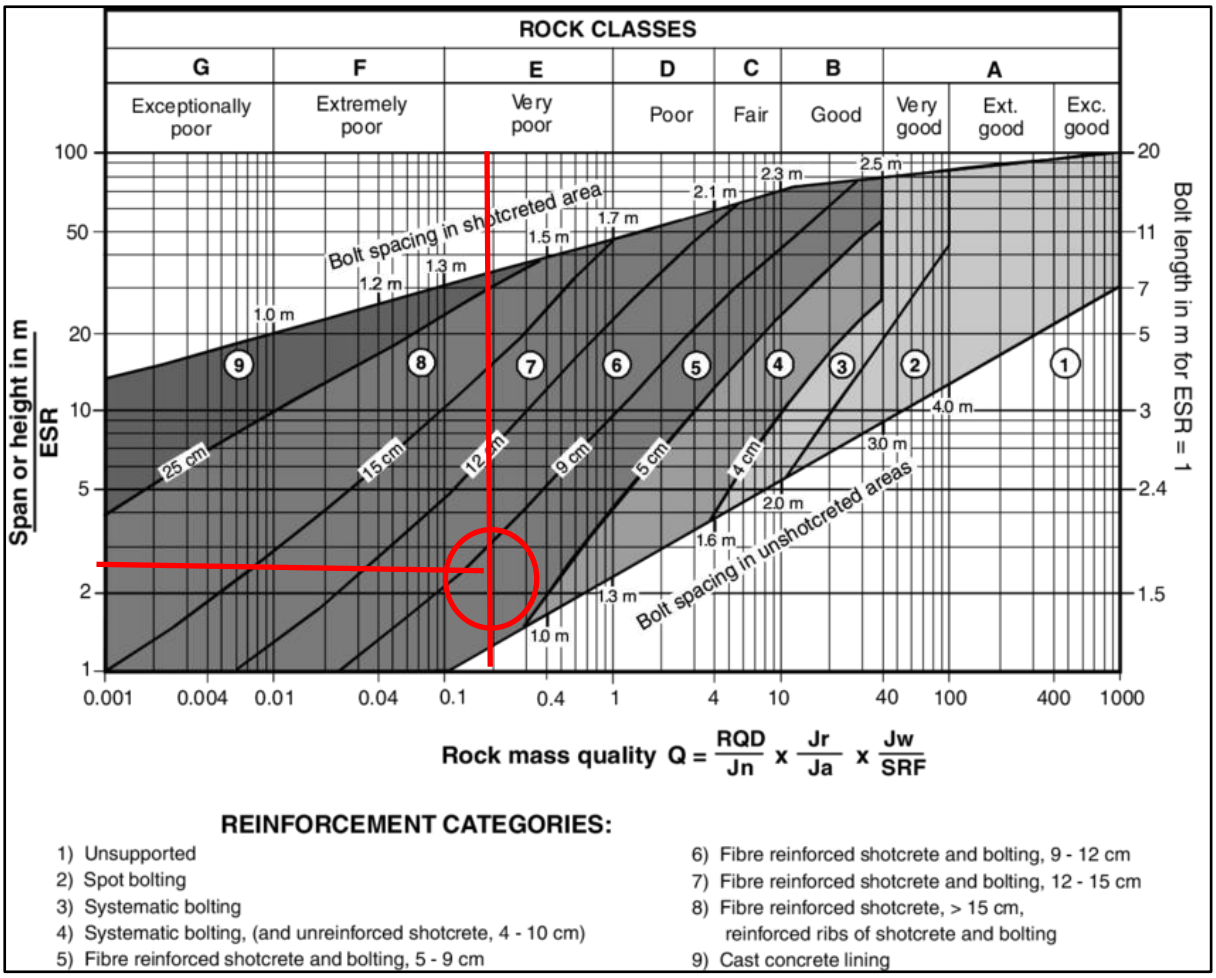


Figure 44: Estimated support categories where poor ground conditions are experienced

The excavation support ratio is 1.3, as this is a permanent opening, and the Q rating was calculated at 0.2. The intersection of these factors suggests that very adverse ground conditions are expected, necessitating stringent support measures. The case study at Northam Platinum is affected by all these factors. The adjusted MRMR was calculated as 32.

The average Q rating of 0.2 and MRMR of 32 with unsupported span were used to assess the stability of the haulage. According to best practices, the factor of safety should be 1.5; however, the factor of safety for haulage falls beneath this recommended threshold, indicating potentially unstable ground conditions (Figure 45).

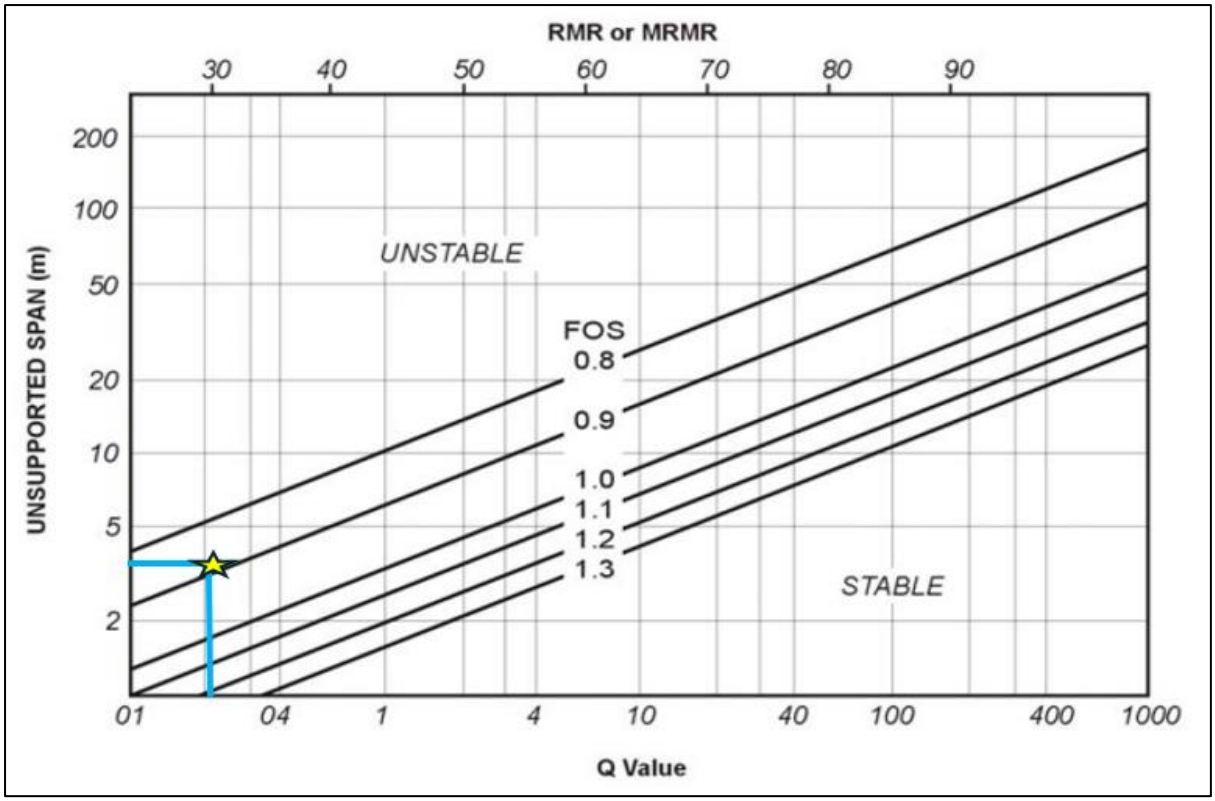


Figure 45: Unsupported span vs Q/RMR/MRMR of the 3.8m span haulages (Stacey & Swart, 2001)

The duration for standing up, as a function of unsupported span RMR values, is illustrated in Figure 46, while the recommended support in accordance with the RMR system is presented in Table 11

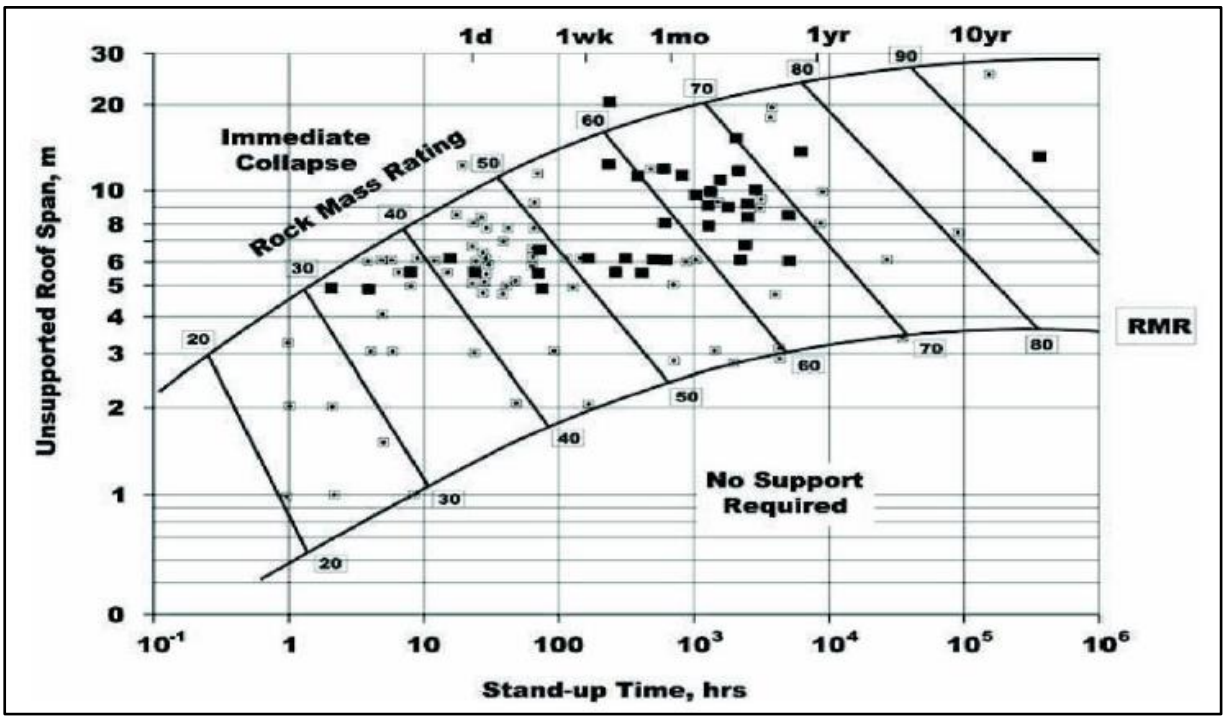


Figure 46: Unsupported span as a function of RMR as sited by Bieniawski and Lowson (2013)

Table 11: RMR classification system guide for excavation and support in rock tunnels (Bieniawski, 1989)

Rock mass class	Excavation	Support		
		Rock bolts (20 mm diam., fully bonded)	*Shotcrete*	*Steel sets*
1. Very good rock RMR: 81-100	Full face: 3 m advance	Generally no support required except for occasional spot bolting		
2. Good rock RMR: 61-80	Full face: 1.0-1.5 m advance; Complete support 20 m from face	Locally bolts in crown, 3 m long, spaced 2.5 m with occasional wire mesh	50 mm in crown where required	None
3. Fair rock RMR: 41-60	Top heading and bench: 1.5-3 m advance in top heading; Commence support after each blast; Commence support 10 m from face	Systematic bolts 4 m long, spaced 1.5-2 m in crown and walls with wire mesh in crown	50-100 mm in crown, and 30 mm in sides	None
4. Poor rock RMR: 21-40	Top heading and bench: 1.0-1.5 m advance in top heading; Install support concurrently with excavation - 10 m from face	Systematic bolts 4-5 m long, spaced 1-1.5 m in crown and walls with wire mesh	100-150 mm in crown and 100 mm in sides	Light ribs spaced 1.5 m where required
5. Very poor rock RMR < 21	Multiple drifts: 0.5-1.5 m advance in top heading; Install support concurrently with excavation; shotcrete as soon as possible after blasting	Systematic bolts 5-6 m long, spaced 1-1.5 m in crown and walls with wire mesh. Bolt invert	150-200 mm in crown, 150 mm in sides, and 50 mm on face	Medium to heavy ribs spaced 0.75 m with steel lagging and forepoling if required. Close invert

The MRMR for the area of interest concerning the haulages, with an initial calculated RMR of 36, averages 32. After applying adjustments of 90% for weathering, 85% for joint orientation, 120% for mining-induced stresses, and 94% for blasting effects, the modified MRMR is.

Adjusted MRMR = 36 x 0.9 x 0.85 x 1.2 x 0.94 = 32

5.4 Numerical Modelling using Vantage Software

The 14-level west footwall drive or haulage was modelled to calibrate the Rock wall condition Factor (RCF) using VANTAGE (Figures 47 & 48). VANTAGE is boundary element software that applies linear elastic modelling. The RCF along the 14 FWD West is above 1.4, indicating poor rock mass conditions (Figure 48). The F-factor was taken as 0.5.

Rockwall Condition Factor (RCF)

The Rockwall Condition Factor is a numerical value that assesses stability and support requirements of rockwalls in underground excavations, particularly tunnels in underground mines. Considering the condition of the rock mass, it is calculated as the ratio of the maximum tangential stress to the strength of the rock. The RCF assists engineers in determining the

appropriate support system for a given excavation based on the anticipated rock wall behavior. (Jager and Ryder, 1999):

The RCF is typically calculated using the following formula:

$$RCF = (3\sigma1 - \sigma3) / (F\sigma_c) \quad [18]$$

Where:

- σ1 and σ3 are the major and minor principal stresses acting normal to the tunnel.
- σc is the uniaxial compressive strength of the rock.
- F is a factor representing the condition of the rock mass, reflecting its strength and stability. The F factor represents downgrading of σc. In good conditions F takes on a value of unity, In a rock mass characterised by significant discontinuity, it is advised that factor F be set at approximately 0.5. For extensive excavations exceeding (>6 x 6m), F may be further reduced by ten percent.

Critical RCF Values:

- A typical RCF table will define critical values that represent different levels of rock stability:
    - **Low RCF (e.g., < 0.7):** Indicates good ground conditions and low risk of rockfalls.
    - **Moderate RCF (e.g., 0.7 to 0.9):** May require some form of support or monitoring, depending on specific conditions.
    - **High RCF (e.g., > 1.4):** Suggests potentially unstable ground and a higher risk of rockfalls, requiring more extensive support or rehabilitation measures.

Figures 47 and 48 illustrate the rockwall condition factor calibrated against different uniaxial compressive strengths. As this haulage traverses different rock types, the strengths will be different. The F factor takes on a value of 0.5 as the expected rock mass is highly discontinuous due to complex geological structures associated with water fissures. The RCF of 1.4 and above indicates that stringent support will be required due to poor ground conditions anticipated.

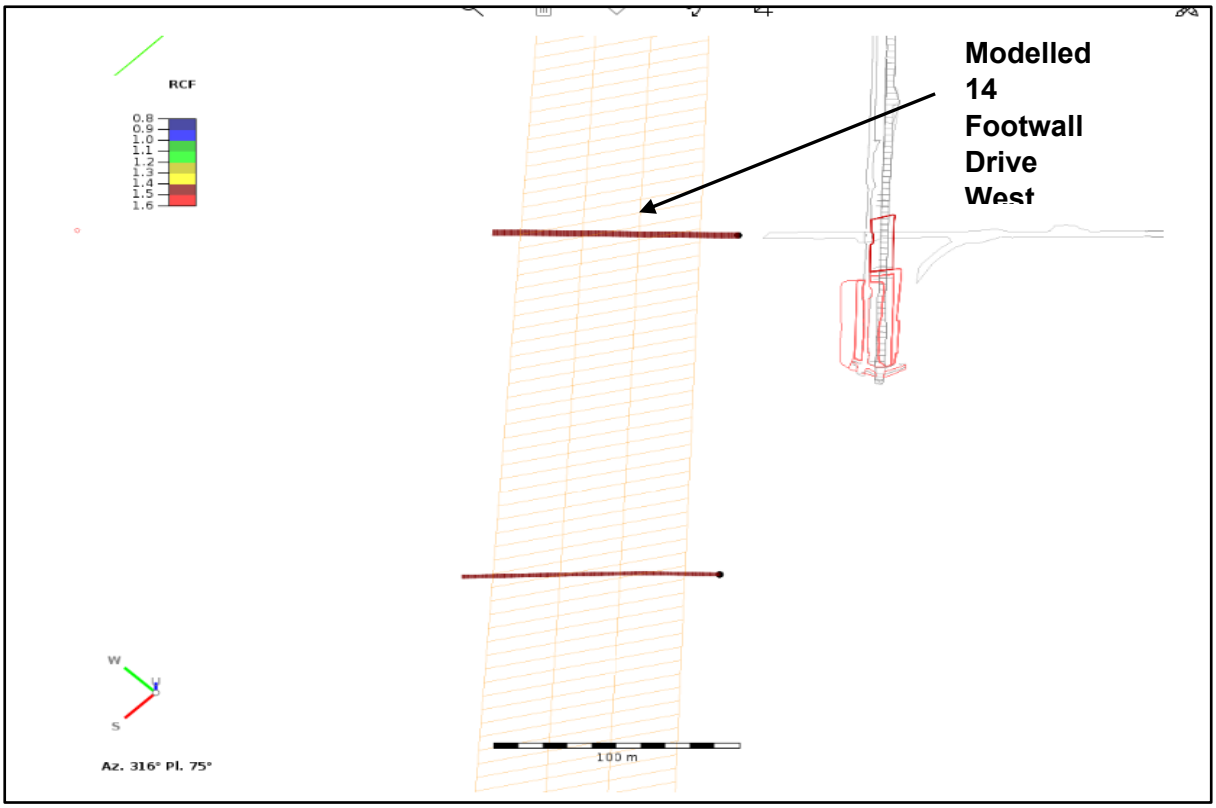


Figure 47: Plan showing 14-footwall drive west haulage traversing Big John Dyke

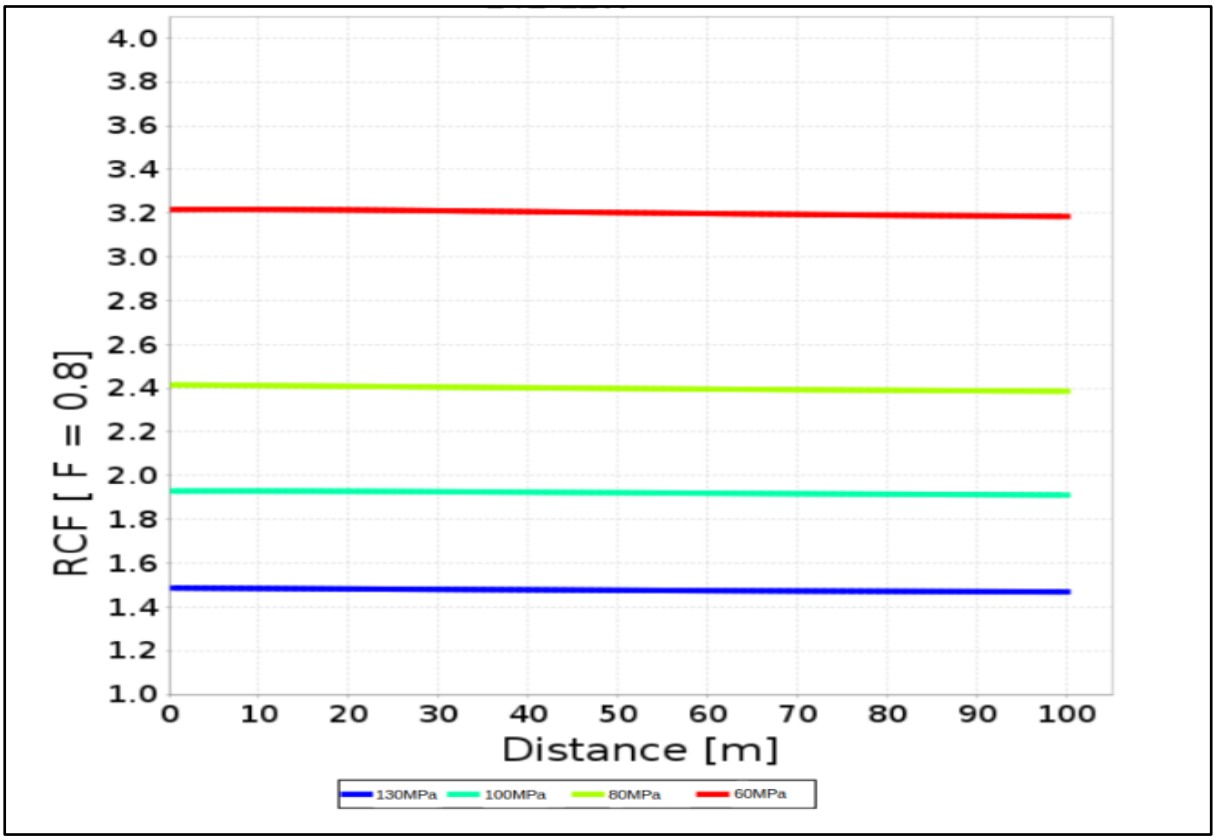


Figure 48: RCF results above 1.4 with UCS values ranging from 60MPa to 130 MPa

5.5 Structural Analysis Using Stereo nets at 16 Footwall Drive East Haulage Introduction

This is a structural analysis for the 16-footwall drive east mining through the Little John Dyke.

Figure 49 illustrates Stereographic plotting with scattered joint sets poles. Shallow, intermediate, and steep angled joints are prominent at 16-footwall drive east.

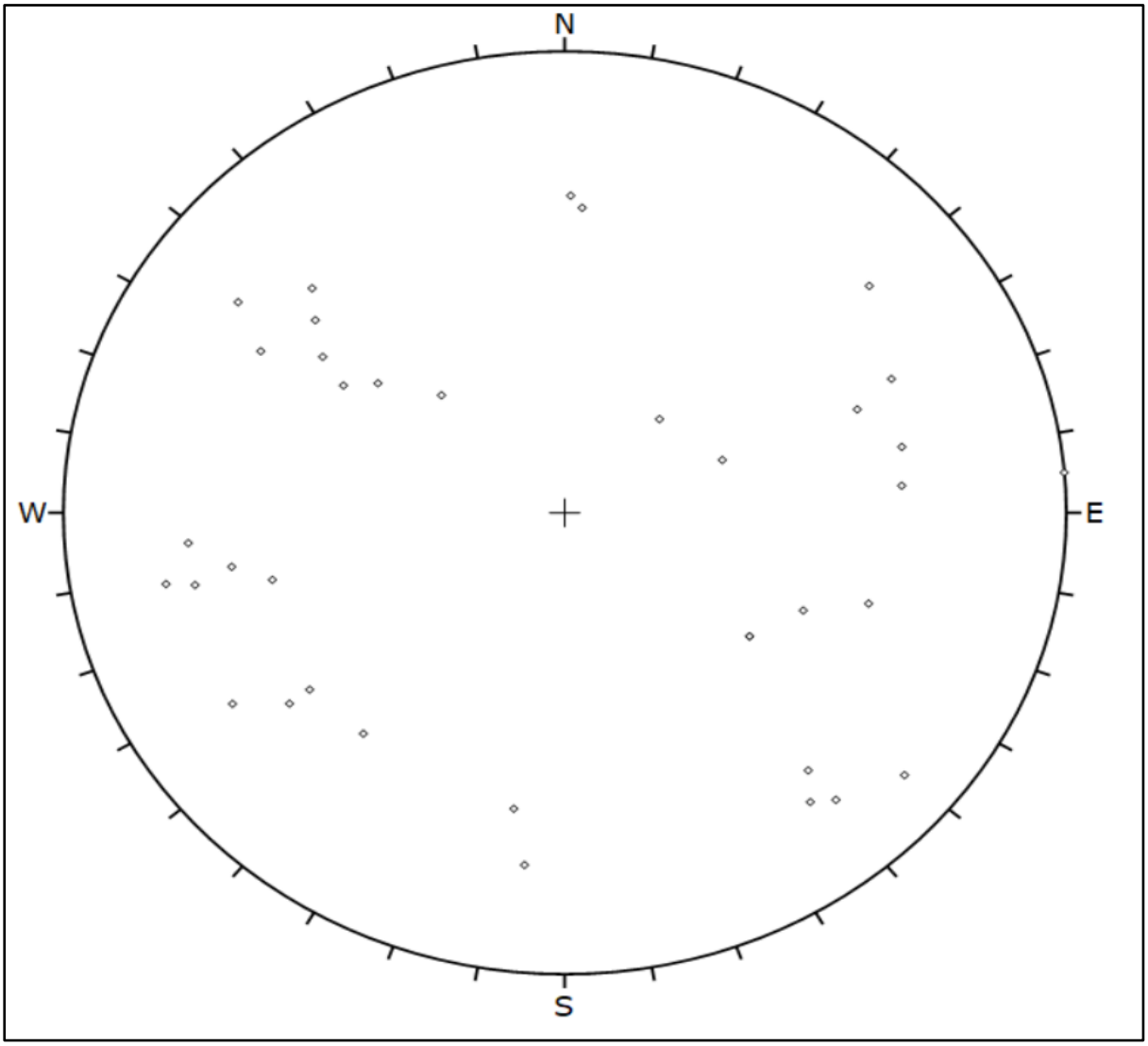


Figure 49: Scatter plot of poles on an equal area hemisphere at 16 Foot Wall Drive east

Figure 50 presents the rosette plot. The NE-SW joint set emerges as the predominant feature, exhibiting an average strike direction of 225° and an average dip of 62°. This particular joint set is designated as the J1 joint set. It generates wedges within the hanging wall, which pose significant challenges for support with rock bolts. Most joints in the southern sections exhibit a westerly dip. Among all the joints mapped, six display a dip angle of less than 60°, indicating the infrequent occurrence of low-angled joints. The J2 joint trends NW-SE, characterised by an average strike direction of 155° and an average dip angle of 70° for the northern section.

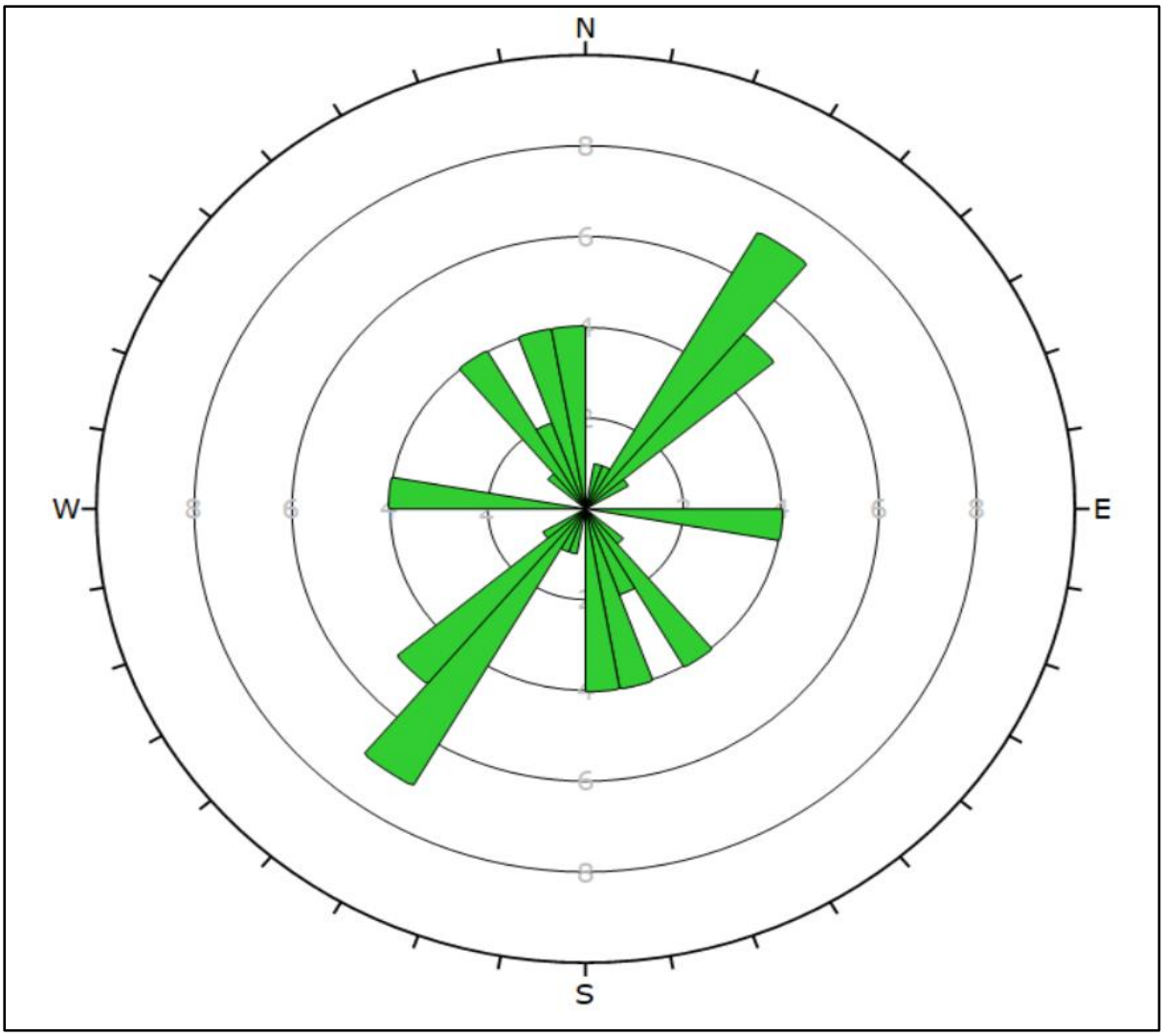


Figure 50: Shows the Rosette Plot indicating the most dominant joint sets

Figure 51 illustrates kinematic analyses, which indicate possible wedge failure due to the intersection of three joints. Wedges and shear zones in the hanging wall can cause a large fall of ground if not properly supported. The projection displays shallow and steep dipping joints with closely spaced joints creating a fall-out thickness of approximately 3.5m.

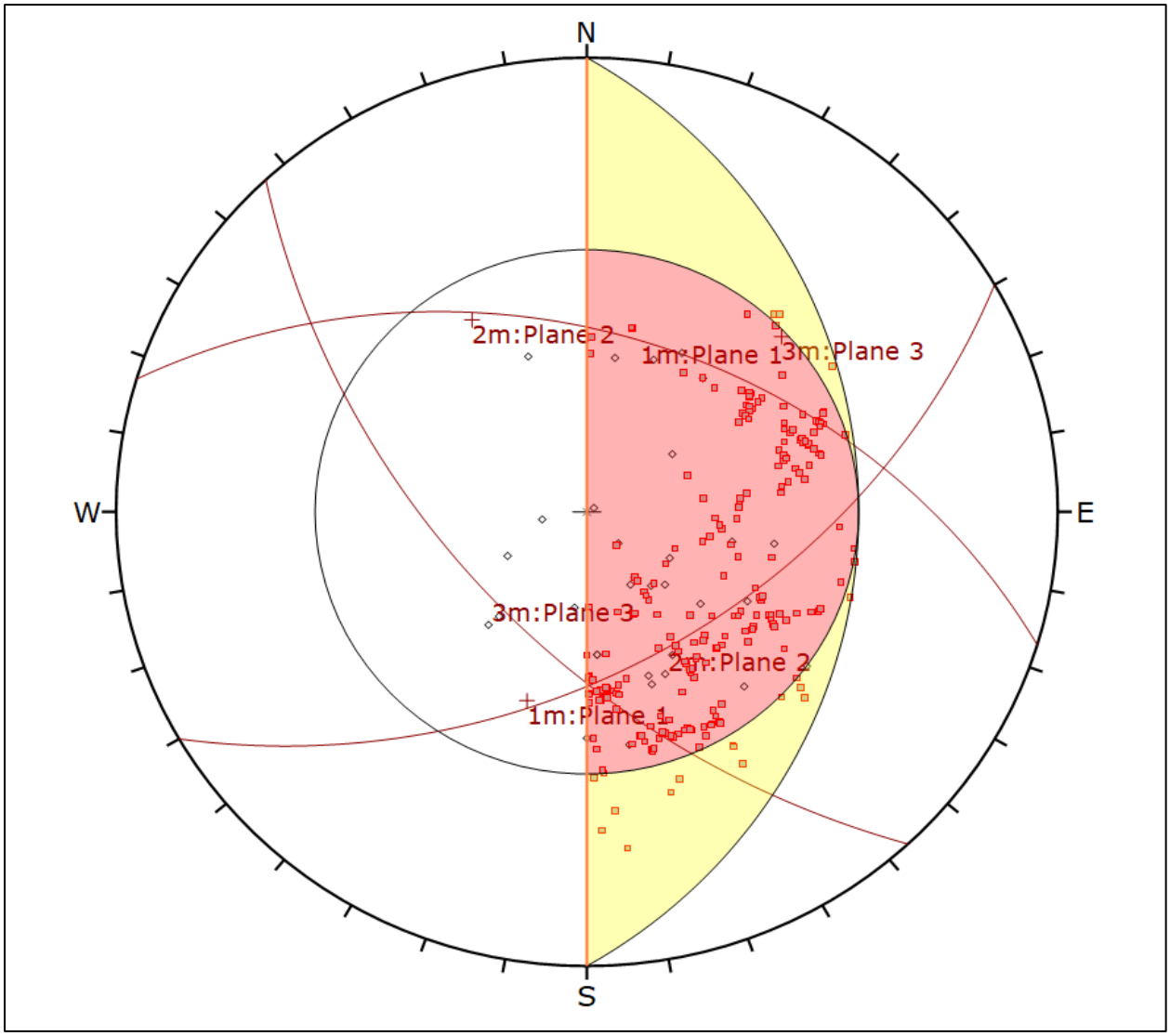


Figure 51: Kinematic Analyses showing possible wedge failure on 16 Footwall Drive East

The unwedge analysis program for the joint sets for the 16 FDE was conducted (Figure 52), A potential unstable block was predicted, featuring an apex height of 3.5m, with the anticipated failure mechanism involving both wedging and sliding. The convergence of the three joint planes is likely to precipitate potential wedge failure at the hanging wall and

sidewalls. Using the 1.8m bolts and long anchors could not contain the wedges in the hanging wall as the factor of safety was calculated below the 1.5 threshold.

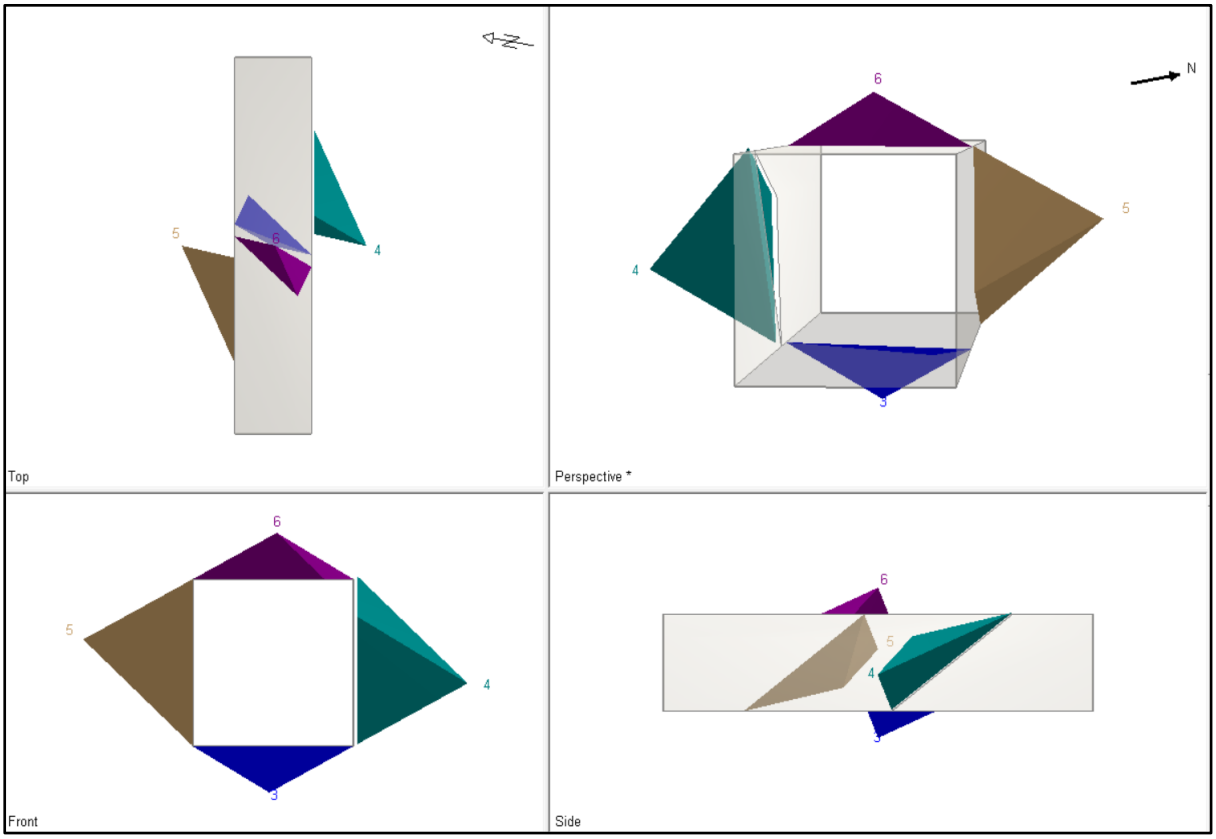


Figure 52: Simulated wedges in the rock mass surrounding the 16 Footwall east haulage

5.6 Rock Mass Classification Analyses at 16 Footwall Drive East Haulage

Rock mass classification data was collected from the core recovered from 16-footwall drive east cover drilling ahead of the development end face. The cover hole data indicated poor rock mass conditions (refer to Appendix I) with an average Q and RMR of 0.3 and 40, respectively. The rock mass classification indicated extremely poor ground conditions due to the stress fractures expected. The GSI ranges between 25-30, indicating poor to very poor ground conditions due to jointed rock mass and the presence of water.

Figure 53 illustrates the Q support chart. The excavation support ratio is 1.3, as this is a permanent opening, and the Q rating was calculated at 0.3. The intersection of these factors indicates that poor ground conditions are expected where stringent support is required. In terms of ground conditions, the MRMR will serve as a superior indicator, as it takes into account the influences of weathering, joint orientation, confining stresses, and blasting. The case study at Northam Platinum is affected by all these factors. The adjusted MRMR was calculated as 32.

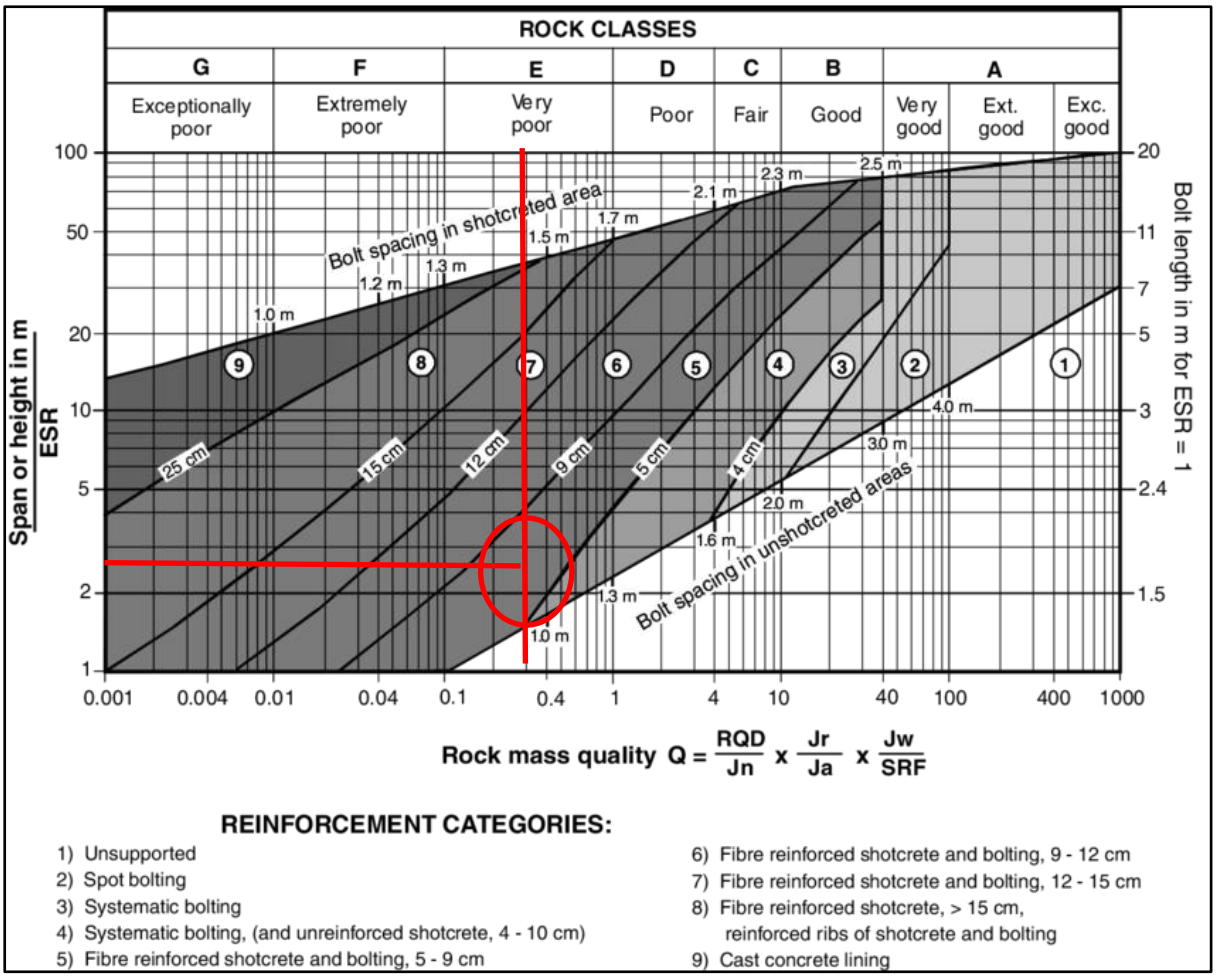


Figure 53 Estimated support categories where very poor ground conditions are experienced

The average Q rating of 0.2 and MRMR of 32 with unsupported were employed to evaluate the stability of the haulage. The recommended safety factor, in accordance with best practices for excavations, should be 1.5; however, the safety factor for the haulage falls below this recommended value, indicating potential unstable ground conditions (Figure 54).

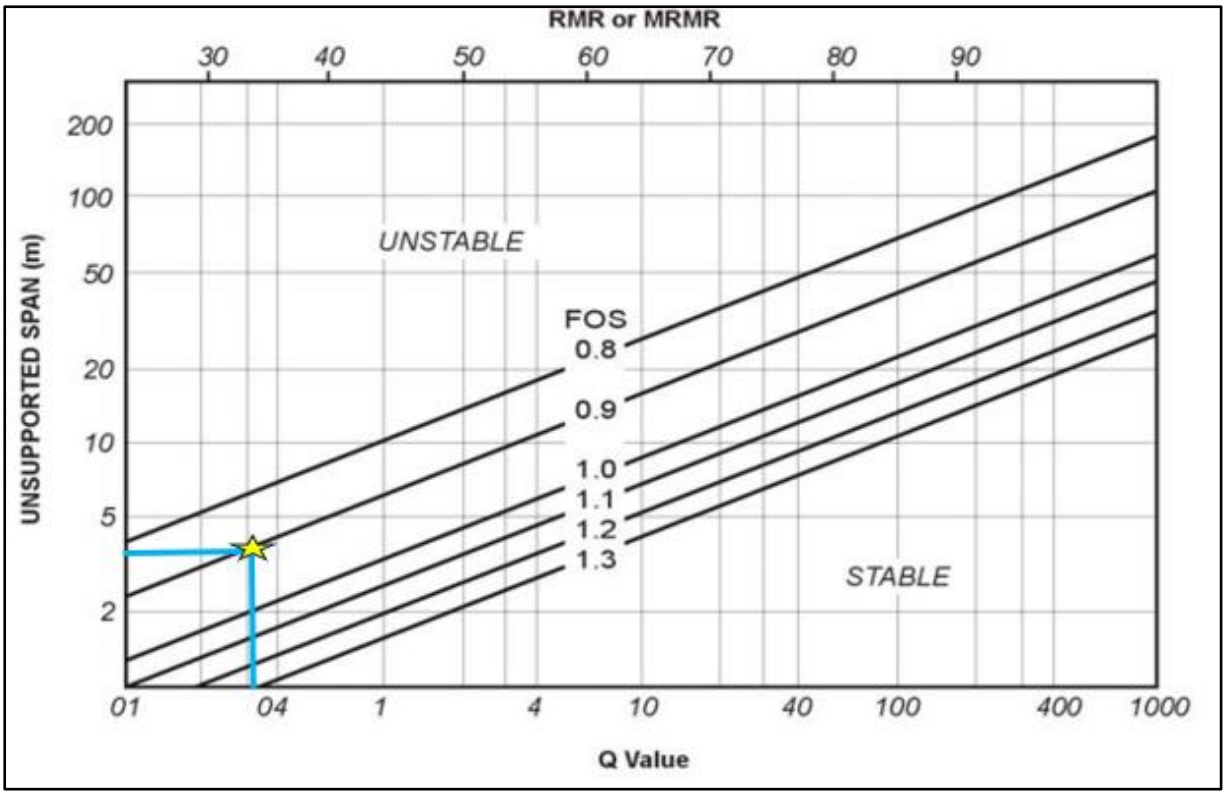


Figure 54: Unsupported span vs Q/RMR of the 3.8m span haulages (Stacey & Swart, 2001)

Stand up time as a function of unsupported span RMR values is given in figure (55)

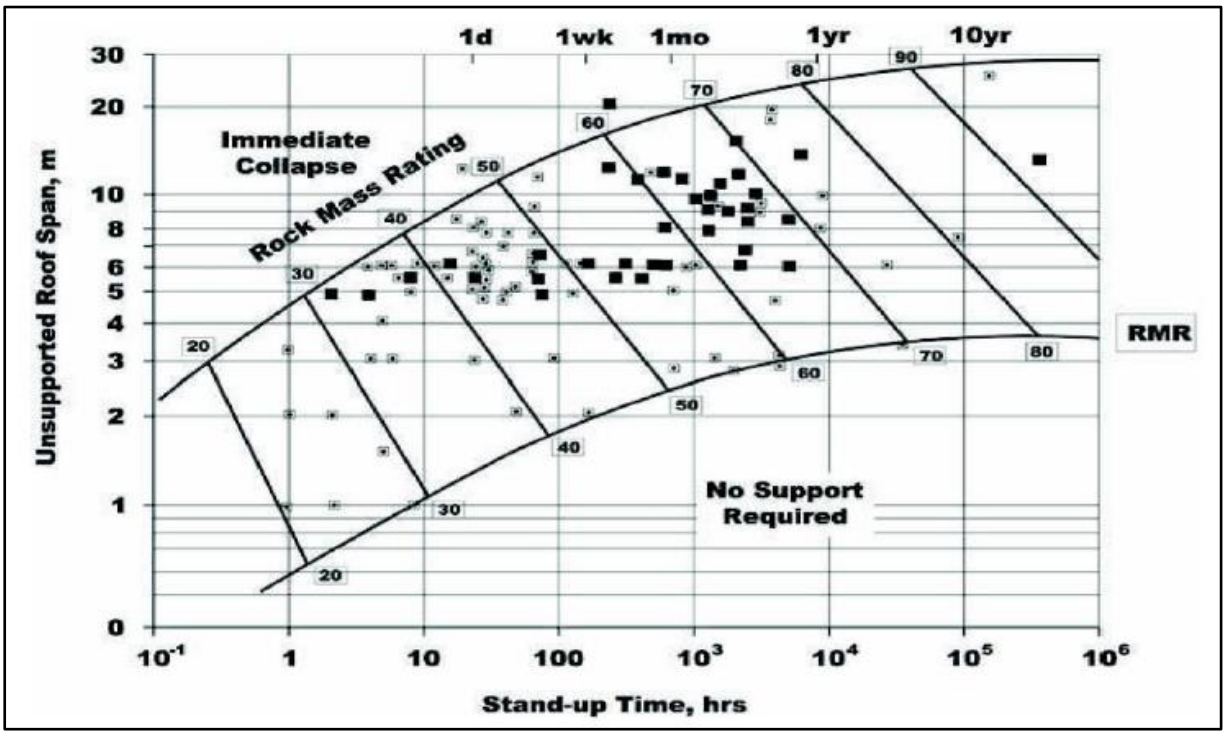


Figure 55: Unsupported span as a function of RMR as sited by Bieniawski and Lowson (2013)

The MRMR for the area of interest concerning the haulages, with an initial calculated RMR of 36, averages 32. Following adjustments of 90% for weathering, 85% for joint orientation, 120% for mining-induced stresses, and 94% for blasting effects, the revised MRMR is.

Adjusted MRMR = 36 x 0.9 x 0.85 x 1.2 x 0.94 = 32

5.7 Numerical Modelling using Vantage Software for RCF Analyses

In addition to the analysed rock mass classification data, the footwall drive or haulage was modelled to calibrate RCF using VANTAGE. The RCF along the 16 FWD East is above 1.4, indicating poor rock mass conditions (Figure 47). The F factor takes on a value of 0.5 as the expected rock mass is highly discontinuous due to complex geological structures associated with water. Figures 56 & 57) illustrate rock wall condition factors calibrated with different uniaxial compressive strengths. As the haulage traverses different rock types, the strengths will differ. The RCF of 1.4 and above indicates that stringent support will be required.

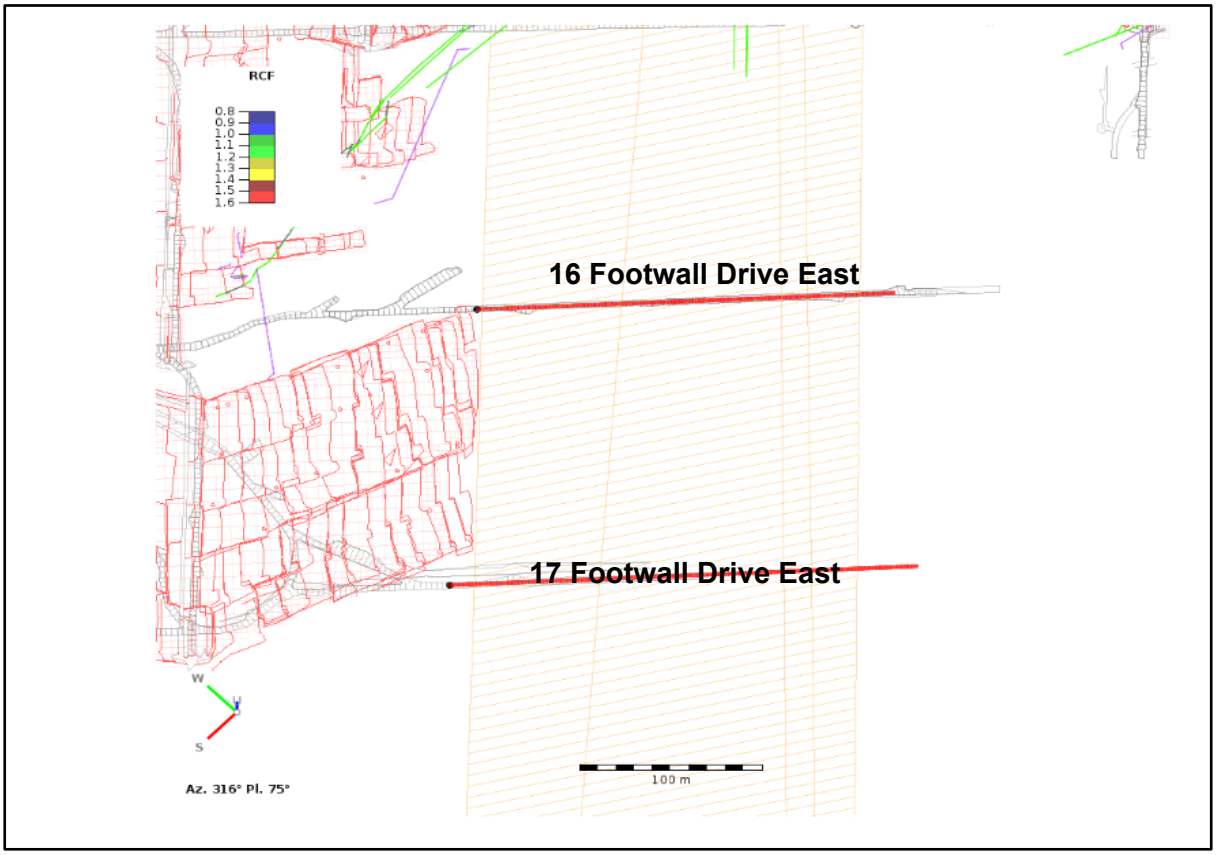


Figure 56 Plan depicting 16 Footwall Drive East and 17 Footwall Drive East

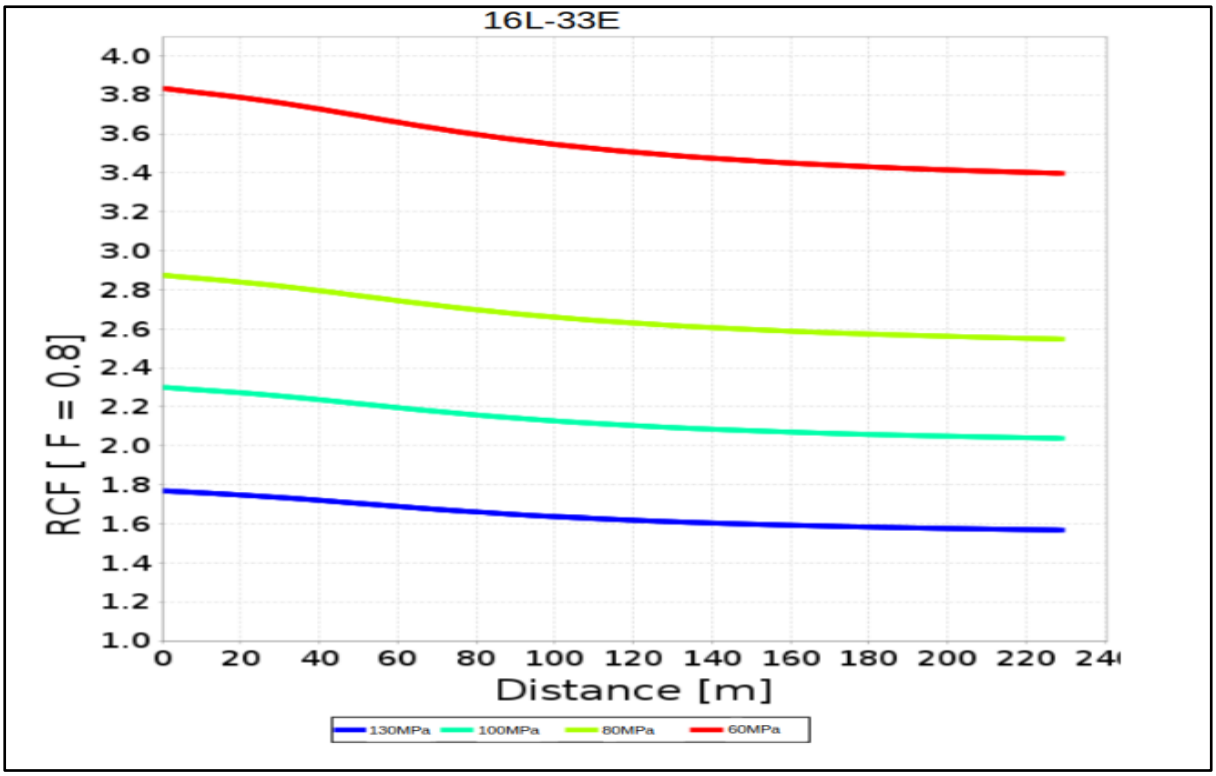


Figure 57: RCF results for 16 footwall drive east at different strengths

5.8 Structural Analyses using Stereo Nets at 17 Footwall Drive East Haulage

Introduction

This is structural analysis for the 17 footwall drive east mining through the Little John Dyke. Figure 58 illustrates Stereographic plotting with scattered joint sets. Intermediate joints with angles and their corresponding strikes directions at the 17- Footwall Drive east haulage.

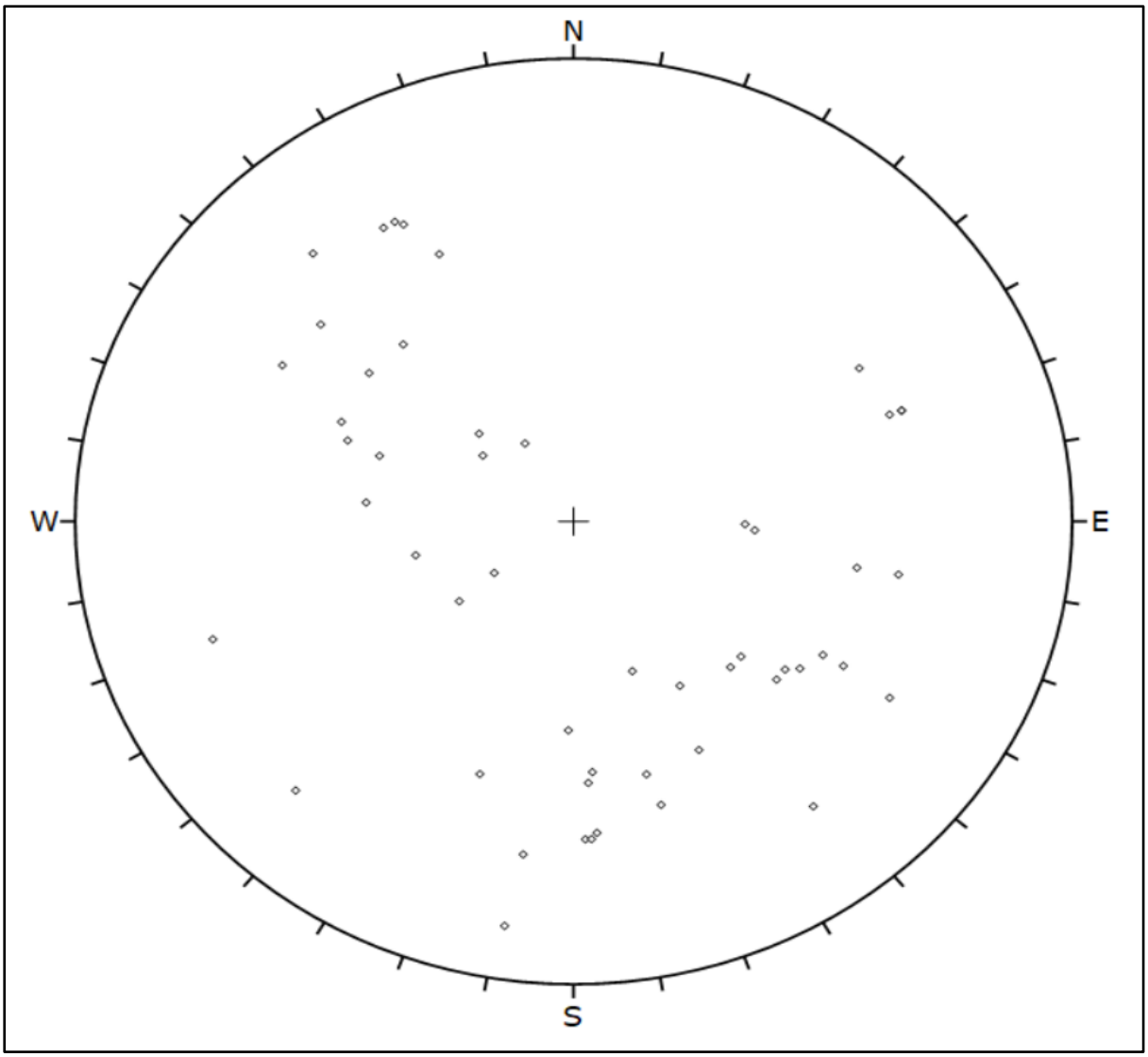


Figure 58: Stereographic plot with poles showing joints at scattered points at 17 FDE

Figure 59 illustrates Rosette plot. The NE-SW joint set is the most dominant one, with an average strike direction of 210° and an average dip of 63°. This set is referred to as the J1 joint set. This set is designated as the J1 joint set. This joint set forms wedges in the hanging wall, which are difficult to support with rock bolts. From the joint mapping (Appendix D), most of the joints dip towards the northeastern direction in the northern sections. Among all the mapped joints, nine exhibited a dip angle below 60°, indicating a scarcity of low-angled joints. The J2 joint trends in an east-west orientation, exhibiting an average strike direction of 260° and a mean dip angle of 70° in the northern section.

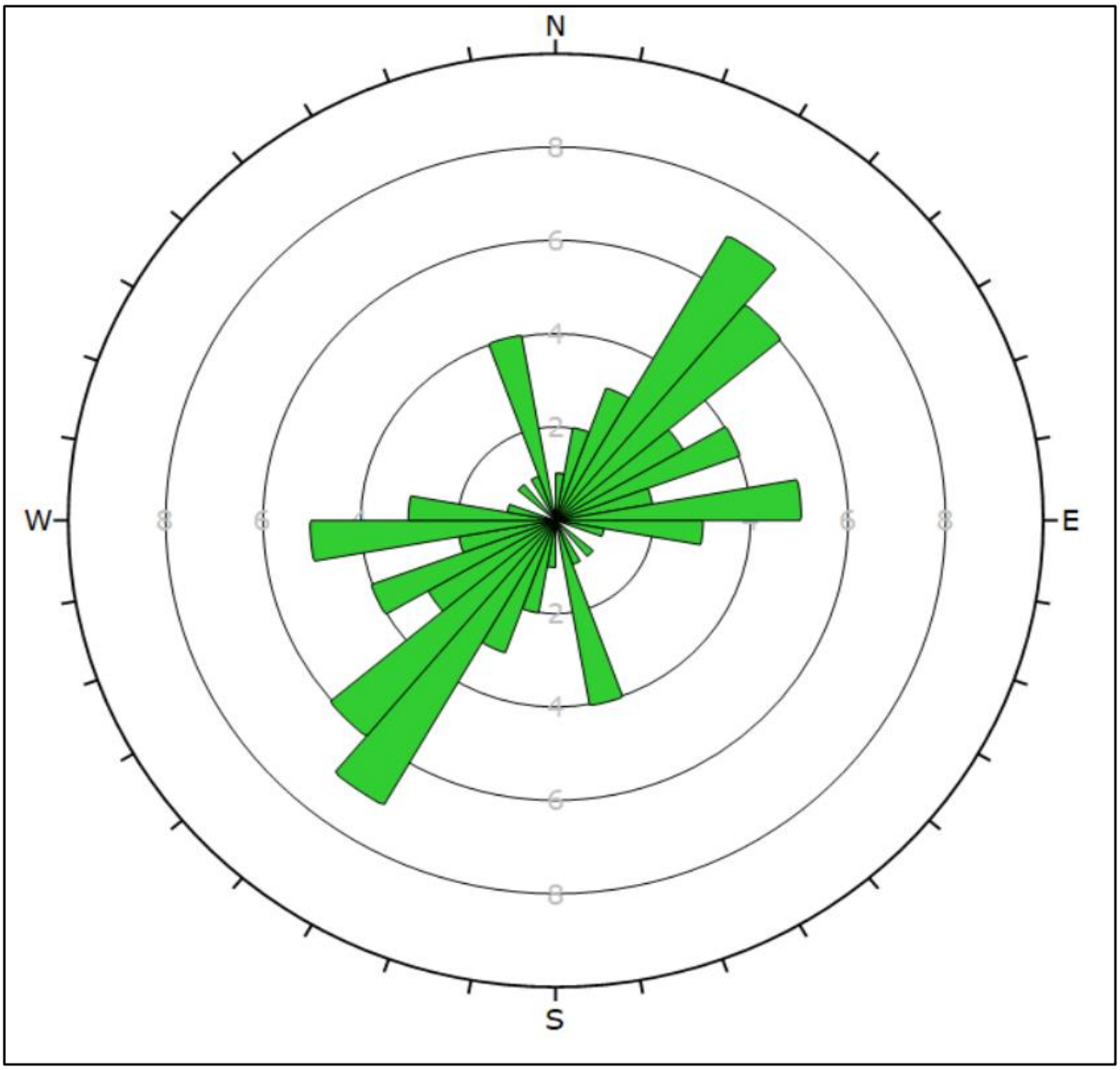


Figure 59: Depicts Rosette Plot showing the most dominant joint sets at 17 FDE

Figure 60 illustrates kinematic analyses, which suggest a potential wedge failure resulting from the convergence of three joint sets. Wedges and shear zones in the hanging wall induce large fall of ground if not properly supported. The projection shows that shallow and steep dipping joints create a fall-out thickness of approximately 3.5m with closely spaced joints.

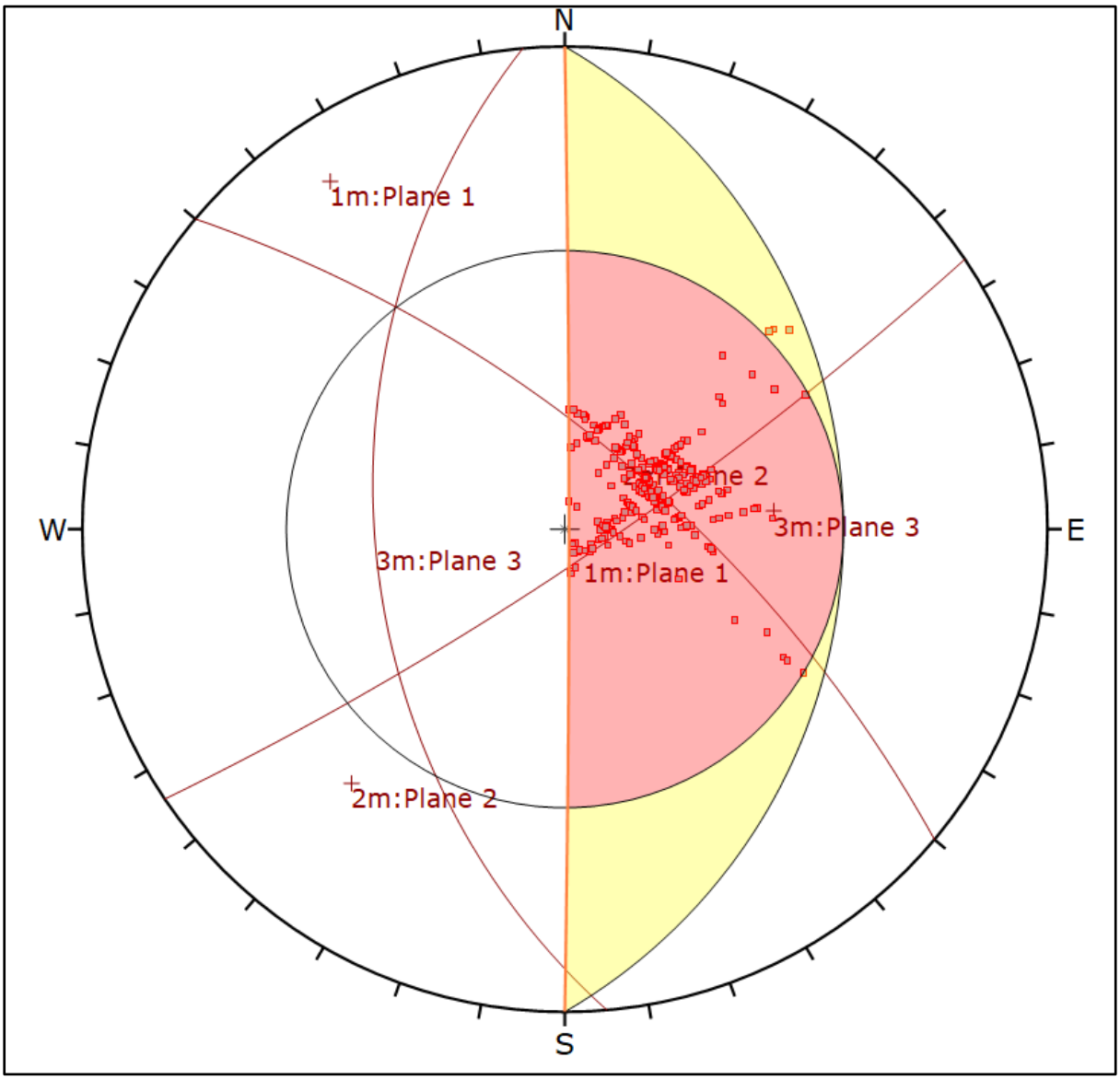


Figure 60: Kinematic analyses showing possible wedge failure on the 17-footwall drive east

The unwedge analysis program concerning the joint sets for the 17 FDE was executed (see Figure 61). A potentially unstable block was identified, featuring an apex height of 3.5m, and the failure mechanism involving wedge instability should be anticipated. The convergence of the three joint planes is expected to precipitate potential wedge failure at the hanging wall and

sidewalls. Using the 1.8m bolts and long anchors could not contain the wedges in the hanging wall, as the factor of safety was calculated below the 1.5 threshold.

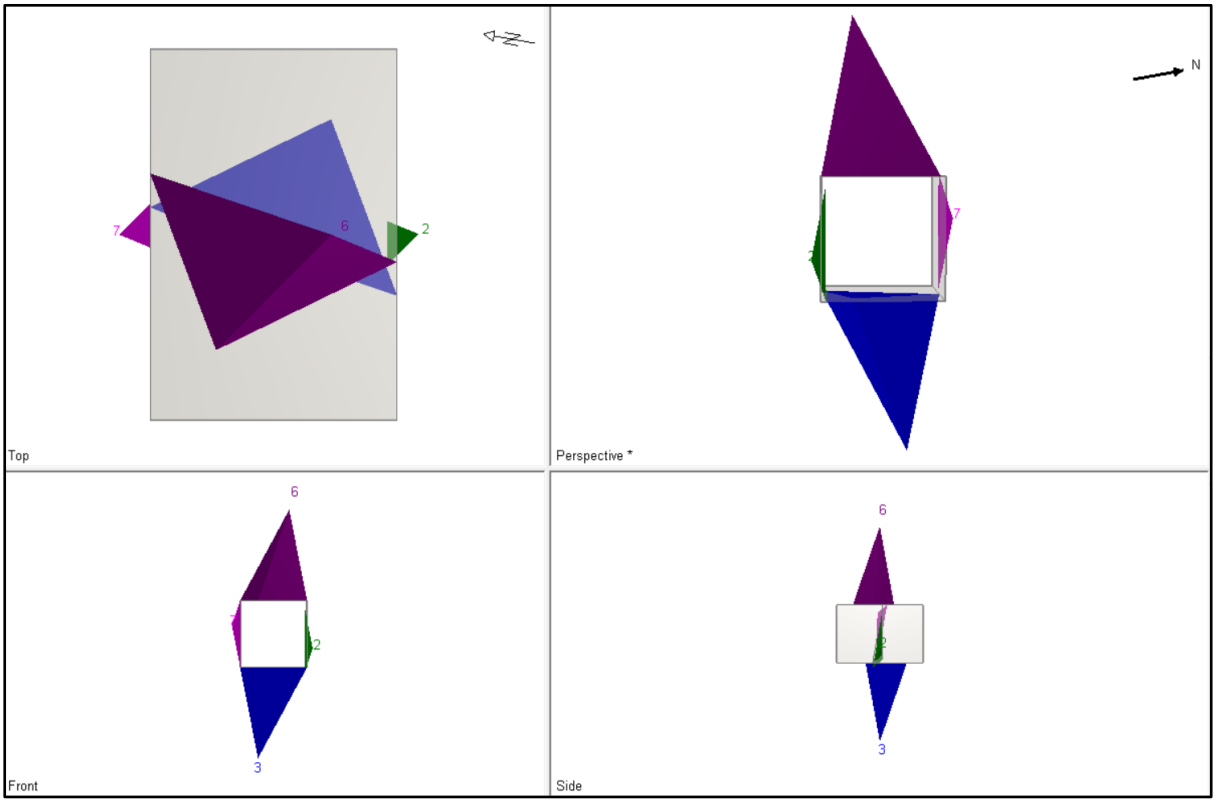


Figure 61: Simulated wedges in the rock mass surrounding the 17 Footwall east haulage

5.9 Rock Mass Classification Analyses at 17 Footwall Drive East Haulage

Rock mass classification data was collected from the core recovered from cover drilling ahead of the development end face. The cover hole data indicated poor rock mass conditions with an average Q and RMR of 0.25 and 37, respectively. Water was intersected near the dyke (Figure 31). The GSI ranges between 25-30, indicating poor to very poor ground conditions due to jointed rock mass and the presence of water.

Rock mass classification will be applied on all cores to determine ground conditions and support requirements. Rock mass classification will be employed on all core samples to ascertain subsurface conditions and necessary support requirements.

Figure 62 illustrates the Q support charts. The excavation support ratio is 1.3, as this is a permanent opening, and the Q rating was calculated at 0.25. The intersection of these factors indicates that poor ground conditions are expected where stringent support is required. The case study at Northam Platinum is affected by all these factors. The adjusted MRMR was calculated as 32 indicating poor ground conditions.

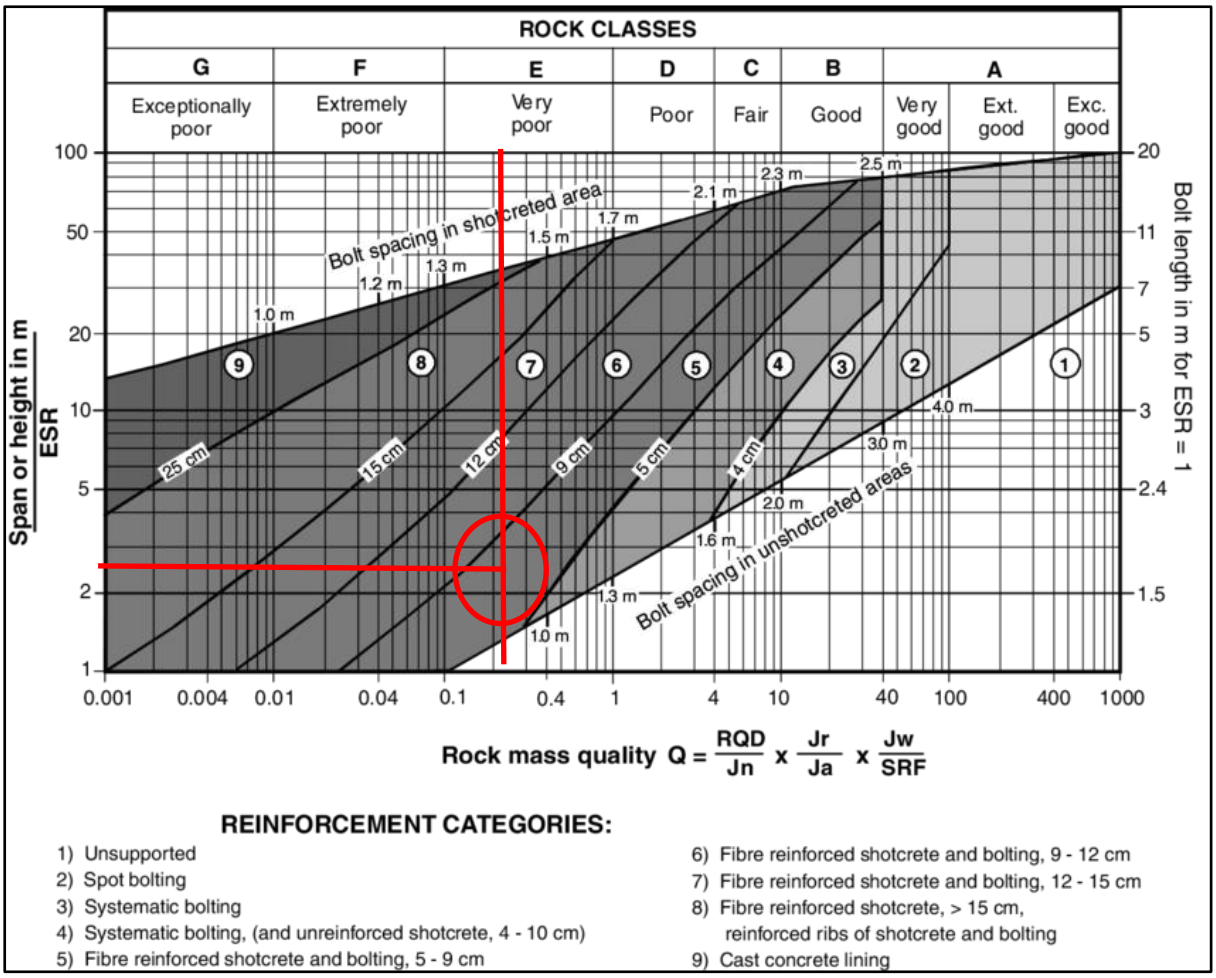


Figure 62 Estimated support categories where very poor ground conditions are experienced

The average Q rating of 0.2 and MRMR of 32 with unsupported span were used to assess the stability of the haulage. The recommended factor of safety according to best practice of excavation should be 1.5, and the haulage quantity is below the recommended threshold, indicating the potential for unstable ground conditions (Figure 63).

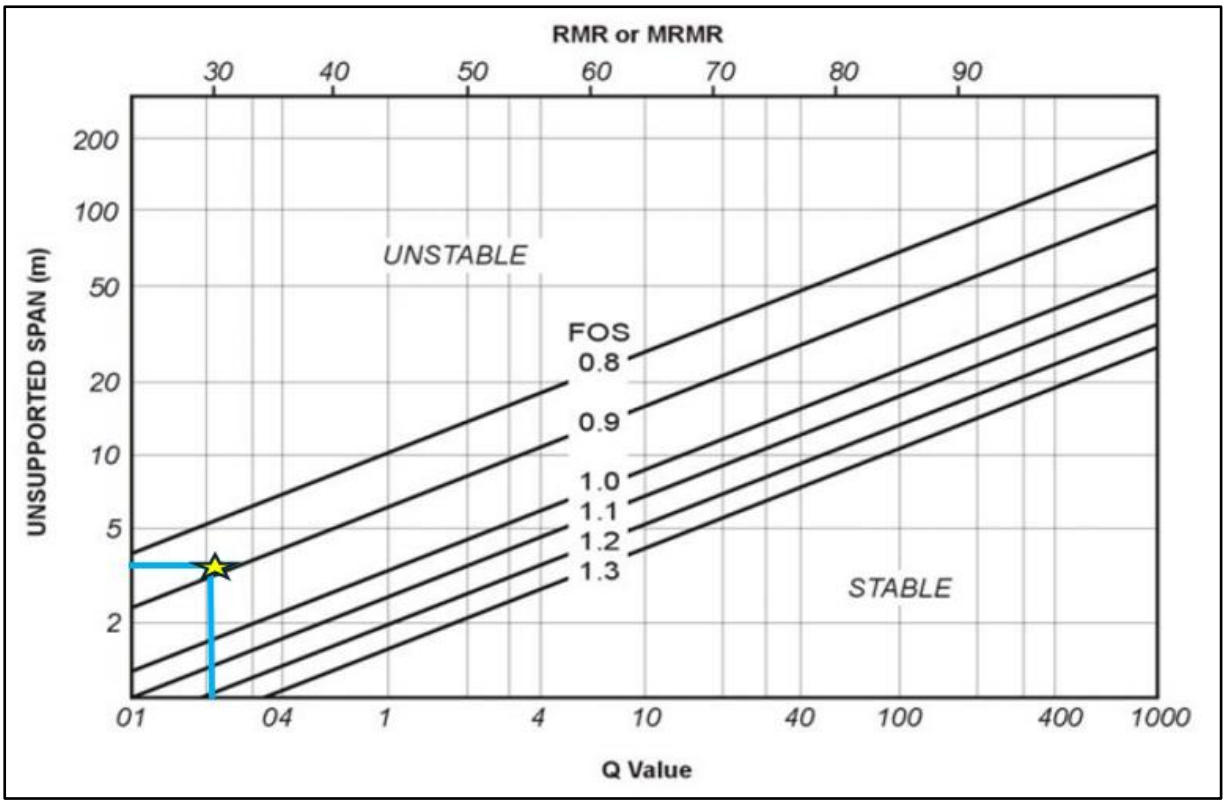


Figure 63: Unsupported span vs Q/RMR of the 3.8m span haulages (Stacey & Swart, 2001)

The standing time as a function of unsupported span RMR values is illustrated in Figure 64, while the suggested support according to the RMR system is presented in the table.

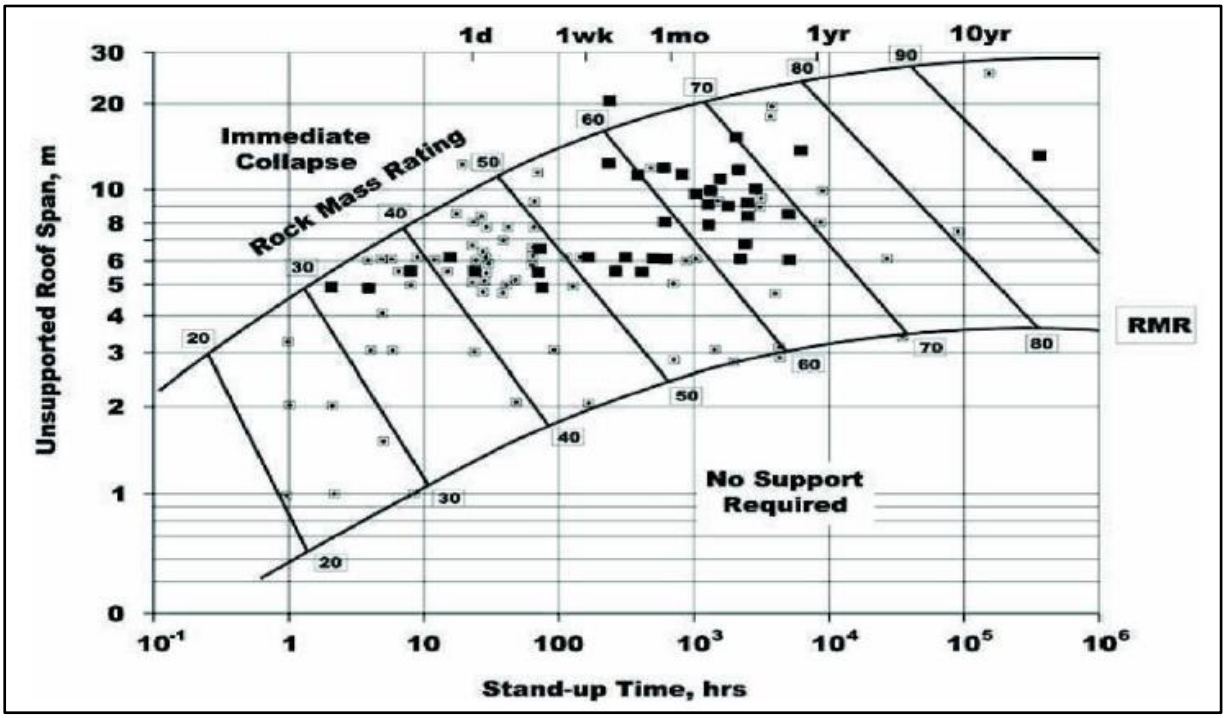


Figure 64: Unsupported span as a function of RMR as sited by Bieniawski and Lowson (2013)

The MRMR for the area of interest concerning the haulages, with an initial calculated RMR of 36, averages 32. After applying adjustments of 90% for weathering, 85% for joint orientation, 120% for mining-induced stresses, and 94% for blasting effects, the recalibrated MRMR is.

Adjusted MRMR = 36 x 0.9 x 0.85 x 1.2 x 0.94 = 32

5.10 Numerical Modelling using Vantage Software for RCF Analyses

In addition to the analysed rock mass classification data, the footwall drive or haulage was meticulously modelled using VANTAGE (Figure 65). The RCF along the 17 FWD East is above 1.4, indicating poor rock mass conditions (refer to Figure 65). The F-factor was taken as 0.8.

Figure 65 illustrates the rock wall condition factor calibrated with different uniaxial compressive strengths. As this haulage will traverse different rock types, the strengths will differ. The RCF of 1.4 and above indicates that stringent support will be required.

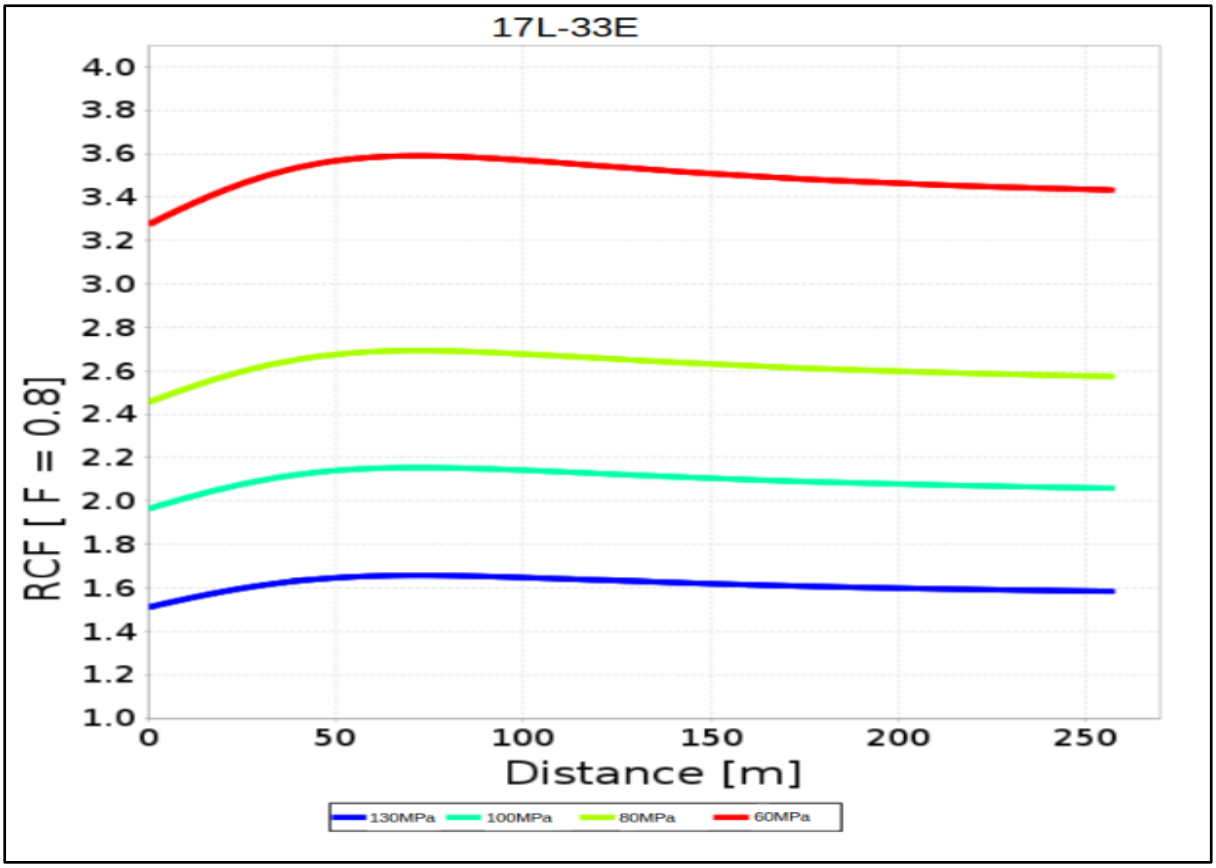


Figure 65: RCF results for 17 footwall drive east at different strengths

5.11 Chapter Summary

This chapter provides a comprehensive overview of the analyses conducted on three development haulages investigated at the Zondereinde Northam Platinum Mine. It offers a concise discussion of stereographic analyses that illustrate anticipated joint set orientations, and possible modes of failure aimed at assisting support design. Additionally, Rockwall Condition Factors to assess possible principal stresses are also evaluated and assist in developing appropriate support. Furthermore, rock mass classifications using Q, RMR, and MRMR are also calculated and assisted in the design. Moreover, fall of ground database will be discussed in the following chapter to determine the actual thickness to be supported on the water fissures. All the above factors will assist in selecting suitable support for the three haulages mining through water-bearing fissures at Zondereinde Northam Platinum Mine. The subsequent chapter discusses the methodology, the choice of support, and the selected support informed on by the aforementioned by the information and case studies.

.

CHAPTER 6 SUPPORT SYSTEMS DESIGN

6.1 Introduction

Under normal ground conditions at Northam Platinum Mine, where the host rock is Norite,1.8m resin bolts are used on a spacing of 1m along and 1.5m across the tunnel. In this study three haulages are mining through water fissures, which contain complex geological features and cannot be supported by normal tendons. This chapter examines the choice of support informed by the aforementioned case studies, rock mass classification systems, numerical modeling, and stereographic projection. This chapter explores the analyses of support design requirements, fall of ground database, and the factor of safety involved. Steel arch sets with void fill is the support system proven effective when supporting this kind of ground condition. Additionally, the arch sets design tests are discussed in this chapter. The test was conducted in the laboratory of the University of Pretoria, which holds accreditation. Different steel sets are discussed below. Different steel sets are discussed below. Mitri and Khan (1990) state that Steel arches are ductile and, given their load-bearing capabilities, have been used extensively in weak ground conditions. Furthermore, this chapter addresses the design of steel arch sets, load deformation tests, and the methodology for approaching water-bearing issues. Based on the analyses presented in the preceding chapter and several case studies conducted abroad and locally, arch sets with void fill and consolidation bolts are recommended. Therefore, arch sets are installed 10m from the poor ground contact after geological drilling. In situations where ground conditions are notably unfavorable, spiling bolts are additionally installed. Moreover, this chapter details the arch sets tests and design properties with void fill and consolidation bolts used in these excavations to support the deadweight in complex water fissures.

6.2 Arch Sets Design

Different companies manufacture these support systems, including Becker Mining (Admin, 2023). The T.H. 29 Steel Arches are used at other mines and at Zondereinde Northam Platinum Mine, where poor ground conditions are intersected. Arch sets are steel supports that can be integrated with other support units to enhance the stability of excavations (Admin, 2023). The ever-challenging geological conditions in mining necessitate the pursuit of innovative and effective methods for ensuring the stability of roadways. The new support structures must adhere to exceptionally rigorous strength standards and exhibit remarkable load-bearing capacities (Rotkegel, 2013). The steel arch supports are durable and well-suited for fractured rock in transportation routes and underground chambers, playing an essential role in the rehabilitation of haulage systems. They are used with void filling and sometimes with consolidation where ground conditions are very poor (Rotkegel, 2013). Arch sets are

designed due to the deterioration of ground conditions resulting from geological features that cannot be effectively contained by conventional tendon support systems. It is equally crucial to fully utilise the support parameters, which can be achieved by enhancing the operational conditions of each individual support arch. This includes ensuring a snug fit between the support and the rock, proper placement on the floor, and appropriate alignment against the sidewall (Rotkegel, 2013).

6.2.1 Test Procedure of Different Sets

This section aimed to determine the load-bearing capacity of four arches commonly manufactured by Bekker Mining. The tests were all static tests. Four hydraulic cylinders were used to apply the loads on all tests of arch sets. These parts document the position of the hydraulic cylinders and measure points for the deflection in arches. The presented test results demonstrate that a conventional steel arch support system can attain a strength increase of up to four times by employing enhanced load distribution. The placement of plated joints within the arch framework significantly affects the overall strength dynamics of these support systems.

Each test was done on one of the roof support structures supplied by Bekker Mining. Four cylinders were used to perform the test. The load on the structure was increased on the pressure gauge in increments of 10 MPa, corresponding to 30 kN. The arch's deflection was measured. (Tests were carried out at the University of Pretoria).

The following four structures were tested:

- D-shaped arch set, A3Y / 3 segment – this structure consists of three segments with a curved top and sides (Figure 66).
- Arch ring set, R1Y /4 segment – this structure consists of four curved segments (Figure 67).
- Square arch sets, AC1Y /3 segment – this structure consists of three segments with a curved top and straight sides (Figure 68).
- Double square arch sets, S-AC1Y / 5 segment – this structure has a double beam section and consists of five segments with a flat top and straight sides (Figure 69).

The following figures reveal the loading positions on the arches

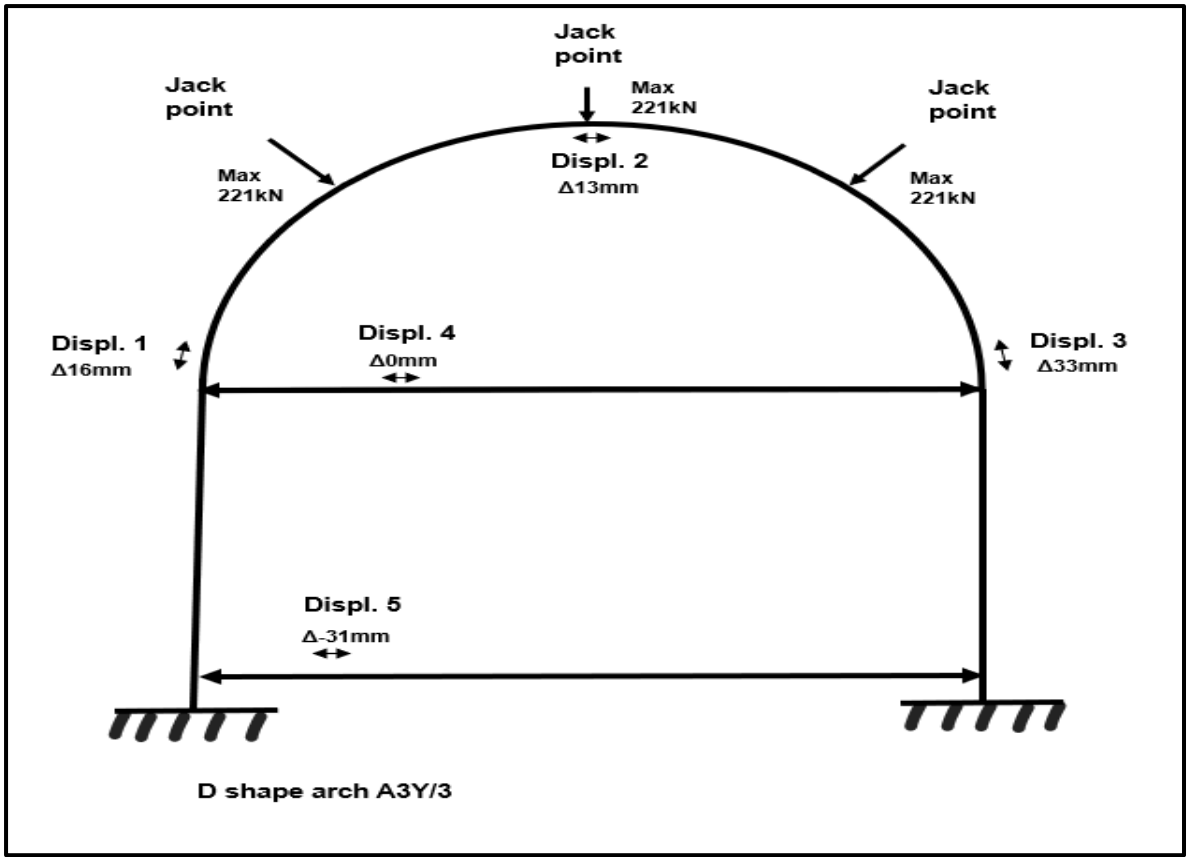


Figure 66: Loading points for D Shaped arch sets, A3Y/3 (University of Pretoria, 2004)

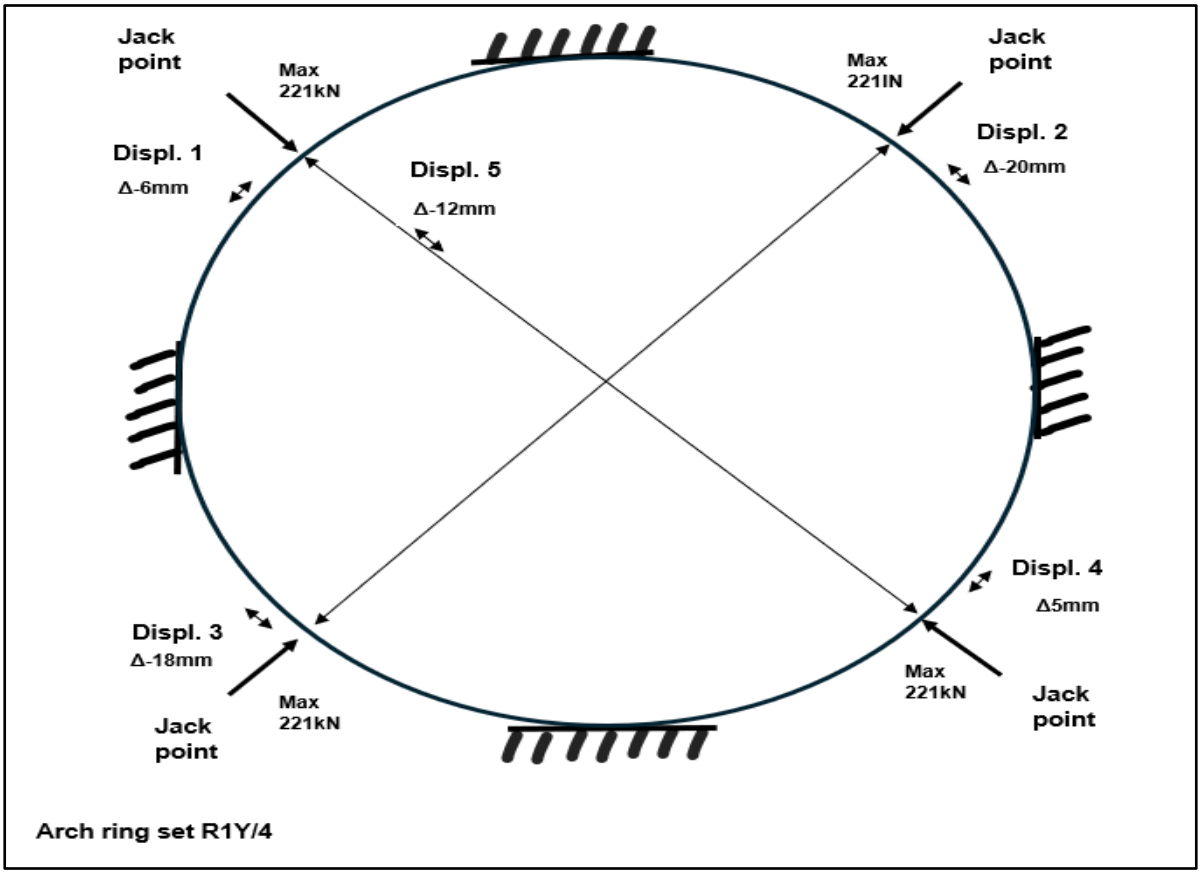


Figure *67*: Loading points for Arch ring sets, R1Y /4 (University of Pretoria, 2004)

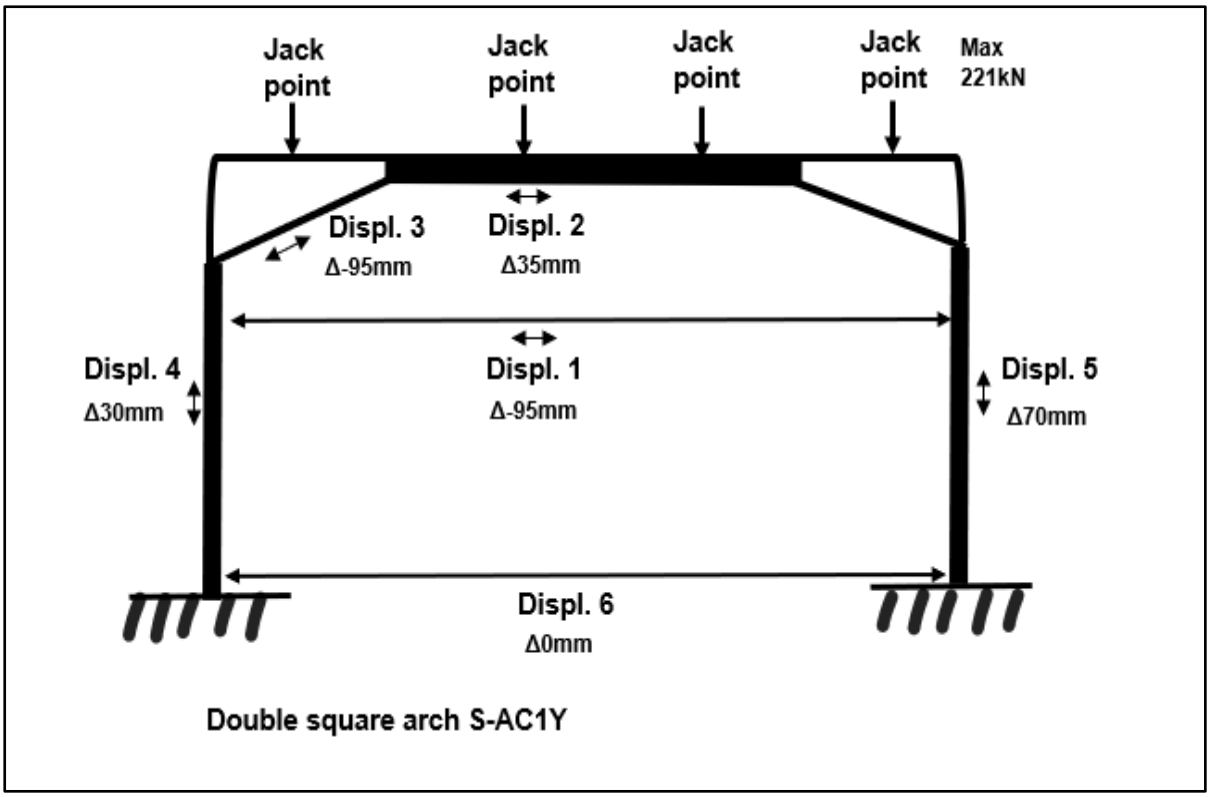


Figure 68: Loading points for the Double square arch, S-AC1Y (University of Pretoria, 2004)

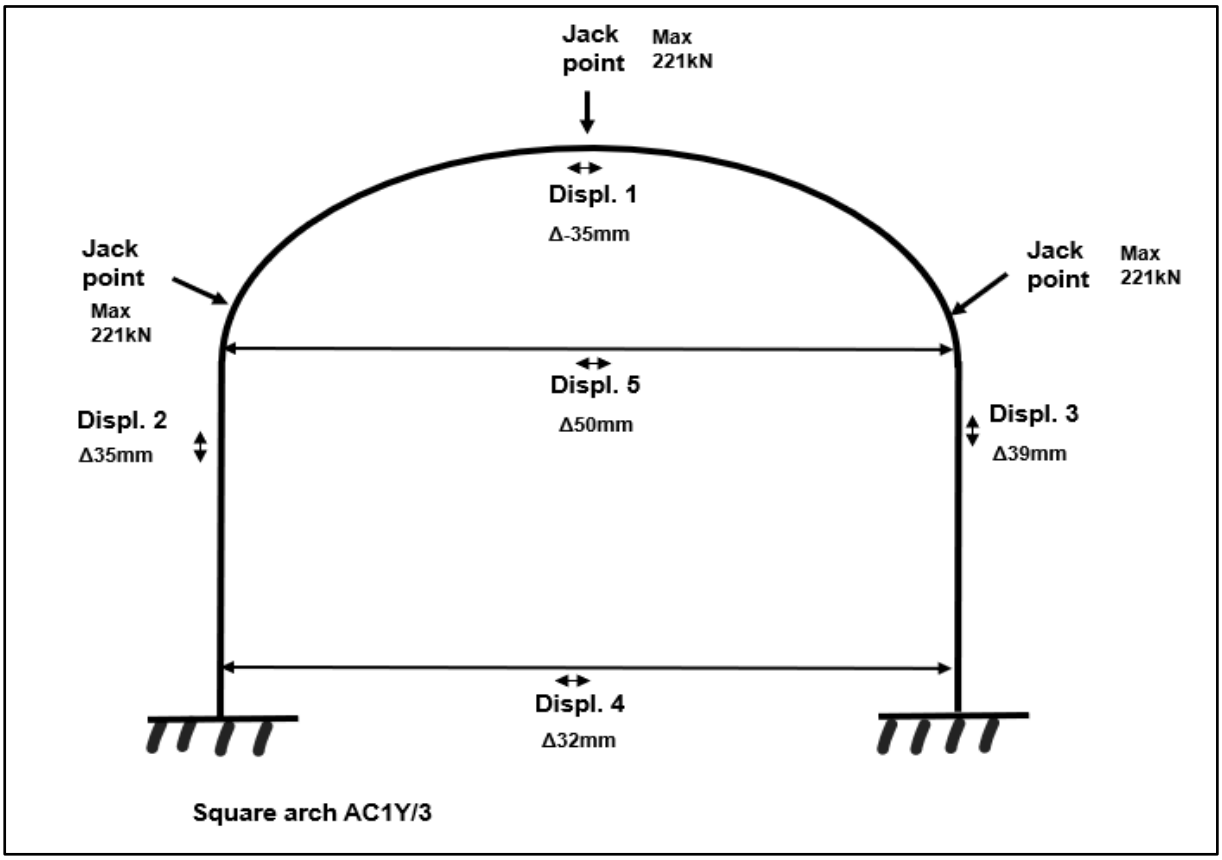


Figure 69: Loading points for the Double square arch, S-AC1Y/3 (University of Pretoria, 2004)

6.2.2 Test Results for Different Arch Sets

The primary aim of these tests was to ascertain the arch's deflection under the load applied. The deflection was measured at different positions for each arch. The measurement points were chosen at the points where the maximum deflection would be expected.

The greatest deflection at the crown of the D-shaped arch set, A3Y/3 (Table 12). The maximum deflection, with a maximum load of 221.9 kN on the bend, was 33mm at displacement 3. The permanent deflection at this point was 13mm. No slipping occurred on the joint.

Table12: Deflections for D-shaped arch set, A 3Y/3 (University of Pretoria, 2004)

Pressure	**Force**	**Disp. 1**	**Disp. 2**	**Disp. 3**	**Disp. 4**	**Disp. 5**
[MPa]	**[kN]**	**[mm]**	**[mm]**	**[mm]**	**[mm]**	**[mm]**
0	0	0	0	0	0	0
10	30.4	2	0	2	1	0
20	60.8	4	2	1	0	-5
30	91.2	6	2	3	0	-10
40	121.6	10	2	8	0	-13
50	152	11	3	10	-1	-15
60	182.4	12	4	13	0	-17
73	221.9	16	13	33	0	-31
0	0	11	8	13	0	-11

Displacements and strains were measured up to failure (Figure 60). Displacements were measured at 5 points (Disp. 1 to Disp. 5). The strains were measured, and the load was applied using the transducer in the hydraulic pressure jack.

Figure 70 indicates load displacement points at A3Y/3 sets. Displacements from Disp. 1 to Disp. 4 points are positive (downward) depending on the height of the rise. Displacement 5 and one point on displacement 4 are negative displacements (upwards). The maximum displacement at disp. 3. is 33 at a load of 221.09 kN.

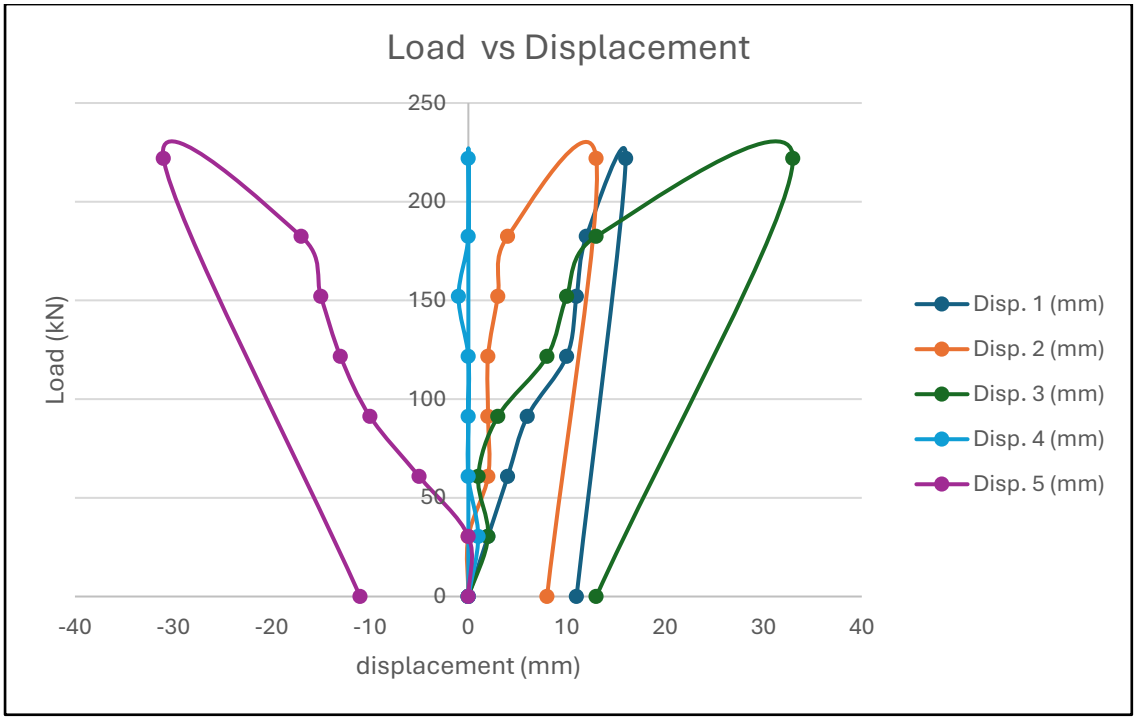


Figure 70: Load displacement curve of 5 points on D shaped arch sets (A 3Y/3)

For the Arch ring set, R1Y/4, the maximum deflection was at Disp. 4 (Table 13). The maximum deflection with a maximum load of 221.9 kN on the crown was 5mm, and on the bend. No slipping occurred on all joints.

Table 13: Deflections for Arch ring set, R1Y/4 (University of Pretoria, 2004)

Pressure	**Force**	**Disp. 1**	**Disp. 2**	**Disp. 3**	**Disp. 4**	**Disp. 5**
[MPa]	**[kN]**	**[mm]**	**[mm]**	**[mm]**	**[mm]**	**[mm]**
0	0	0	0	0	0	0
10	30.4	-1	-2	-1	0	0
20	60.8	-2	-4	-2	0	0
30	91.2	-4	-7	-4	0	-5
40	121.6	-4	-9	-7	0	-3
50	152	-4	-10	-10	0	-3
60	182.4	-4	-15	-15	4	-9
73	221.9	-6	-20	-18	5	-12
0	0	-3	-5	-7	5	-3

Displacements and strains were measured up to failure (Figure 61). Displacements were measured at 5 points (Disp. 1 to Disp. 5). The strains were measured, and the load was applied using the transducer in the hydraulic pressure jack.

Figure 71 indicates load displacement points at R 1Y/4 sets. Displacements from Disp. 1 to Disp. 3 and Disp. 5 are negative (upwards) depending on the height of the rise. Displacement 4 is positive (downwards). The maximum displacement at point 4. is 5mm at a load of 221.09 kN.

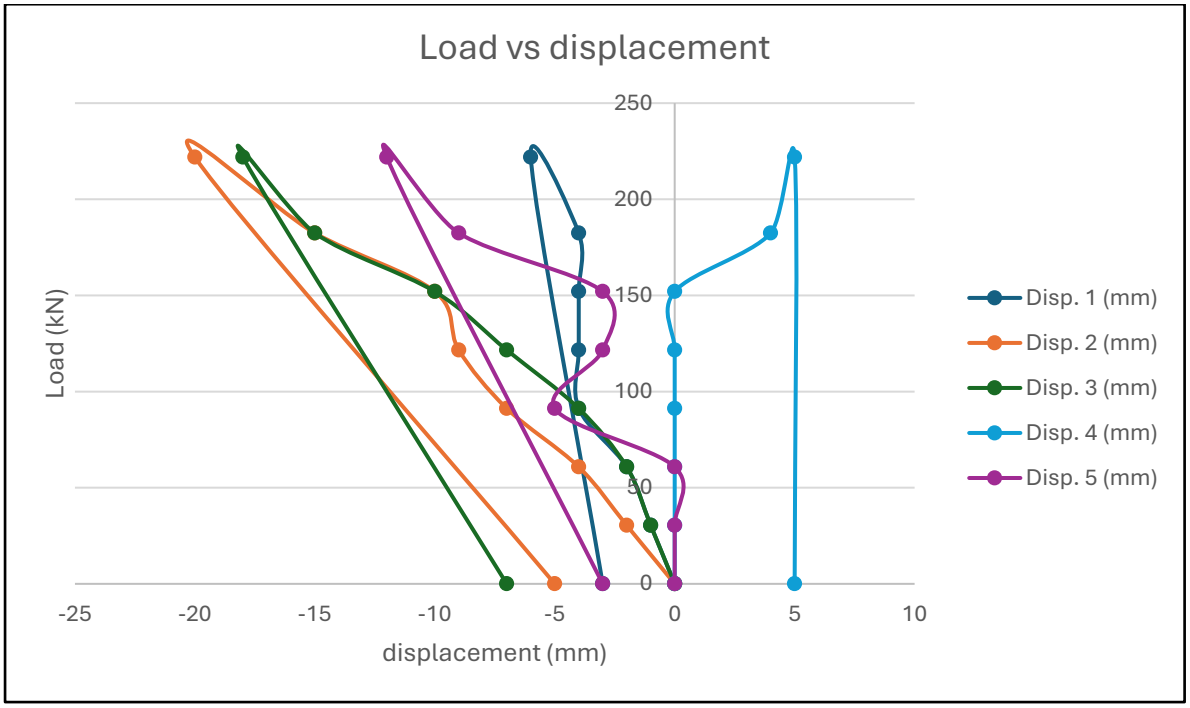


Figure 71: Load displacement curve of 5 points Ring arch sets (R 1Y/4)

The greatest deflection occurred at the crown for the Square Arch set, AC1Y/3 (Table 14). The deflection with a load of 221.9 kN on the crown bend was 70mm. Moreover, on the bend, it was 33mm. The permanent deflection at this point was 53mm. No slipping occurred on the joint.

Table 14: Deflections for Square arch set, AC1Y/3 (University of Pretoria, 2004)

Pressure [MPa]	Force [kN]	Disp. 1 [mm]	Disp. 2 [mm]	Disp. 3 [mm]	Disp. 4 [mm]	Disp. 5 [mm]
0	0	0	0	0	0	0
10	30.4	-10	5	4	5	10
20	60.8	-20	9	9	8	15
30	91.2	-38	15	17	12	25
38	115.52	-85	30	33	20	55
40	121.6	-85	30	36	23	65
50	152	-95	35	37	23	65
60	182.4	-95	35	39	23	65
73	221.9	-95	35	39	23	70
0	0	-53	23	30	30	47

Displacements and strains were measured up to failure (Figure 62). Displacements were measured at 5 points (Disp. 1 to Disp. 5). The strains were measured, and the load was applied using the transducer in the hydraulic pressure jack.

Figure 72 indicates load displacement points at A 3Y/3 sets. Displacements from Disp. 2 to Disp. 5 points are positive (downward) depending on the height of the rise. Displacement 1 is negative displacement (upwards). The maximum displacement at point 3. is 70mm at a load of 221.09 kN.

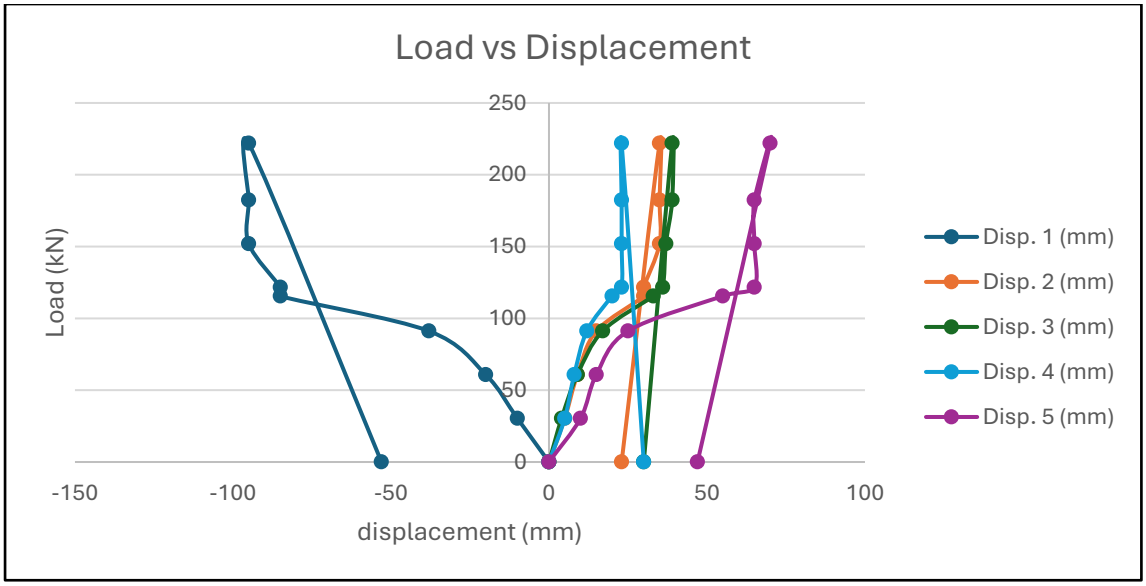


Figure 72: Load displacement curve of 5 points for square sets (AC1Y/3)

The maximum deflection was at the crown for the Double Square Arch set, S-AC1Y/5 (Table 15). The deflection with a load of four times 221.9 kN on the crown and 95mm. The permanent deflection at this juncture measured 53mm, resulting in a permanent deformation of 54.1%. Slippage was observed at the joint located at the center of the crown.

Table 15: Deflections for Double square arch set, S-AC1Y/5 (University of Pretoria, 2004)

Pressure	**Force**	**Disp. 1**	**Disp. 2**	**Disp. 3**	**Disp. 4**	**Disp. 5**
[MPa]	**[kN]**	**[mm]**	**[mm]**	**[mm]**	**[mm]**	**[mm]**
0	0	0	0	0	0	0
10	30.4	-5	5	4	5	10
20	60.8	-10	9	9	8	15
30	91.2	-15	15	17	12	25
33	100.32	-25	20	33	20	55
38	115.52	-25	20	36	23	45
50	152	-15	25	37	23	35
60	182.4	-25	35	39	23	65
73	221.9	-35	35	39	23	50
0	0	-24	25	32	32	50

Displacements and strains were measured up to failure (Figure 63). Displacements were measured at 5 points (Disp. 1 to Disp. 5). The strains were measured, and the load was applied using the transducer in the hydraulic pressure jack.

Figure 73 indicates load displacement points at A 3Y/3 sets. Displacements from Disp. 2 to Disp. 5 points are positive (downward) depending on the height of the rise. Displacement 1 is negative displacement (upwards). The maximum displacement at point 3. is 50mm at a load of 221.09 kN.

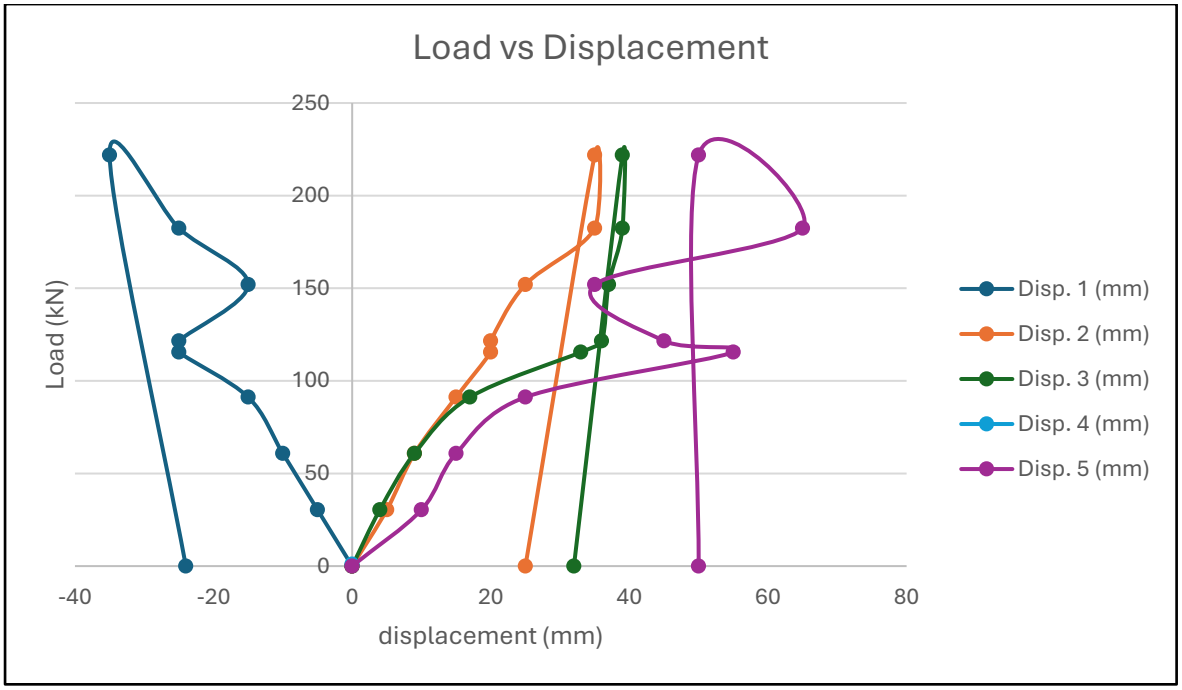


Figure 73: Load displacement curve of 5 points for square sets (AC1Y/3)

6.2.3 Support Design Criteria Requirements

A vital component in the stability analysis and design of ground support for rock mass is the factor of safety (Rahimi *et al.,* 2020). The factor of safety (FOS) pertaining to the gravitational fall of ground is expressed by Equation 18 as described by (Li, 2017): A crucial element in the stability analysis and design of ground support for rock masses is the factor of safety (Rahimi *et al*., 2020). The factor of safety (FOS) related to gravitational failure of the ground is articulated in Equation 19, as outlined by Li (2017):

$$\text{FOS} = \frac{\text{Load capacity of the support system}}{\text{Total load on the support system}} \quad [19]$$

An acceptable factor of safety is 1.5 and above.

The demand for ground support necessary to sustain the dead weight under static conditions can be determined using Equation 20, as outlined by Cai and Kaiser (2018).

$$Ground\ support\ demand = \rho g d f \quad [20]$$

Where

ρ represents the density of rock (kg/m³).

g denotes the acceleration due to gravity (m/s²).

and df signifies the depth of failure or the displacement of the rock (m)

The gravity fall of ground recorded in all tunnels at Zondereinde Northam platinum Mine was analysed for normal ground conditions in 2010 (Zondereinde Mine COP, 2024). The maximum fall-out thickness was 1.3m (Figure 74).

The required support resistance (SRreq) capacity of the support system is delineated by the support and resistance, which can be calculated based on the tributary area theory. Support resistance is characterised as the force divided by the area. The support resistance (expressed in kN/m²) is directly proportional to the height of the fall, which is

$F/A = pgh$

Where: F = load carried by support unit (N)

A = tributary area (m²)

ρ = rock density (kg/m³)

$$SRreq = \rho gh \quad [21]$$

ρ is the density of rock (kg/m³).

g is the gravitational acceleration (≈ 10 m/s²).

h is the thickness of the potential fall (m)

The requisite support resistance to accommodate a 100% fallout thickness of 1.3m is 37.6kN/m² for Norite. The current primary support used in development comprises 20mm diameter, full-column grouted bolts. The bolts offer a minimum support resistance of 110 kN/m² when configured with a spacing of 1m by 1.5m. A factor of safety of 2 can be achieved.

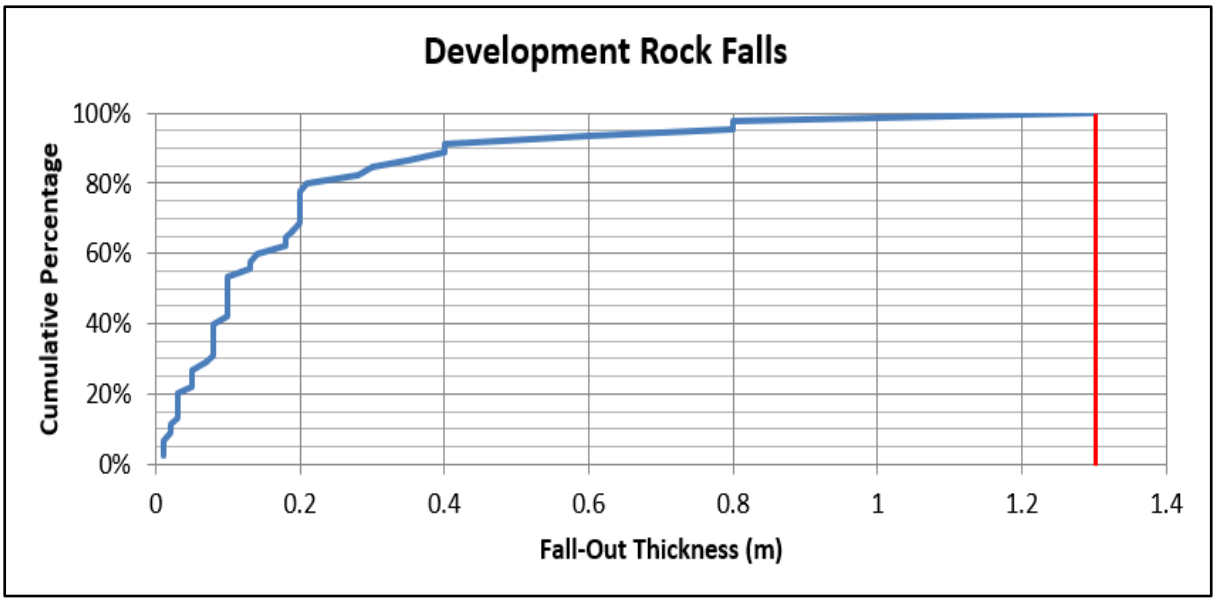


Figure 74: Depicts recorded fall-out thickness in tunnels with normal ground conditions at Zondereinde Northam Platinum Mine

The fall of ground database recorded for water-bearing fissures was conducted in 2012 with stereographic analyses. The 100% fall-out thickness is up to 3.5m (Figure 75)

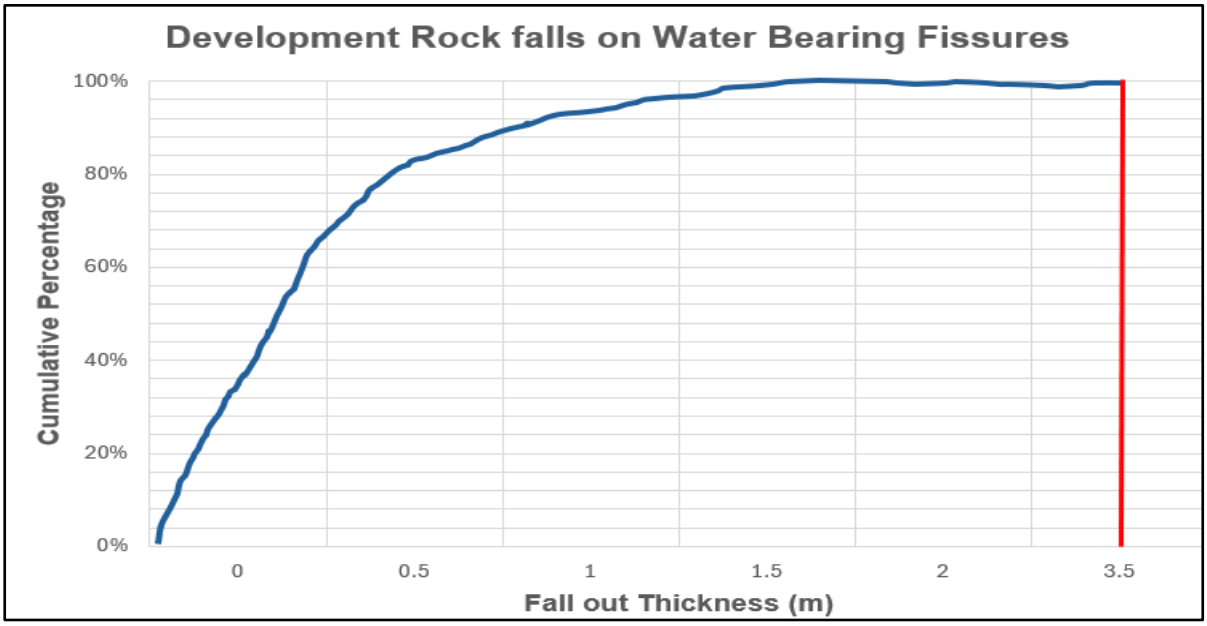


Figure 75: Depicts recorded fall-out thickness where water fissures are intersected at Zondereinde Northam Platinum Mine

The support resistance required for a 100% fall-out thickness of 3.5m is 101.2 kN/m². If the resin bolts are used at 1m by 1.5m, an FOS of 1 is achieved, less than 1.5. In addition to the low safety factor, poor ground conditions are expected.

Arch sets with maximum load of 221 kN/m² will offer a factor of safety of 2.2 when supporting the poor ground conditions

6.2.4 Conclusions on the Selection of Support (Arch Sets)

The main conclusion derived from these four tests is that arches can sustain the greatest load without yielding to collapse. The tests performed represent the worst of what could be anticipated in the typical application of these arches. The support resistance required for 100% fall-out thickness water fissures at Zondereinde Northam Platinum Mine of 3.5m is 101.2 kN/m². If the resin bolts are used at 1m by 1.5m, an FOS of 1 is achieved, and the bolt length is less than the fall out thickness. Hence, arch sets with void fill are the preferred choice of support due to their bearing load capacity, resulting in a factor of safety of at least 2. The conclusion drawn from this statement is that arches would be capable of supporting a higher load in the typical application than what was utilised in the tests. These support units will be able to support the water fissures expected at the development ends at Zondereinde Northam Platinum Mine. The arch sets have proven to be an effective support in most case studies abroad and locally discussed in this research.

6.3 Spiling Bolts

6.3.1 Introduction

These bolts have also been utilised in Norwegian tunnels over the past decade. The bolts are normally used when traversing through weak rocks and weak zones. Spiling bolts are utilised to provide structural support to the ground in front of the tunnel face (Chen *et al*., 2008). They are installed in a fan shape orientated 15 degrees relative to the tunnel axis, see Figure 64. They secure stability before the next blast by supporting the ground ahead.

The spiling bolts are used when poor ground conditions are present to maintain stability ahead of mining faces. The spacing of the bolts is contingent upon the condition and quality of the rock mass. Poor quality requires denser spacing of bolts. In rock masses exhibiting Q values below 0.1, the spacing of bolts should not surpass 0.4 to 0.5m (Holmoy & Aagaard, 2002). The spacing may be further reduced to 25-30cm in extremely poor ground conditions. The spacing of the bolts must be modified to accommodate local conditions. The length of the bolt depends on the excavation process. The diameter of spiling bolts is usually 32mm. The length of the spiling bolts used is usually 6m, and the blasting round used is 1m when mining through water fissure at Zondereinde Northam Platinum Mine.

6.3.2 Description

Figure 76 illustrates consolidation bolts installed on a fan-shaped, shallow angle to support the area ahead of the face. The consolidation bolts are used as additional support when ground conditions are extremely poor.

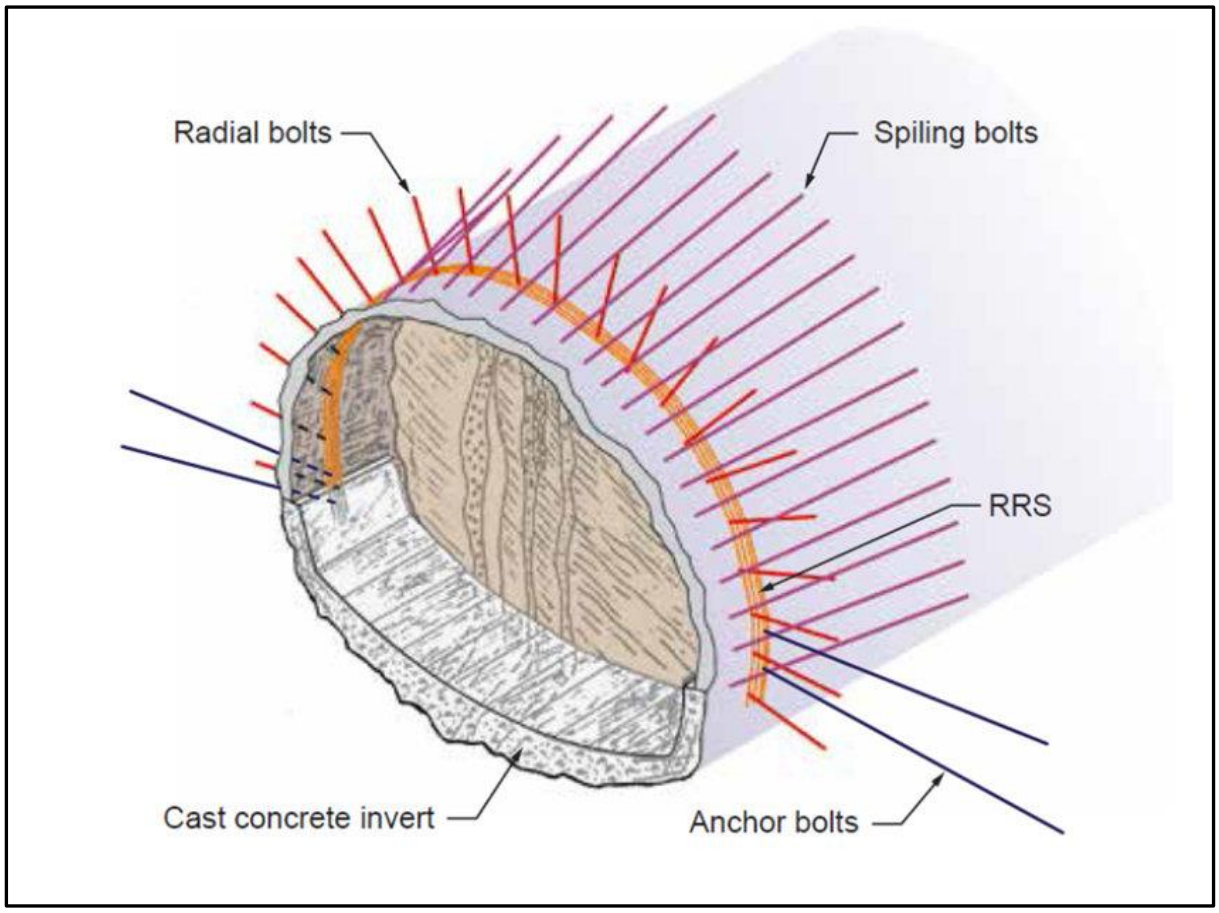


Figure 76: Schematic view depicting spiling bolts in tunnel (Holmoy & Aagaard, 2002)

6.4 Conclusion Support Design

This research study aimed to mine through water-bearing fissures with complex geological structures at Zondereinde Northam Platinum Mine. The collection of geological data facilitated the prediction of expected rock mass behaviour and the characterisation of the rock mass. The empirical and numerical analysis methods were employed to design the support for mining through water fissures. The study revealed that mining through water fissures necessitates implementing a combination of design approaches. Rock mass classification, kinematic analyses, fallout thickness data base and numerical analyses were used to design support. In conjunction with case studies at other mines the support recommended is arch sets with void fill on haulages. The above chapter analysed different types of arch sets that can cater to poor ground conditions induced by water fissures. These arch sets can carry up to 700kN of the demand to be supported.

6.5 Methodology for Developing Through Water-Bearing Fissures at Zondereinde Northam

Footwall drives, or haulages, at the Zondereinde Northam Platinum Mine, must develop through complex water-bearing fissures to access all sections of the mineable orebody. The process typically entails temporarily stopping the haulage or development end short of intersecting an anticipated major geological feature. Geological cover, double-cover, and ring seal cover drilling then commence, depending on the intrusion's presence and rate of water flow.

Cover boreholes are drilled 120m ahead of the development end face to determine ground conditions. These holes also warn of any water or gas intersections. Double cover is usually drilled where water-bearing fissures are anticipated. De-watering boreholes are also drilled to reduce the water coming from the structures.

Ring cover sealing is required when water yields exceed 5000 litres per hour. Ring cover sealing involves drilling 15m-long holes circularly around and ahead of the excavation periphery to divert water from the planned tunnel position and consolidate the surrounding rock mass (Figure 77). Figure 77 shows a five-ring cover array plan.

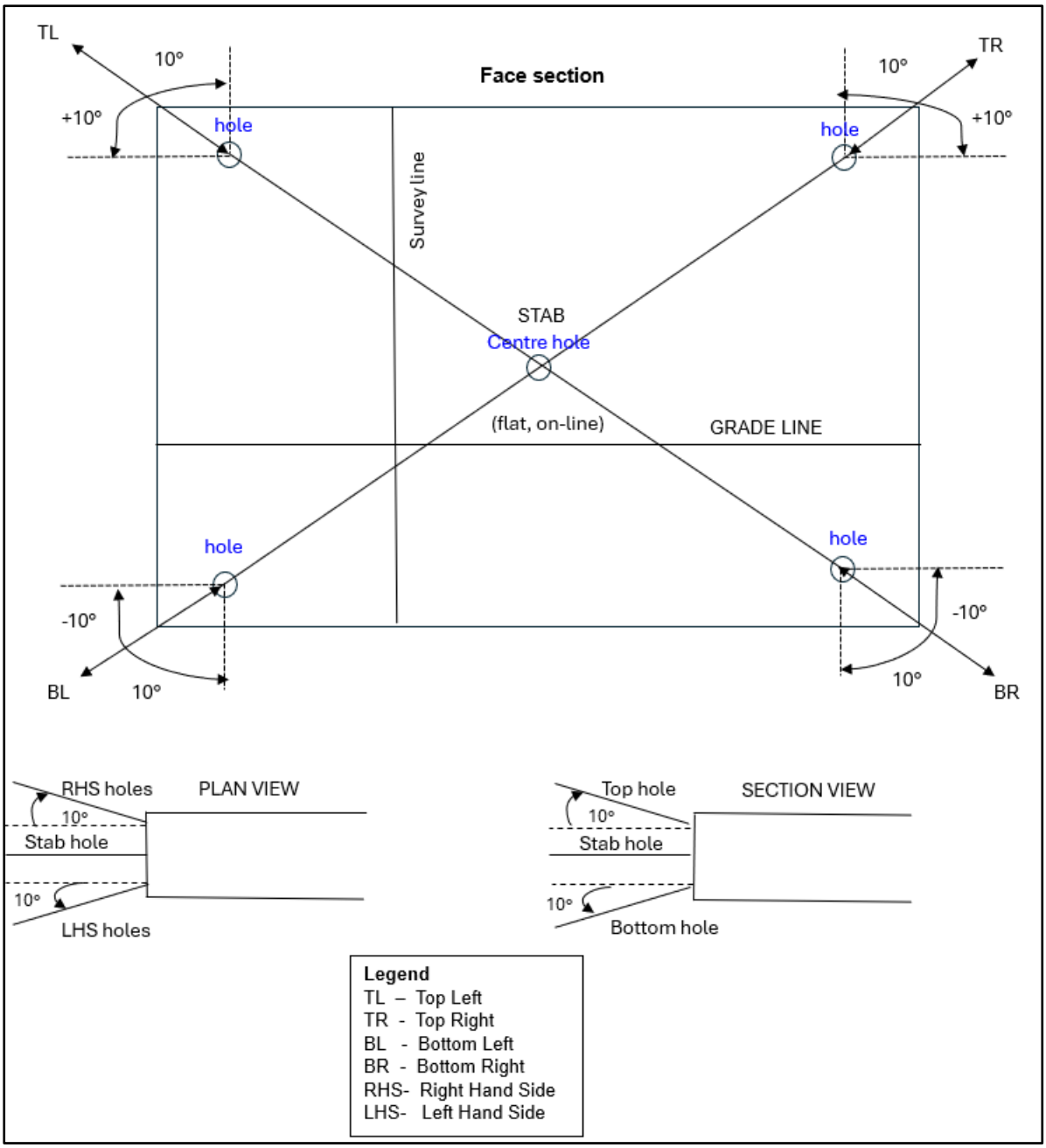


Figure 77: Plan showing a five-hole ring cover array for de-watering of the rock mass ahead of the face

Figure 78 above illustrates a nine-hole ring cover where lots of water is expected.

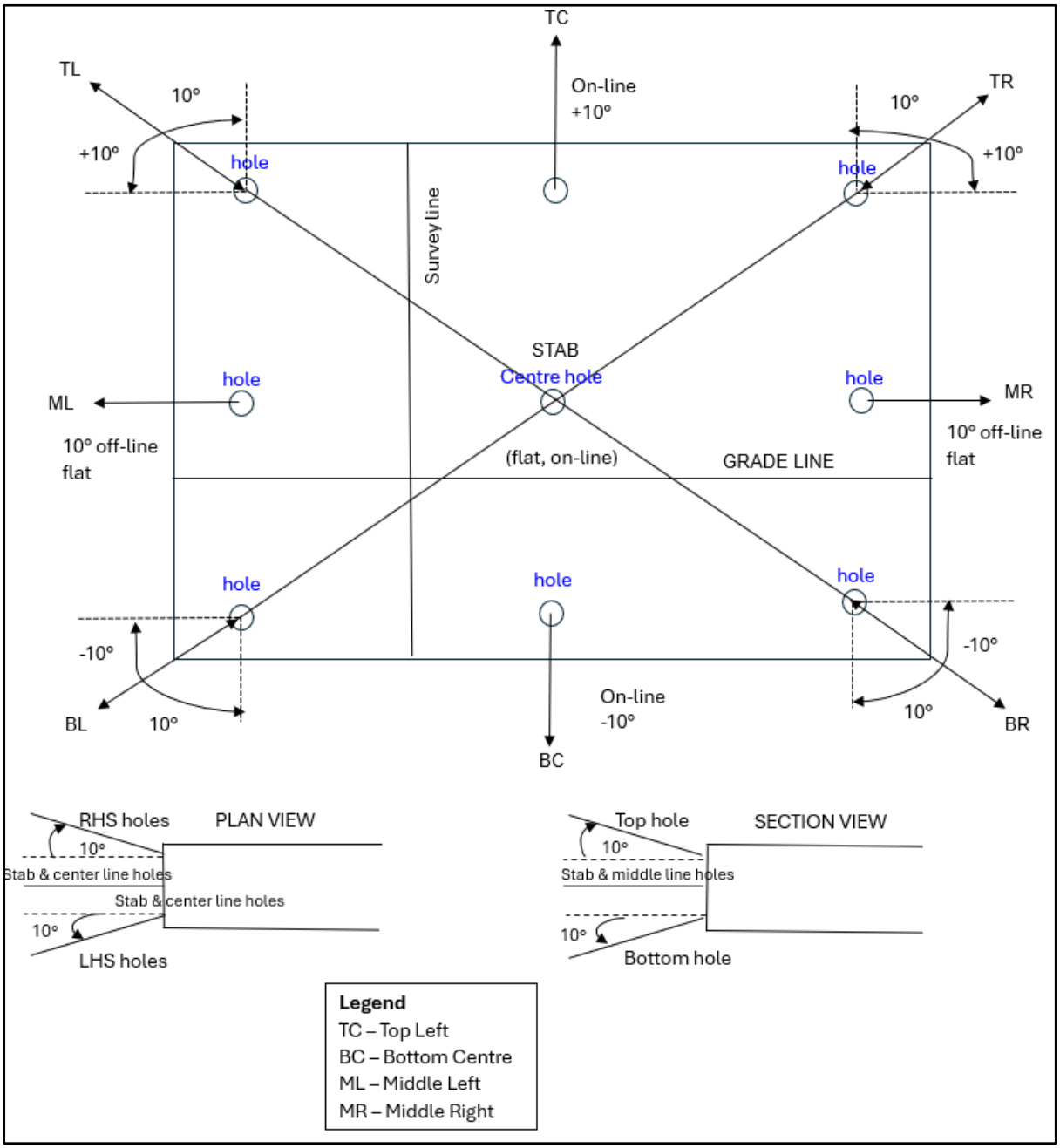


Figure 78: Plan showing a nine-hole ring cover array for de-watering of the rock mass ahead of the face

Once geological drilling has been completed, the footwall drive or haulage can continue developing under restricted conditions. These conditions entail increasing the excavation dimensions from 3.7m high by 2.9m wide to 3.8m high by 3.8m wide within 10m of the anticipated water exposure. This is done intentionally to accommodate arch-set installation, which requires larger excavation dimensions, especially where rail-bound equipment is utilised for transportation.

Face advances are generally limited to a maximum of 1m supported with follow-behind arch sets (arch sets may not exceed 2m from the face after a face advance). Smooth wall blasting is employed when the final row of holes features charges lighter than usual, detonated subsequent to the main charge, to limit the confinement of the holes and mitigate damage to the sidewalls.

Table 16 illustrates comparisons between Zondereinde Northam Platinum Mine and several other case studies in terms of dyke material, mining strategy, rock mass classification, support strategy and blast design. It can be deduced that there are similarities in terms of mining through complex geological features.

Table 16: Similarities with all case studies including Zondereinde Northam Platinum Mine

	Dyke material	**Mining strategy**	**RMR/MRMR**	**Support**	**Blast design**
Northam (Zondereinde Mine)	Associated with shear zones and infilled joints	Increase dimension, Reduce face advance	30-40	Arch sets, Spiling	Smooth wall blasting, Emulsion
Case study 1 (Himalayas-(THPS)	Highly weathered, Biotite schist	Reduce face advance	20	Steel ribs, shotcrete	Hand scalers
Case Study 2 (Gecimez tunnel)	Black Sea coast, Basalt, highly jointed	Reduce face advance	20	shotcrete	Smooth wall blasting, Emulsion
Case study 3 (Norway Tunnel collapse	Swelling Clay	Reduce face advance	20	Sets	Smooth wall blasting, Emulsion
Case study 4 (Taulekoa)	Running Dyke, Serpentinite ferromagnesium, and chlorite material	Increase dimension, Reduce face advance	40	Ring sets with void fill, spiling	Hand scalers

Additional Case studies (Twin Tunnels in Iran)	Calcareous Shale, heavily jointed rock mass	Reduce face advance	20	Sets	Smooth wall blasting, Emulsion
Quench tunnel in Algeria	Weak argillite Soil	Reduce face advance	15	Sets	Smoothwall
Tunnel developed on swelling clay	Swelling clay bounded by water	Reduce face advance	15	Sets	Smoothwall
Spud Shaft	Running Dyke, Serpentinite ferromagnesium, and chlorite material	Increase dimension, Reduce face advance	40	Arch sets, spiling, shotcrete	Smooth wall blasting, Emulsion
Case study 3 (Beatrix 4)	Squeezing rock Smectite.	Reduce face advance	38-40	Ring sets with void fill	Continuous moiling

6.6 Chapter Summary

Arch sets and void fill are suitable supports for mining through water fissures based on all the aspects discussed in previous chapters. The methodology is also discussed, where water sealing and increasing the tunnel dimension are necessary to accommodate the arch sets.

CHAPTER 7 CONCLUSIONS AND RECOMMENDATIONS

This research delineates studies that identify appropriate methods and support for the development of tunnels through water-bearing fissures at Northam Platinum Mine. Several case studies were examined, including mining through the Himalayas in India. Geological exploration and underground observations were conducted on the three mining tunnel faces to collect geotechnical information to determine ground conditions. The geotechnical information collected assisted in predicting the rock mass behaviour on the three haulages.

The geotechnical/geological data gathered from the cores drilled ahead of mining faces in these developments revealed that the dykes comprise a heterogeneous rock mass, which is disintegrated and contains shear zones and closely spaced joints. The study revealed that mining through water fissures necessitates implementing case studies, empirical design and numerical analyses for support design. Empirical methods were used to classify ground conditions and behaviour. Rock Mass classification systems, NGI (2022), Bieniawski (1989), and the most appropriate system for this study is MRMR by Laubscher (1990) as it caters for effects of blasting, weathering, and joint orientation to classify the quality of the rock mass to specify support requirements in mining through these fissures. The dominant joint sets anticipated when the three haulages are mining through water fissures were also determined using Dips software. The stereographic projection employing kinematic analyses revealed wedges in the hanging wall and sidewall, which require intense support. The fall-out thickness was determined as 3.5m with wedges and disintegrated rock mass when mining through water fissures. The unstable layer extends beyond the 1.8m tendons support, and the ground condition is friable for any tendon support. The RCF was calculated to a value beyond 1.4 indicating poor ground conditions due to the anticipated stress fracturing. Based on the empirical methods, numerical analyses, Stereographic projection and kinematic analyses used from Dips software, fall out thickness database and case studies, the suitable support for mining through water fissures is arch sets with void fill. Proper blasting practice is essential in mining through water fissures. It is advisable to employ smooth wall blasting in mining operations conducted through water fissures to mitigate damage to the adjacent rock mass. Adequate training and coaching of workers on drilling practice is required. The methodology of mining through water fissures is to start by drilling ring cover ahead of mining faces. The cover regulates the volume of water, while sealing is implemented to minimise water levels. The second step is to increase the dimension of tunnels to accommodate machinery and sets. The last step is to reduce face advance to 1m and install arch sets 1m before the blast and 2m after blast. Consolidation bolts may also be installed as additional support at the discretion of the Rock Engineer.

7.1 Recommendation for Future Research Work

More case studies need to be conducted and published regarding mining through water fissures in platinum and gold mines in South Africa. This endeavour should encompass all stages of development.

Effective mining and support design concerning water geological fissures results in safe mining and profits by accessing ore reserves. Proper rock mass classification systems need to be applied and formulated to determine the rock's behaviour. Stoping layouts approaching water fissures can also be studied, and mining methods can be proposed.

Reference List

Admin, 2023. Becker Mining's steel arch roof support systems stabilize the rock mass in unstable underground conditions. Engineering & Mining Africa magazine.

Aicha, B. & Mezhoud, S., 2021. Numerical Modeling of The Behavior of Tunnel in Soft Surrounding Rock. A Case Study of Djebel El-Ouahch Tunnel, Algeria, Department of Civil Engineering, University of Mentouri Constantine, pp. 3-30.

Akgun, H., Muratli, S. & Kockar, M. K., 2014. Geotechnical investigations and preliminary support design for the Geçilmez tunnel: A case study along the Black Sea coastal highway, Giresun, northern Turkey. Tunnelling and Underground Space Technology*, 40(4),* pp. 277-299.

Alvesson, M. & Spicer, A., 2019. Neo-Institutional Theory and Organization Studies: A mid-life Crisis? Organization Studies*,* 40(2), pp. 199–218.

Anagnostou, G., 2006. Tunnel stability and deformations in water-bearing ground. Swiss Federal Institute of Technology, Zurich: Switzerland.

Askaripour, M., Saeidi , A., Mercier-Langevin, P. & Rouleau, A., 2022. A Review of Relationship between Texture Characteristic and Mechanical Properties of Rock. Geotechnic*s*, 2(1*),* pp. 262-296.

Attewell, P. B. & Sandford, M. R., 1974. Intrinsic shear strength of a brittle, anisotropic rock-I. Experimental and mechanical interpretation. International Journal of Rock Mechanics and Mining Sciences and Geomechanics Abstracts*,* Volume 11, pp. 423-430.

Barton, N., 2002. Some New Q-Value Correlations to Assist in Site Characterization and Tunnel Design. International Journal of Rock Mechanics and Mining Sciences, 39, 185-216. https://doi.org/10.1016/S1365-1609(02)00011-4.

Barton, N. & Grimstad, E., 1994. The Q-system following twenty years of application in the NMT support selection. In Norwegian in fachzeitschrift, Bergmekanikk, Geoteknikk, 12(6), pp. 428-436.

Barton, N., Lien, R. & Lunde, J., 1974. Engineering Classification of Rock Masses for the Design of Tunnel Support. Rock Mechanics, 6(4), pp. 189-236.

Behrestaghi, M.H.N., Rao, K. S. & Ramamurthy, T., 1996. Engineering geological and geotechnical responses of schistose rocks from dam project areas in India. Engineering Geology, 44(1-4)*,* pp. 183-201.

Bhandari, P., 2020. What Is Qualitative Research? | Definition, Uses & Methods. 12 June. Role of Organizational Psychology in Dealing with Human Resources and the Performance of the Organizations.

Bieniawski, Z. T., 1989. Engineering Rock Mass Classifications: A Complete Manual for Engineers and Geologists in Mining, Civil, and Petroleum Engineering: New York: Wiley & Sons. pp. 29-205.

Bieniawski, Z. T. & Lowson, A. R., 2013. Critical assessment of RMR-based tunnel design practices: A practical engineer's approach. Society for Mining, Metallurgy, and Exploration *(SME),* pp. 180-198.

Bobet, A., 2003. Effect of pore water pressure on tunnel support during static and seismic loading. Tunneling and Underground Space Technology, 18(4), pp. 377–393.

Boggs Jr, S., 2009. Petrology of Sedimentary Rocks. 2nd Edition, Cambridge University Press. Cambridge.

Bouzeran, I., Pierce, M., Andrieux, P. & Williams, E., 2019. Accounting for rockmass heterogeneity and buckling mechanism in the study of excavation performance in foliated ground at Westwood mine. Conference on Deep and High Stress Mining, 24 - 25 June, pp. 29-41.

Brady, B. H. G. & Brown, E. T., 2006. Rock Mechanics for Underground Mining. Golder Associates, Brisbane, Australia, London: Klumer Academic publishers.

Butscher, C., Mutschler, T. & Blum, P., 2016. Swelling of clay-sulfate rocks: a review of processes and controls. Rock Mechanics and Rock Engineering, pp. 153-160.

Carter, T.G. & Marinos, V., 2020. Putting Geological focus back into Rock Engineering Design, Rock Mechanics and Rock Engineering, 53(4), pp. 25-165.

Chen, Z., Zhang, J.M., Ho, K., Wu, F.Q., Li, Z.K., 2008. Landslides and Engineered Slopes. From the Past to the Future, Two Volumes + *CD-ROM.* 1st Edition ed. London: Proceedings of the 10th International Symposium on Landslides and Engineered Slopes, Department of engineering & Technology.

Chikande, T. & Zvarivadza, T., 2016. Review of support system used in poor ground conditions in platinum room and pillar mining. The Journal of The Southern African Institute of Mining and Metallurgy, 116(4), pp. 323 - 332.

Deere, D. U., 1963. Technical Description of Rock Cores for Engineering Purposes. Rock Mechanics and Engineering Geology, 1(1), pp. 16–22.

Deere, D. U. & Deere, D. W., 1988. The Rock Quality Designation (RQD) Index in Practice."Rock Classification System for Engineering Purposes, ASTM STP 984, Louis Kirkaldie, Ed., American Society for Testing and Material, Philadelphia, pp. 91–101.

Dey, K. & Murthy, S. R., 2010. Investigations on impact of Blasting in tunnels. International Journal of Geotechnical Earthquake Engineering, 1(2), pp. 59–71.

Diwakar, K. C., Dangi, H., Kadel, S., Hu, L., 2022. Challenges in Tunneling in the Himalayas: A Survey of Several Prominent Excavation Projects in the Himalayan Mountain Range of South. Geotechnics, 2(4), pp. 802–824.

Du, Preez, D. & Villiers, W. D., 2018. Investigating the different support methods for various geological structures encountered in hard rock mining within the Eastern Limb of the Bushveld Igneous Complex South Africa. Geology, Engineering, Environmental Science

Esterhuizen, G. S. & Streuders, S. B., 1998. Rockfall hazard evaluation using probabilistic keyblock analysis. The Journal of The South African Institute of Mining and Metallurgy, 97(2), pp. 57-62.

Faris, N. T., 2022. Design of tunnel support for single zones with swelling clay. Degree Project In Civil Engineering, *Division of Soil and Rock Mechanics,* pp. 4-44.

Goricki, W., Schubert, G. & Riedmueller, G., 2004. New developments for the design and construction of tunnels in complex rock masses. International Journal of Rock Mechanics and Mining Sciences, *41(3),* pp. 720-730.

Hadjigeorgiou, J. & Harrison, J. P., 2011. Uncertainty and sources of error in rock engineering. Paper presented at the 12th ISRM Congress, Beijing, China, October 2011.

Haile, A,T., Grave, D.M, Sevume, C., Le Bron, K., 1998. Strata Control in tunnels and an evaluation of support units and systems currently used with a view to improve the effectiveness of support,8 stability and safety of tunnels. CSIR Division of Mining Technology (GAP 335). Pp. 18-21.

Hoek, E., 1994. Strength of rock and rock masses. ISRM News Journal, Volume 2, pp. 4-16.

Hoek, E. & Brown, E. T., 1980. Underground Excavations in Rock. Institution of Mining and Metallurgy, pp. 18-377.

Hoek, E., Kaiser, P. K. & Bawden, W. F., 1995. Support of Underground Excavation in Hard Rock. Rotterdam, The Netherlands: AA Balkema.

Holmoy, K. H. & Aagaard, B., 2002. Spiling bolts and reinforced ribs of sprayed concrete replace concrete lining. Tunnelling and Underground Space Technology, *17(4).* pp. 403-413.

Hongri, Z., Sheng, Y., Zhang, G., Dong, Z., Liu Y., 2014. The Influence of Coal Mining on Groundwater Resources and the Analysis of Water Resources Protection Countermeasure. Project on Mine disaster Prevention and Control, pp. 398-406.

Hunter, D. R., 1975. The Regional Geological Setting of the Bushveld Complex (An Adjunct to the Provisional Tectonic map of the Bushveld Complex); Economic Geology Research Unit, University of the Witwatersrand: Johannesburg, South Africa, pp. 18.

Humphrey, W. A., 1910. The Geology of the Rustenburg and Zeerust Bushveld South of the Dwarsberg, Pretotia: Union of South Africa, Mines Department.

Hussain, S., Rehman, Z.U., Mohammad, N., Tahir, M ., 2018. Numerical Modeling for Engineering Analysis and Designing of Optimum Support Systems for Headrace Tunnel. Advances in Civil Engineering, pp. 1–12.

Jager, A.J. & Ryder, J. A., 1999. A handbook on Rock Engineering Practice for Tabular Hard Rock Mines. Safety in Mines Research Advisory Committee (SIMRAC), pp 100-350.

Jakubec, J, Lagace, D, Boggis, B, Clark, L.M & Lewis, P.A., 2018, 'Underground mining at Ekati and Diavik diamond mines', in Y Potvin & J Jakubec (eds), Caving 2018*:* Proceedings of the Fourth International Symposium on Block and Sublevel Caving, Australian Centre for Geomechanics, Perth, pp. 73-88, https://doi.org/10.36487/ACG_rep/1815_03_Jakubec

Jakubec, J. & Laubscher, D. H., 2000. The MRMR Rock Mass Rating Classification System in Mining Practice. Mass Min, 29th October, pp. 413 - 421.

JHA, A., 2022. Influence of Geological Conditions on Design and Construction of Tunnel.

Kahraman, S., Rostami, J. & Naeimipour, A., 2016. Review of Ground Characterization by Using Instrumented Drills for underground mining and construction. Rock Mechanics and Rock Engineering, *49,* pp. 585-602.

Kaiser, P. K., Diederichs, M.S., Martin, C.D., Sharp, J., & Steiner, W., 2000. Underground works in hard rock tunneling and mining. Paper presented at the ISRM International Symposium, Australia, November.

Laubscher, D. H., 1990. A Geomechanics Classification System for the Rating of Rock Mass in Mine Design. Journal of the South African Institute of Mining & Metallurgy, 90(10), pp. 257-272.

Laubscher, D. H. & Taylor, H. W., 1976. The importance of geomechanics classification of jointed rock masses in mining operations. In Exploration for rock engineering, pp. 119-128.

Leedy, P. & Ormrod, J., 2001. Practical Research Planning and Design. 7 ed. Upper Saddle River and Thousand Oaks,CA. Merrill Prentice Hall and SAGE Publications.

Li, C., 2017. Principle of Rockbolting Design. Journal of Rock Mechanics and Geotechnical Engineering, 9(3), pp. 396–414.

Maranda, A., 2011. ANFO Detonation Parameters. Central European Journal of Energetic Materials, Volume vol. 8,no. 4, pp. 280-291.

Marinos, P. & Hoek, E., 2001. Estimating the geotechnical properties of heterogeneous rock masses such as Flysch. Bulletin of Engineering Geology and the Environment 60(2), pp. 85-92.

Marinos, P., Marinos, V. & Hoek, E., 2000. The Geological Strength Index (GSI): A characterization tool for assessing engineering properties of rock masses. Underground works under special conditions, Publisher:Taylor and Francis, pp. 87-94.

Marinos, V., Goricki, A. & Malandrakis, E., 2018. Determining the principles of tunnel support based on the engineering geological behaviour types:example of a tunnel in tectonically disturbed heterogeneous rock in Serbia. Bulletin of Engineering Geology and the Environment, 23 March, pp. 16–20.

Mathew, W., 1997. The use of advanced analytical Technigues to enable Batch and Source Matching of Homemade explosivesBulk Explosive, pp 17-200.

Mathews, K.E., Hoek, E., Wylie, D.C., Stewart, S.B.V. 1981. Prediction of stable excavation spans for mining at depths below 1000m in hard rock mines, pp 25-102.

Matsukura, Y., Hashizume, K. & Oguchi, C. T., 2002. Effect of microstructure and weathering on the strength anisotropy of porous rhyolite. Engineering Geology, January, 63(1-2), pp. 39-47.

Mauriya, K. V., Yadav, P. . K. & Angra, V. K., 2010. Challenges and Strategies for Tunnelling in the Himalayan Region. Mumbai, Indian Geotechnical Conference, GEOtrendz.

Miglianico, M., Dubreuil, P., Miquelon, P. & Bakker, A. B., 2020. Strength Use in the Workplace: A Literature Review. Journal of Happiness Studies, *21(3),* pp. 737-764.

Mikula, P. A. & Lee, M. F., 2007. Empirical Performance Chart for Ground Support in Seismic Conditions at Mt Charlotte. Proceedings of the Fourth International Seminar on Deep and High Stress Mining, Australian Centre for Geomechanics, Perth, Volume 1, pp. 324-334.

Mitri, H. S. & Khan, U. H., 1990. Design guidelines for steel arch supports in underground mining. Mining Science and Technology, *13(1),* pp. 37–44.

Mizens, G. A. & Maslov, A. V., 2015. Sandstones from the molasse formation in the southern part of the Uralian foredeep. Lithology and Mineral Resources*, 50,* August, pp. 407–431.

Moser, A. & Korstjens, I., 2017. Series: Practical guidance to qualitative research. Part 1: Introduction. Eur J Gen Pract. December, Volume 23, pp. 271-273.

Moss, A. & Kaiser, P. K., 2022. An operational approach to ground control in deep mines. Journal of Rock Mechanics and Geotechnical Engineering*, 14(1)*, pp. 67-81.

Mouton, J. & Marais, H., 1994. Basic concepts in the methodology of the social sciences. Pretoria, HSRC Studies in Research Methodology, pp. 100-290.

NGI, 2022. Using the Q-System: Rock mass classification and support design. Norway: NGI.

Nguyen, Q. P., Nguven, V.M., Nguven, K.C., Nguven, N.H., 2021. Influence of Groundwater Level Rise on The Geomechanical Changing Process in The Tunnel Surrounding Jointed Rock Mass and in The Tunnel Support Structure. 2420(1). AIP Conference Proceedings.

Nihayat, T. F., 2022. Design of tunnel support for single zones with swelling clay. Division of Soil and Rock Mechanics, pp. 4-44.

Nikolic, M., Bonacci, T.R.,, Ibrahimbegovic, A., 2016. Overview of the numerical methods for the modeling of rock mechanics problems, 23(2). pp. 627-637.

Oelofse, J. M. & Judeel, J., 1999. Tunneling through a Running Dyke on Tau Lekoa Mine - Vaal River Operations. September. Conference Proceedings, Johannesburg.

Özbek, A., Gül, M., Karacan, E. & Alca, Ö., 2018. Anisotropy effect on strengths of metamorphic rocks. Journal of Rock Mechanics and Geotechnical Engineering, 10(1), pp. 164-175.

Palmstrom, A., 1982. The Volumetric Joint Count - a Useful and Simple Measure of the Degree of Jointing. Proceedings of 4th International Congress IAEG Congress, 10-15 December, Vol. 2, pp. 221–228.

Palmstrom, A., 2005. Measurements of and Correlations between Block Size and Rock Quality Designation (RQD).Tunnelling and Underground Space Technology, 20, pp. 362–377.

Palmstrom, A. & Broch, E., 2006. Use and misuse of rock mass classification systems with particular reference to the Q-system. Tunneling Underground Space Technology, 21, pp. 575-593.

Park, E. S., Martin, C. D. & Christiansson, R., 2004. Numerical simulation of the mechanical behavior of discontinuous rock masses. In Proceedings of the Numerical modeling in micromechanics via particle methods. International PFC Symposium, October. pp. 85–91.

Peck, W., 2000. Determining the stress reduction factor in highly stressed jointed rock. Australian Centre for Geomechanics, 35(2), pp. 57–60.

Pells, P.J.N. & Bertuzzi, R., 2007. Limitations of Rock Mass Classification Systems For Tunnel Support Designs, Pells Sullivan Meynink, Australia, pp 10-50.

Potvin, Y. & Hadjigeorgiou, J., 2020. Ground support for underground mines. Australian Centre for Geomechanics, pp. 100–190.

Potvin, Y., 1988. Empirical Open Stope Design in Canada, “Doctoral Thesis’’, The University of British Columbia, Vancouver, pp 1-50.

Potvin, Y., Dight, P. M. & Wesseloo, J., 2012. Some pitfalls and misuses of rock mass classification systems. The Journal of The Southern African Institute of Mining and Metallurgy, 112(8), pp. 697-702.

Potvin, Y. & Hadjigeorgiou, J., 2015. Empirical ground support design of mine drives.Perth, Australian Centre for Geomechanics, pp. 419–430.

Rahimi, B., Sharifzadeh, M. & Feng, X. T., 2020. Ground behaviour analysis, support system design and construction strategies in deep hard rock mining-Justified in Western Australian's mines. Journal of Rock Mechanics and Geotechnical Engineering, 12(1), pp. 1-20.

Ramamurthy, T. (1993) Strength, Modulus Responses of Anisotropic Rocks: In: Hudson, J.A., Ed., Compressive Rock Engineering, Vol. 1, Pergamon, Oxford, pp.313–329.

Rehman, H., Naji, A., Kim, J. J. & Yoo, H. K., 2018. Empirical Evaluation of Rock Mass Rating and Tunneling Quality Index System for Tunnel Support Design. Applied Sciences, 8(5), pp. 426-791.

Renshaw, C. E., Myse, T. A. & Brown, S. R., 2003. Role of heterogeneity in elastic properties and layer thickness in the jointing of layered sedimentary rocks. Geophysical Research Letters, 30(24).

Roland, P., Viktor, P., Robert, A. & Andres, P., 2016. Rock structure control of groundwater flow and stability – disposal of hazardous waste in abandoned mines. Engineering Geology, pp. 1-25.

Rotkegel, M., 2013. ŁPw Steel Arch Support – Designing and Test Results. Journal of Sustainable Mining, 12(1), pp. 34–40.

Russo, A. & Hormazabal, E., 2016. A Methodology to Select Valid Results from Lab Tests to Estimate Properties of Intact Rock with Microdefects. SRK Consulting (Chile).

Ryder, J. A. & Jager, A. J., 2002. A textbook on Rock Mechanics for tabular hard rock mines: The Safety in Mines Research Advisory Committee *(*SIMRACK*).* Johannesburg, pp. 127-470.

Sahu, A. K., Padhy, R. & Dhir, A., 2020. Envisioning the Future of Behavioral Decision-Making: A Systematic Literature Review of Behavioral Reasoning Theory. Australasian Marketing Journal *(*AMJ*),* 28 (4), pp. 145-159.

Saroglou, H., 2013. Engineering Behaviour of anisotropic and heterogeneous layered rocks. Global view of Engineering Geology and the Environment – Wu & Qi (eds)*,* pp. 721–731.

Schubert, W., Goricki, A. & Riedmuller, G., 2003. The guideline for the geomechanical design of underground structures with conventional excavation*.* Ground characterization and coherent procedure for the determination of excavation and support during design and construction, pp. 13–18.

Sellers, E. J., 2011. Controlled blasting fo enhanced safety. The Journal of the Southern African Institute of Mining and Metallurgy*,* 111(1,) pp. 11-16.

Selmer - Oslen, R. & Palmstrom, A., 1989. Tunnel collapses in swelling clay zones. Tunnels & tunneling*, Vol. 21,* pp. 49-58.

Sharifzadeh, M., Tarifard , A. & Moridi, M. A., 2013. Time-dependent behavior of tunnel lining in weak rock mass based on displacement back analysis method. Tunnelling and Underground Space Technology*,* September, Volume 38, pp. 348-358.

Sharifzadeh, M. Z., Feng, X.T., Zhang, X., Qiao, L. & Zhang, Y., 2017. Challenges in multi-scale hard rock behaviour evaluation at deep underground excavations*.* In Proceedings of the 12th Iranian and 3rd Regional Tunneling Conference: Tunneling and Climate change*,* pp. 53-72*,* Nov 27-29, 2017. Tehran: Iranian Tunneling Association (IRTA*).*

Singh, S. P., 1992. Mining industry and blast damage. Journal of Mines, Metals and Fuel*,* 1(12), pp. 465–468.

Somodi, G., 2021. Study of Rock Mass Rating (RMR) and Geological Strength Index (GSI) Correlations in Granite, Siltstone, Sandstone and Quartzite Rock Masses. *Applied Sciences*, 11(8), pp. 1-13.

Spaun, G. & Nickmann, M., 2006. Engineering geological classification of weak rocks. *In* Proceedings of the 10th international IAEG congress*,* September, Volume 492, pp. 1-9.

Stacey, T. R. & Swart, A. H., 2001. Rock Engineering Practice for Shallow and Open cast MIne*s*. Johannesburg: Safety in Mines Research Advisory Committee, pp. 3–35.

Stacey, T. R., 2001. *Best Practice Rock Engineering Handbook for "Other" Mines.* Braamfontein : The Safety in Mines Research Advisory Committee (SIMRAC).

Stacey, Rockscience

Stanchits, S., Mayr, S., Shapiro, S. & Dresen, G., 2011. Fracturing of porous rock induced by fluid injection. *Tectonophysics,* 503(1-2), pp. 129–145.

Swart, A. H. & Handley, M. F., 2005. The design of stable stope spans for shallow mining operations. The Journal of The South African Institute of Mining and Metallurgy*,* Volume 105, pp. 265–285.

Vitali, O. P., Celestino, T. B. & Bobet, A., 2021. New modeling approach for tunnels under complex ground and loading conditions. International Journal of Geotechnical and Geoenvironmental Engineering, 44(1*),* pp. 1-8.

Vithal, R. & Jansen, J., 2019. Designing Your First Research Proposal. A Manual for Beginning Researchers*. 2 edition*. pp. 1-64.

Villaescusa, E., Drover, C., Kusui, A., 2016. Ground support design for sudden and violent failures in hard rock tunnels. Conference: 9th Asian Rock Mechanics Symposium AT Bali Indonesia.

Wang, J. J., Zhao, T. L., Chai, H. J. & Tang, S. C., 2016. Failure of a rock slope 16.5 years after excavation in repeated strata of sandstone and mudstone. *Environmental Earth Sciences,* Volume 75, pp. 1–14.

Watson, B., 2004. A rock mass rating system for evaluating stope stability on the Bushveld Platinum mines. Journal of the Southern African Institute of Mining and Metallurgy*,* 104(4), pp. 229–238.

Yilmaz, O., 2023. Drilling and blasting designs for parallel hole cut and v-cut method in the excavation of underground coal mine galleries. Scientific Reports, 13(1), pp. 244.

APPENDICES

Appendix A: Classification of individual parameters used in the Tunnelling Quality Index Q (Ryder & Jager, 2002)

1. JOINT SET NUMBER (J_n)	
DESCRIPTION	***VALUE***
A. Massive, few random joints	**1.0**
B. One joint set	**2.0**
C. One joint set plus random joints	**3.0**
D. Two joint sets	**4.0**
E. Two joint sets plus random joints	**6.0**
F. Three joint sets	**9.0**
G. Three joint sets plus random joints	**12.0**
H. Four or more joint sets, random heavily jointed	**15.0**
I. Crushed rock	**20.0**

2. JOINT ROUGHNESS NUMBER (J_r)			
DESCRIPTION	***VALUE***		
	Discontinuous	Undulating	Planar
A. Rough or irregular	**4.0**	**3.0**	**1.5**
B. Smooth	**3.0**	**2.0**	**1.0**
C. Slickensided	**2.0**	**1.5**	**0.5**
D. +5mm thick gouges	**1.5**	**1.0**	**1.0**

3. ROCK QUALITY DESIGNATION (RQD)	
DESCRIPTION	***VALUE***
A. Very poor	**0 - 25**
B. Poor	**25 - 50**
C. Fair	**50 - 75**
D. Good	**75 - 90**
E. Very good	**90 - 100**
Note 1: Where RQD<10, use value of 10	
and if RQD>100, use value of 100	

4. JOINT ALTERATION NUMBER (J_a)			
DESCRIPTION	**Fill<1mm**	**Fill 1-5mm**	**Fill>5mm**
A. Tightly healed, hard rockwall joints,(Quartz)	**0.8**	**1.0**	**2.0**
B. Unaltered joint walls	**1.0**	**2.0**	**3.0**
C. Non-cohesive mineral (Calcite)	**2.0**	**4.0**	**6.0**
D. Serpentinite/Talc Infill	**3.0**	**6.0**	**10.0**
E. Clay	**4.0**	**8.0**	**12.0**
F. Shattered Zones or crushed rock	**5.0**	**10.0**	**12.0**

5. JOINT WATER (J_w)	
DESCRIPTION	**VALUE**
A. Dry	**1.0**
B. Wet/Moist	**0.8**
C. Dripping water (< 5litres/min)	**0.5**
D. Gushing >10l/min	**0.1**

6 STRESS REDUCTION FACTOR (SRF)	
DESCRIPTION	***VALUE***
A. No shear, faults,	**1.00**
B. One shear/fault or major E-W joints with opposing dips.	**2.50**
C. One shear/fault and blocky ground	**4.00**
D. Multiple faults or dykes	**6.00**
E. Curved Low Angled joints or domes	**7.50**
F. Joints sub // to advance direction (same/opposing dips)	**8.00**
H. Multiple faults/Wide shears mylonite zones	**10.00**

Appendix B Rock Mass Rating System (Bieniaswski, 1989)

A. CLASSIFICATION PARAMETERS AND THEIR RATINGS

Parameter			Range of values						
1	Strength of intact rock material	Point-load strength index	>10 MPa	4 - 10 MPa	2 - 4 MPa	1 - 2 MPa	For this low range - uniaxial compressive test is preferred		
		Uniaxial comp. strength	>250 MPa	100 - 250 MPa	50 - 100 MPa	25 - 50 MPa	5 - 25 MPa	1 - 5 MPa	< 1 MPa
	Rating		15	12	7	4	2	1	0
2	Drill core Quality *RQD*		90% - 100%	75% - 90%	50% - 75%	25% - 50%	< 25%		
	Rating		20	17	13	8	3		
3	Spacing of discontinuities		> 2 m	0.6 - 2 . m	200 - 600 mm	60 - 200 mm	< 60 mm		
	Rating		20	15	10	8	5		
4	Condition of discontinuities (See E)		Very rough surfaces Not continuous No separation Unweathered wall rock	Slightly rough surfaces Separation < 1 mm Slightly weathered walls	Slightly rough surfaces Separation < 1 mm Highly weathered walls	Slickensided surfaces or Gouge < 5 mm thick or Separation 1-5 mm Continuous	Soft gouge >5 mm thick or Separation > 5 mm Continuous		
	Rating		30	25	20	10	0		
5	Ground water	Inflow per 10 m tunnel length (l/m)	None	< 10	10 - 25	25 - 125	> 125		
		(Joint water press)/ (Major principal σ)	0	< 0.1	0.1, - 0.2	0.2 - 0.5	> 0.5		
		General conditions	Completely dry	Damp	Wet	Dripping	Flowing		
	Rating		15	10	7	4	0		

B. RATING ADJUSTMENT FOR DISCONTINUITY ORIENTATIONS (See F)

Strike and dip orientations		Very favourable	Favourable	Fair	Unfavourable	Very Unfavourable
Ratings	Tunnels & mines	0	-2	-5	-10	-12
	Foundations	0	-2	-7	-15	-25
	Slopes	0	-5	-25	-50	

C. ROCK MASS CLASSES DETERMINED FROM TOTAL RATINGS

Rating	100 ← 81	80 ← 61	60 ← 41	40 ← 21	< 21
Class number	I	II	III	IV	V
Description	Very good rock	Good rock	Fair rock	Poor rock	Very poor rock

D. MEANING OF ROCK CLASSES

Class number	I	II	III	IV	V
Average stand-up time	20 yrs for 15 m span	1 year for 10 m span	1 week for 5 m span	10 hrs for 2.5 m span	30 min for 1 m span
Cohesion of rock mass (kPa)	> 400	300 - 400	200 - 300	100 - 200	< 100
Friction angle of rock mass (deg)	> 45	35 - 45	25 - 35	15 -25	< 15

E. GUIDELINES FOR CLASSIFICATION OF DISCONTINUITY conditions

Discontinuity length (persistence) Rating	< 1 m 6	1 - 3 m 4	3 - 10 m 2	10 - 20 m 1	> 20 m 0
Separation (aperture) Rating	None 6	< 0.1 mm 5	0.1 - 1.0 mm 4	1 - 5 mm 1	> 5 mm 0
Roughness Rating	Very rough 6	Rough 5	Slightly rough 3	Smooth 1	Slickensided 0
Infilling (gouge) Rating	None 6	Hard filling < 5 mm 4	Hard filling > 5 mm 2	Soft filling < 5 mm 2	Soft filling > 5 mm 0
Weathering Ratings	Unweathered 6	Slightly weathered 5	Moderately weathered 3	Highly weathered 1	Decomposed 0

F. EFFECT OF DISCONTINUITY STRIKE AND DIP ORIENTATION IN TUNNELLING**

Strike perpendicular to tunnel axis		Strike parallel to tunnel axis	
Drive with dip - Dip 45 - 90°	Drive with dip - Dip 20 - 45°	Dip 45 - 90°	Dip 20 - 45°
Very favourable	Favourable	Very unfavourable	Fair
Drive against dip - Dip 45-90°	Drive against dip - Dip 20-45°	Dip 0-20 - Irrespective of strike°	
Fair	Unfavourable	Fair	

Appendix C: Stereographic Plot data investigated at 14 FDW, 16 FDE and 17 FDE

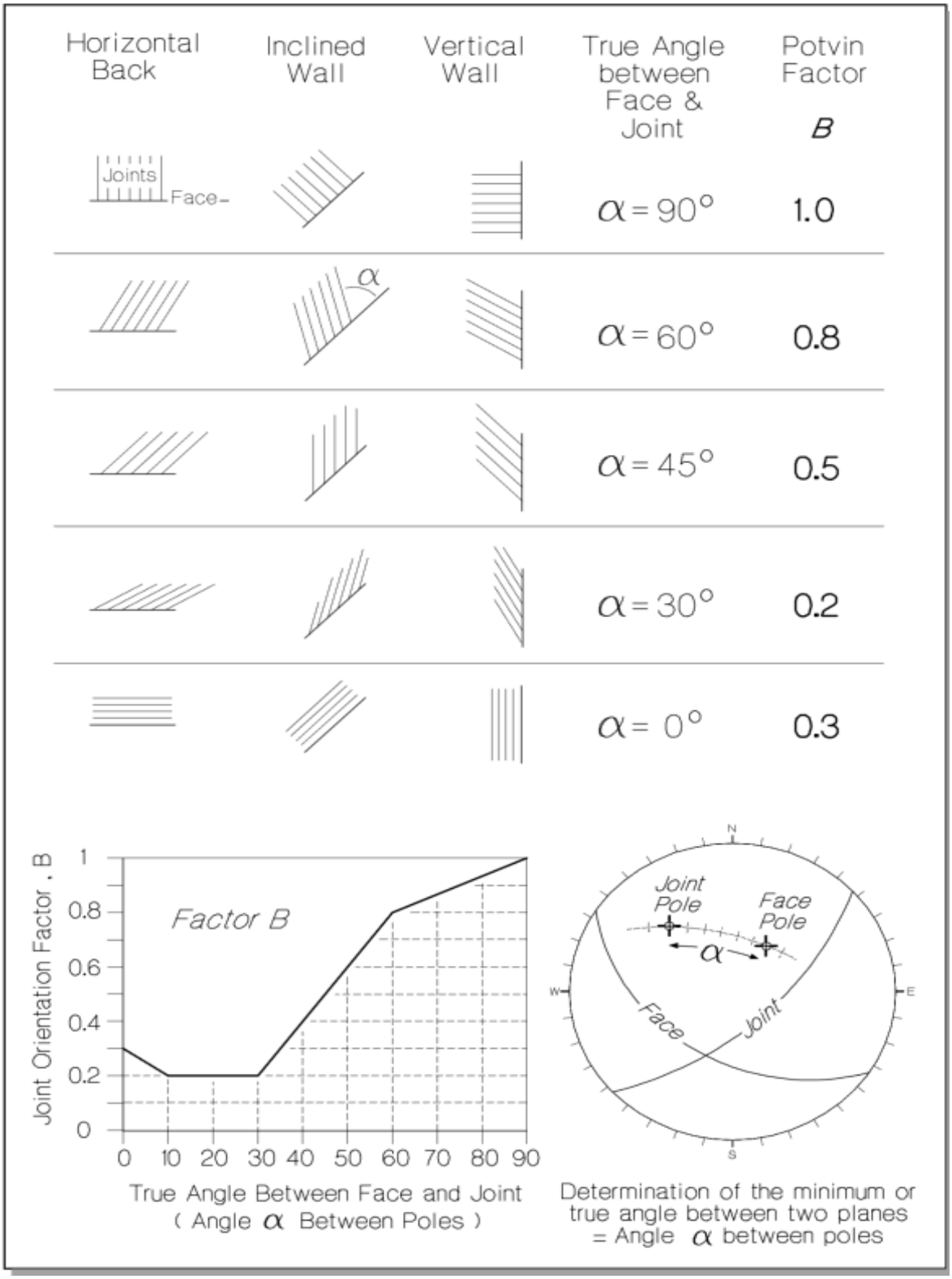
16E Joints sets		17E Joints sets		14W Joint sets	
Dip angle (°)	**Strike angle (°)**	**Dip angle (°)**	**Strike angle (°)**	**Dip angle (°)**	**Strike angle (°)**
60	300	50	86	70	120
67	240	55	120	68	125
68	250	60	220	55	119
70	250	58	150	65	126
69	358	62	169	71	121
56	310	59	170	50	127
70	250	70	160	60	130
60	019	89	180	65	129
69	357	68	240	80	120
80	360	65	220	69	129
57	320	75	170	40	121
83	009	80	166	38	127
59	357	78	165	35	125
57	356	63	150	45	128
45	329	69	206	48	123
67	280	70	200	49	129
76	322	74	201	60	126
48	311	65	190	58	126
38	340	60	205	59	123
48	315	70	200	58	122
59	345	54	204	60	127
58	333	58	207	60	123
68	356	61	160	67	127
72	008	65	155	89	128
73	301	68	160	61	123
60	280	58	240	71	129
58	305	59	200	65	125
56	307	48	205	63	127
64	300	64	204	64	125
65	344	67	205	58	126
67	342	56	206	69	127
64	350	62	169	72	123
62	348	59	160	65	122
69	349	57	170	73	126
48	355	62	188	68	122

Appendix D UCS test 2011 (CSIR)

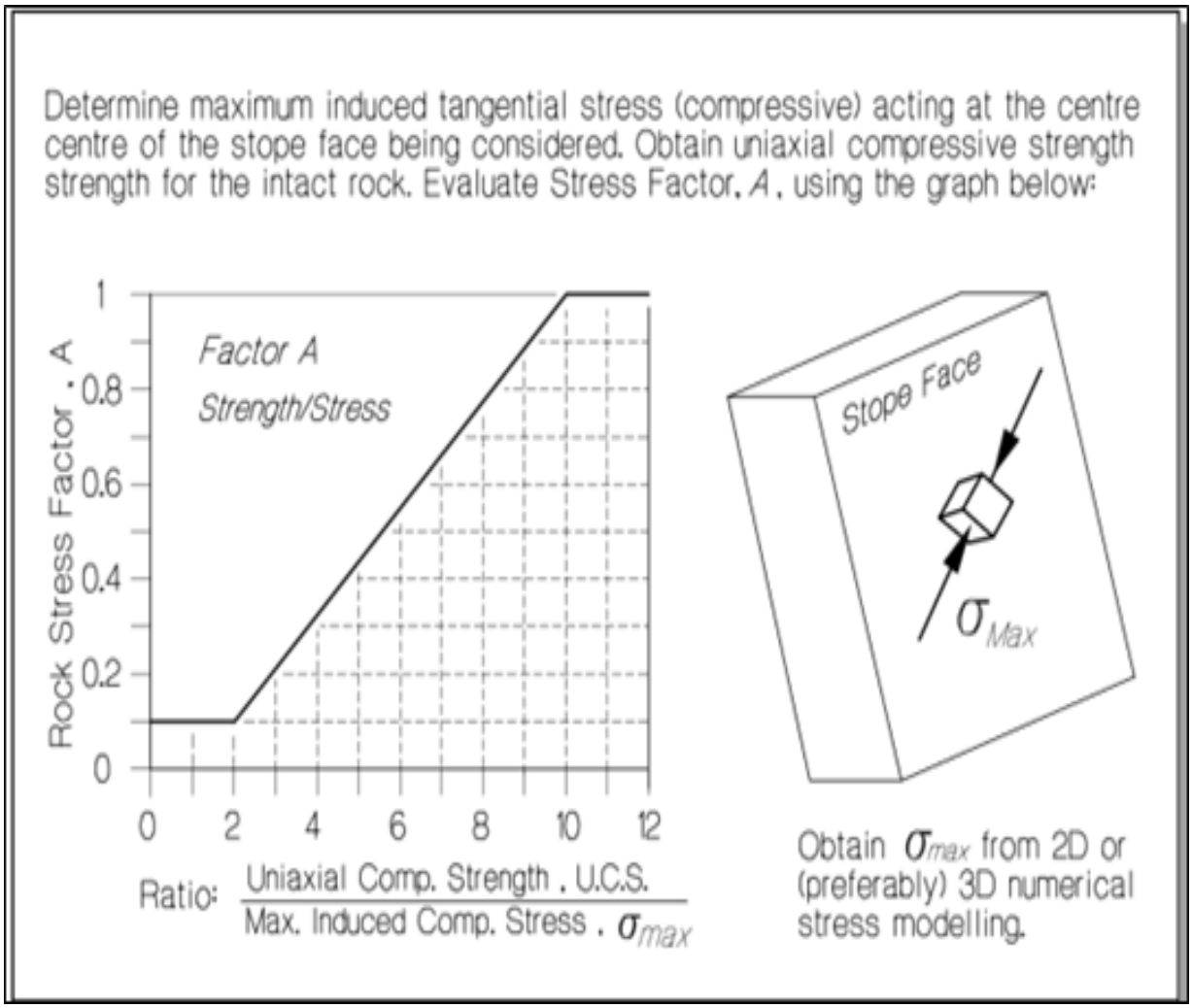
Rock Strength information

Approx. Distance from the Merensky Reef (m)		Rock Type	Uniaxial Compressive Strength Range (UCS) MPa
Above	Below		
28 - 30		Bastard Unit	100 +
24 - 28		Merensky Anorthosite	100 +
19 - 24		Leuco Norite	90 - 110
15 - 19		Merensky Cyclic Unit	88 - 98
9 - 15		Norite	89 - 94
2 - 9		Mela Norite	75 -118
HW - 2		Merensky Pyroxenite	84 - 118
0	0	Merensky Reef	85 - 98
	FW - 2	P2 Dunite	84 - 99
	2 - 4	P1 Anorthosite	87 - 108
	4 - 5	Harzburgite	88 - 96
	5 - 19	UG 2 Pyroxenite	85 - 148
	19 - 21	Dunite/Harzburgite	105 - 140
	21 - 22	UG2	70 - 110
	22 - 37	UG1 Pyroxenite	60 - 115
	37 - 38	UG1	67 - 70
	38 - 42	Anorthosite	69 - 108
	45 - 47	Norite	78 - 92

Appendix E Determination of Joint Orientation Factor, B, for Stability Graph analysis (Hutchinson and Diederichs 1996)

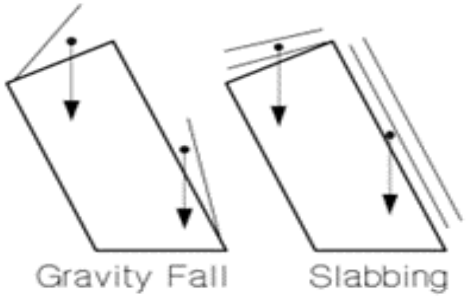


Appendix F Rock stress factor A, for stability analysis (Potvin, 1988)

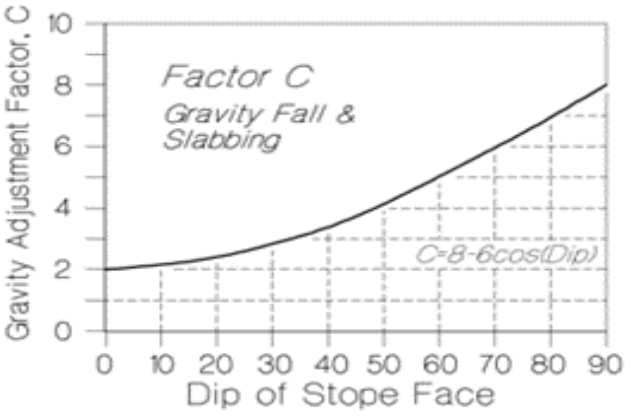


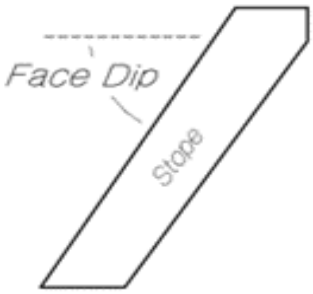
Appendix G Determination of Gravity Adjustment Factor, C, for Stability Graph analysis (Potvin, 1988)

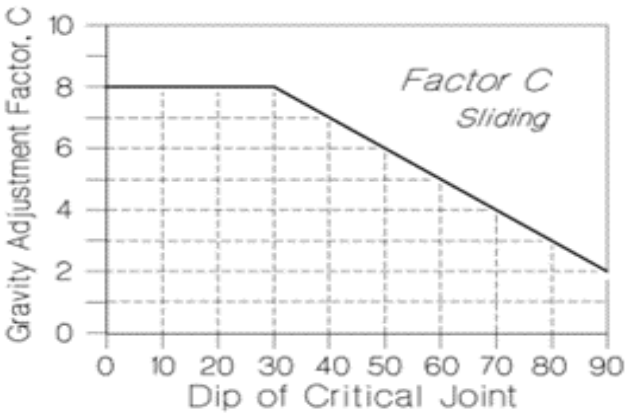
1) Determine the most likely mode of structural failure in case study using the figures below:

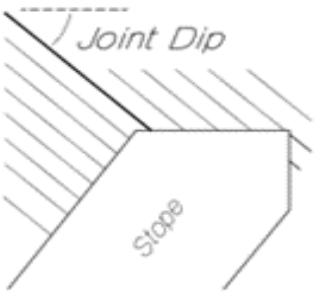


2) Next determine the gravity adjustment factor, *C*, based on the failure mode using the appropriate chart below.









Appendix H: Geological core logging sheet for 14 FDW Borehole 14073

GEOTECHNICAL CORE LOGGING SHEET

Logged by:	T.Chauke	Core diameter:	AXT
Date:	Aug-23	Hole ID:	14073	Hole inclination:	10

Depth (m)		TCR (m)	SCR (m)	Pieces >10cm	RQD	Geotechnical Interval (m	Rock Type	Weathering (1-5)	Hardness (1-5)	Rock Competence			Jointing Distribution (# of joints)				Joint Surface Condition				Q	RMR
From	To									Solid (m)	Matrix (m)	Matrix Type (1-5)	0°-30°	30°-60°	60°-90°	Total Number	Macro (1-5)	Micro (1-9)	Infill Type (1-9)	Wall Alt (1-3)		
3.00	6.00	3	3	1.2	40	3	Norite +dyke	5	5	3	0.22	5	1	1	1	3	1	2	3	1	0.5	45.485
6.00	8.80	2.8	2.8	1.3	46	3	Norite +dyke	5	5	3	0.94	5	1	1	2	4	1	2	3	1	0.75	48.126
8.80	11.80	3	3	1.46	49	3	Norite	5	5	3	91	4	9	2	1	12	1	7	3	1	0.0357	28.293
11.80	14.80	3	3	1.58	53	3	Norite	5	5	3	0	4	4	5	2	11	1	2	3	1	0.2727	41.536
14.80	17.80	3	3	1.3	43	3	Norite	5	5	3	0.26	5	3	5	1	9	1	2	3	1	0.1667	38.328
17.80	20.80	3	3	1	33	3	Norite +dyke	5	5	3	0	5	3	4	2	9	1	2	3	1	0.3333	42.843
20.80	23.80	3	3	1.1	37	3	Norite +dyke	5	5	3	0.2	5	5	5	1	11	1	7	3	1	0.039	28.859
23.80	26.80	3	3	1.1	37	3	Norite +dyke	5	5	3	0.3	5	4	3	1	8	1	7	3	1	0.0536	30.934
26.80	29.80	3	3	1.2	40	3	Norite +dyke	5	5	3	0	5	5	5	2	12	1	6	3	1	0.0833	33.812
29.80	32.80	3	3	1.2	40	3	Norite +dyke	5	5	3	0	5	4	4	2	10	1	5	3	1	0.12	36.188
32.80	35.80	3	3	1.3	43	3	Norite +dyke	5	5	3	0	5	2	5	1	8	1	4	3	1	0.0938	34.58
35.80	38.80	3	3	2	67	3	Norite +dyke	5	5	3	0	5	2	4	2	8	1	4	3	1	0.1875	39.095

Appendix I: Geological core logging sheet for 16 FDE borehole 15071

GEOTECHNICAL CORE LOGGING SHEET

Logged by:	T.Chauke	Core diameter:	AXT
Date:	Aug-23	Hole ID:	15071	Hole inclination:	10

Depth (m)		TCR	SCR	Pieces	RQD	Geotechnical	Rock Type	Weathering	Hardness	Rock Competence			Jointing Distribution (# of joints)				Joint Surface Condition					
From	To	(m)	(m)	>10cm		Interva			(1-5)	Solid (m)	Matrix (m)	Matrix Type	0°-30°	30°-60°	60°-90°	Total Number	Macro (1-5)	Micro (1-9)	Infill Type	Wall Alt (1-3)	Q	RMR
3.00	6.00	3	3	1.2	40	3	Norite +dyke	5	5	3	0.22	5	3	1	1	5	1	7	5	1	0.3333	42.843
6.00	8.80	2.8	2.8	1.1	39	3	Norite +dyke	5	5	3	0.94	5	1	1	2	4	1	2	4	1	0.3274	42.726
8.80	11.80	3	3	1.2	40	3	Norite +dyke	5	5	3	0	5	9	5	1	15	1	7	3	1	0.3125	42.423
11.80	14.80	3	3	1.7	57	3	Norite +dyke	5	5	3	0	4	4	5	2	11	1	2	3	1	0.1574	37.955
14.80	17.80	3	3	1.2	40	3	Norite +dyke	5	5	3	0.26	5	3	1	1	5	1	2	3	1	0.3333	42.843
17.80	20.80	3	3	1.1	37	3	Norite +dyke	5	5	3	0.2	5	3	1	1	10	1	2	2	1	0.3056	42.276
20.80	23.80	3	3	1.3	43	3	Norite +dyke	5	5	3	0	5	3	1	1	6	1	2	3	1	0.2708	41.491
23.80	26.80	3	3	1.2	40	3	Norite +dyke	5	5	3	0.3	4	3	1	2	6	1	2	4	1	0.3333	42.843
26.80	29.80	3	3	1.5	50	3	Norite +dyke	5	5	3	0	5	3	1	2	7	1	7	4	1	0.3125	42.423
29.80	32.80	3	3	1.1	37	3	Norite +dyke	5	5	3	0	4	3	1	2	5	1	3	5	1	0.3056	42.276
32.80	35.80	3	3	1.3	43	3	Norite +dyke	5	5	3	0	5	3	1	2	10	1	3	6	1	0.3611	43.365
35.80	38.80	3	3	1.4	47	3	Norite +dyke	5	5	3	0	4	3	1	2	10	1	4	5	1	0.2917	41.973

Appendix J: Geological core logging sheet for 17 FDE borehole 14072

GEOTECHNICAL CORE LOGGING SHEET

Logged by:	T.Chauke	Core diameter:	AXT
Date:	Aug-23	Hole ID:	14072	Hole inclination:	10

Depth (m)		TCR	SCR	Pieces	RQD	Geotechnical	Rock Type	Weathering	Hardness	Rock			Jointing Distribution (# of joints)				Joint Surface Condition					
From	To	(m)	(m)	>10c		Interval		(1-5)	(1-5)	Solid (m)	Matrix (m)	Matrix	0°-30°	30°-60°	60°-90°	Total Number	Macro (1-5)	Micro (1-9)	Infill Type	Wall Alt (1-3)	Q	RMR
3.00	6.00	3	3	1	33	3	Norite +dyke	5	5	3	0.22	5	1	4	1	6	1	2	3	1	0.25	41
6.00	8.80	2.8	2.8	1.3	46	3	Norite +dyke	5	5	3	0.94	5	1	3	2	6	1	2	3	1	0.5	45.5
8.80	11.80	3	3	1.46	49	3	Norite	5	5	3	0	4	5	4	1	10	1	7	3	1	0.04	29.5
11.80	14.80	3	3	1.58	53	3	Norite	5	5	3	0	5	4	5	2	11	1	2	3	1	0.27	41.5
14.80	17.80	3	3	1.3	43	3	Norite	5	5	3	0.26	5	2	5	1	8	1	2	3	1	0.19	39.1
17.80	20.80	3	3	1	33	3	Norite +dyke	5	5	3	0	5	2	4	2	8	1	2	3	1	0.38	43.6
20.80	23.80	3	3	1.1	37	3	Norite +dyke	5	5	3	0.2	5	2	2	1	5	1	7	3	1	0.09	34
23.80	26.80	3	3	1.1	37	3	Norite +dyke	5	5	3	0.3	5	1	1	1	3	1	7	3	1	0.14	37.3
26.80	29.80	3	3	1.2	40	3	Norite +dyke	5	5	3	0	5	1	5	2	8	1	6	3	1	0.13	36.5
29.80	32.80	3	3	1.2	40	3	Norite +dyke	5	5	3	0	5	4	4	2	10	1	5	3	1	0.12	36.2
32.80	35.80	3	3	1.3	43	3	Norite +dyke	5	5	3	0	5	2	5	1	8	1	4	3	1	0.09	34.6
35.80	38.80	3	3	2	67	3	Norite +dyke	5	5	3	0	5	2	5	2	9	1	4	3	1	0.17	38.3